2013

NMDA RECEPTORS IN THE DORSAL VAGAL COMPLEX OF NORMAL AND DIABETIC MICE

Eva C. Bach
University of Kentucky, ecbach2@uky.edu

STUDENT AGREEMENT:

I represent that my thesis or dissertation and abstract are my original work. Proper attribution has been given to all outside sources. I understand that I am solely responsible for obtaining any needed copyright permissions. I have obtained and attached hereto needed written permission statements(s) from the owner(s) of each third-party copyrighted matter to be included in my work, allowing electronic distribution (if such use is not permitted by the fair use doctrine).

I hereby grant to The University of Kentucky and its agents the non-exclusive license to archive and make accessible my work in whole or in part in all forms of media, now or hereafter known. I agree that the document mentioned above may be made available immediately for worldwide access unless a preapproved embargo applies.

I retain all other ownership rights to the copyright of my work. I also retain the right to use in future works (such as articles or books) all or part of my work. I understand that I am free to register the copyright to my work.

REVIEW, APPROVAL AND ACCEPTANCE

The document mentioned above has been reviewed and accepted by the student's advisor, on behalf of the advisory committee, and by the Director of Graduate Studies (DGS), on behalf of the program; we verify that this is the final, approved version of the student's dissertation including all changes required by the advisory committee. The undersigned agree to abide by the statements above.

Eva C. Bach, Student

Dr. Bret N. Smith, Major Professor

Dr. Bret N. Smith, Director of Graduate Studies

NMDA RECEPTORS IN THE DORSAL VAGAL COMPLEX OF NORMAL AND DIABETIC MICE

DISSERTATION

A dissertation submitted in partial fulfillment of the requirements for the degree of Doctor of Philosophy in the Department of Physiology in the College of Medicine at the University of Kentucky

By

Eva Claudia Bach

Lexington, Kentucky

Director: Dr. Bret N. Smith, Professor of Physiology

Lexington, Kentucky

2013

ABSTRACT OF DISSERTATION

NMDA RECEPTORS IN THE DORSAL VAGAL COMPLEX OF NORMAL AND DIABETIC MICE

The dorsal vagal complex (DVC), containing the nucleus of the solitary tract (NTS) and the dorsal motor nucleus of the vagus nerve (DMV), plays a pivotal role in autonomic regulation. Afferent fibers from peripheral organs and higher brain centers synapse in the NTS, which integrates these synaptic connections as well as information from systemically circulating hormones and metabolites. The integrated information is relayed to the dorsal motor nucleus of the vagus nerve (DMV), which in turn, projects motor fibers to elicit parasympathetic control of digestive and other viscera. Physiological functions mediated by the DVC are disrupted in diabetic patients and synaptic plasticity within the DVC has been linked to these complications. N-methyl-D-aspartic acid (NMDA) receptors have been extensively studied for their involvement in synaptic plasticity in a variety of central nervous system disorders; and their activation in the DVC modulates hepatic glucose production and feeding behavior. Although chronic disease can alter NMDA function, changes in DVC expression and/or sensitivity of NMDA receptors in diabetic states has not been addressed. Using whole cell electrophysiology, functional properties of the nuclei in the DVC were investigated in normoglycemic and type 1 diabetic mice. Preterminal NMDA (preNMDA) receptors were discovered to tonically modulate excitatory neurotransmission on terminals contacting DMV neurons. While these preNMDA receptors were not found to differentially modulate tonic excitatory neurotranmission, soma-dendritic NMDA receptor responses of NTS neurons were augmented in type 1 diabetic mice. Through the use single-cell PCR, increased NMDA receptor responses could be correlated to neurons that mediate excitatory neurotransmission and would argue that augmented NMDA receptor responses increase vagal output. In general, enhancing vagal output decreases activity of connected peripheral organs. Molecular approaches were employed to corroborate the observed functional NMDA receptors changes to their protein and mRNA expression levels. Overall, results argue that NMDA receptors are involved in synaptic plasticity in DVC of type 1 diabetic mice to enhance excitatory neurotransmission. This modulation may potentially serve as a

physiological counter regulatory mechanism to control pathological disturbances of gastrointestinal homeostatic reflex responses.

KEYWORDS: NMDA, Dorsal Vagal Complex, Electrophysiology, Type 1 diabetes, Synaptic Plasticity

Eva Bach

November 6, 2013

NMDA RECEPTORS IN THE DORSAL
VAGAL COMPLEX OF NORMAL AND DIABETIC MICE

Bret N. Smith
Director of Dissertation

Bret N. Smith
Director of Graduate Studies

November 6, 2013

This dissertation is dedicated to my mom and stepdad, Christine and Manfred Jakober, for their unwavering support throughout this journey

ACKNOWLEDGEMENTS

First of all, I would like to express my gratitude to my doctoral advisor Dr. Bret Smith. Over the last few years his guidance and expertise in neurophysiology and brainstem circuitry along with enthusiasm and support for my studies have been invaluable. While guiding me though the process of my doctoral studies, he provided me with the freedom to develop and experimentally explore my own hypothesis driven ideas. His doors were always open to discuss these ideas, results and/or any experimental and/or technical challenges.

I would also like to thank the members of my advisory committee, Dr. Brian Delisle, Dr. Olivier Thibault and Dr. Timothy McClintock. The expertise in their respective fields, not only assisted me with technical designs of my studies, but also often provided me with a new perspective to be appreciated especially in the context of interpreting results. This guidance and their constructive criticism, not only helped shape these studies, but also fostered my critical thinking skills.

The Grant Writing Workshop and its participating faculty tutors deserve similar acknowledgement. Given the complexity of grant writing, I am thankful to have had these dedicated tutors step me though the grant writing process,

I would like to thank all present and past members in the Smith Laboratory. I would like to point out a few members, in respect to specific roles they played in helping me throughout graduate school. Dr. Camille Blake not only invested a substantial amount of time into editing my documents, but was a supportive friend and troubleshoot companion. In respect to the molecular

approaches used throughout this dissertation, I would like to thank Katalin Halmos and Dr. Peter Gyarmati, for their help and patience. The same goes for Dr. Robert Hunt, who was especially instrumental in teaching me electrophysiology.

My family, which has always supported me in whichever way possible, certainly cannot be forgotten in my mentioning. I can't thank them enough for their emotional support and encouragement.

I am grateful also for the family of friends, I have found in Lexington. Thank you to all of my graduate student and climbing friends that have laughed and enjoyed the things I love with me and were there when I needed help.

I would like to say thanks to my boyfriend Dr. Ryan Woods, who, patiently edited my dissertation and provided me with countless laughs and encouragement during times of frustration. On this note, I just cannot leave out my four-legged best friends, Loki and Enzo, who certainly never fail to entertain.

Table of Contents

List of Tables

List of Figures

Chapter 1: Introduction

The Dorsal Vagal Complex

Circuit organization and neurotransmission in the Dorsal Vagal Complex

The dorsal vagal complex (DVC) of the caudal brainstem regulates central parasympathetic reflex and integrative functions, including those of the digestive system. Viscerosensory inputs mediated by cranial nerves VII, IX and X in conjunction to centrally-originating afferents form synapses in the nucleus of the solitary tract (NTS). The NTS consists of a heterogeneous population of cells, which incorporates mechanical stimuli from peripheral organs as well as from circulating hormones and metabolites, and transmits this information to other autonomic centers including the dorsal motor nucleus of the vagus nerve (DMV) (Browning and Travagli, 2011; Kalia and Mesulam, 1980a; Kalia and Mesulam, 1980b; Travagli, 2007; Travagli et al., 2006). The DMV contains preganglionic motor neurons that project back to peripheral organs. As a unit, the fiber tracts, the NTS, and the DMV mediate the vago-vagal reflex (Browning and Travagli, 2011; Kalia and Mesulam, 1980a; Kalia and Mesulam, 1980b; Travagli, 2007; Travagli et al., 2006).

DMV neurons maintain tonic pacemaker activity (Travagli et al., 1991a). This input, however, is tightly regulated by predominantly GABAergic and glutamatergic presynaptic neurons of the NTS (Davis et al., 2004; Glatzer et al.,

2007; Travagli, 2012). GABAergic inputs maintain a tonic inhibitory drive that dominates the regulation of vagal outflow, with glutamatergic inputs serving a phasic excitatory role (Gao and Smith, 2010; Travagli et al., 1991b). An enhanced excitatory drive to DMV neurons and subsequent increase of vagal output would be expected to invoke stimulation of peripheral organs to aid in maintaining appropriate energy homeostasis, and glucose homeostasis in particular (Zsombok and Smith, 2009). Increased vagal outflow lowers hepatic gluconeogenesis, enhances pancreatic exocrine function (i.e. release of insulin) and stimulates gastric emptying (Ahren et al., 1996; Pocai et al., 2005b; Saltzman and McCallum, 1983).

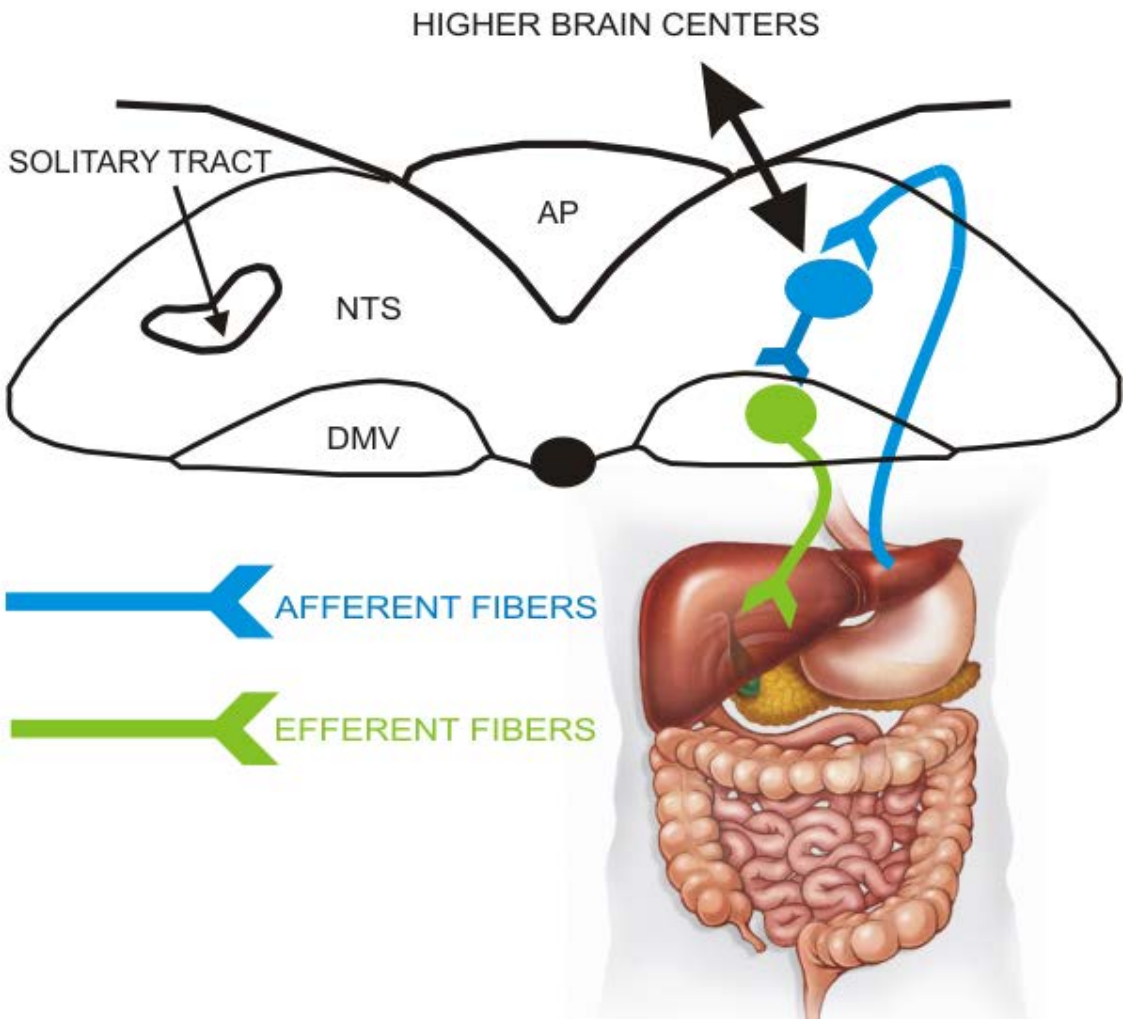

Figure 1.1 Schematic of gastrointestinal reflex-arc of the brainstem.

DMV= Dorsal Motor Nucleus of the Vagus, NTS= Nucleus of the Solitary Tract

Energy homeostasis in the DVC and pathological consequences

Homeostatic gastric reflex responses are a good example of a response mediated by the DVC that can be modulated by a complex array of peripheral as

well as CNS signals (Barber and Burks, 1983; Barber and Burks, 1987; Travagli et al., 2006). Furthermore, it exemplifies a response whose homoeostatic imbalance can lead to pathological complications (Saltzman and McCallum, 1983). Gastric reflexes are in part controlled by mechanical as well as chemoactivation. Therefore, when the stomach becomes full and consequently experiences mechanical distension and chemoactivation of various satiety signals, vagal afferents that synapse in the NTS become activated to trigger the cessation of feeding (Barber and Burks, 1983; Barber and Burks, 1987; Travagli et al., 2006). Synaptic inputs also arise from higher brain centers, notably the hypothalamic nuclei, which provide additional signals related to the overall metabolic status (Obici et al., 2002; Pocai et al., 2005a).

The collective input from these various signals, as well as those of peripheral hormones and metabolites discussed below, help fine-tune parasympathetic reflex responses of the gastrointestinal organs including the stomach. It is, therefore, not surprising that incongruence between these collective signals can result in pathological outcomes. In the context of the stomach, gastroparesis has been well established as a pathological symptom of diabetic patients (Saltzman and McCallum, 1983; Zsombok and Smith, 2009).

Diabetes mellitus is a metabolic disease of glucose characterized by the body's inability to maintain glucose homeostasis. This can arise either from pancreatic β-cell islet destruction and the concomitant inability of the body to synthesize insulin (Type 1 diabetes), or abnormal insulin secretion and insulin resistance (Type 2 diabetes) (Zimmet et al., 2001).

Beyond synaptic inputs to the DVC, signaling the status of various metabolic functions, fenestrated capillaries surrounding this region of the brain provide a direct indication on the status of circulating hormones and metabolites (Gross et al., 1990; Merchenthaler, 1991). Of particular interest is the ability of this nucleus to directly respond to hormones and metabolites that mediate glucose homeostasis. Glucose itself modulates efferent activity of the DVC through subpopulation of cells in the NTS and the DMV that respond to changing glucose concentrations by altering their firing properties. These glucose-sensitive neurons respond to both hypoglycemic as well as hyperglycemic conditions to elicit vagal efferent responses conducive to maintaining and reestablishing glucose homeostasis (Babic et al., 2012; Balfour et al., 2006; Balfour and Trapp, 2007; Browning and Travagli, 2010; Ferreira et al., 2001; Pocai et al., 2005b).

In conjunction with glucose, other metabolites that have been well established for their peripheral role in glucose homeostasis have a direct effect on neurons within the DVC. A few of these hormonal players include insulin, leptin and glucagon-like peptide-1 (GLP-1). In particular, insulin as well as leptin modulate synaptic input to the DMV and on NTS neurons through the activation of insulin and leptin receptors, respectively, that results in a decrease of glutamate release on gastric related neurons. Both were shown to act in a PI3K-dependent mechanism suggesting their activation of signaling cascades similar to those observed in peripheral organs and hypothalamic nuclei (Blake and Smith, 2012; Williams and Smith, 2006; Williams et al., 2007). GLP-1 activity has been shown to enhance both the excitatory and inhibitory activity to pancreatic-

projecting neurons in the DMV (Wan et al., 2007). Collectively the direct effects of metabolites and hormones at the level of the DVC, suggests that they are important players in minute to minute efferent output modulation.

The complexity of the synaptic rules governing homeostatic gastrointestinal reflex responses elicited by the DVC emphasizes the need to better understand these principles and how they can be modulated under physiological as well as pathological circumstances. A more comprehensive understanding of their mechanisms may serve as a potential tool to manipulate glucose homeostasis and prevent symptoms of diabetic patients. As a result, studying the DVC in the context of diabetes has garnered increased attention in the global epidemic of metabolic disorders (Zsombok and Smith, 2009).

The role of the CNS in the diabetes epidemic

Diabetes, in particular Type 2 diabetes, is emerging as one of the most prevalent diseases of the developed world (Zimmet et al., 2001). Due to its effects on peripheral organs that modulate hormone homeostasis, diabetes has classically been treated as a peripheral disease, but the pathological involvement of the CNS has garnered increased attention more recently when various studies linked changes neuronal responses and synaptic reorganization of central nervous system (CNS) to glucose dysregulation and diabetes (Levin et al., 1999; Obici et al., 2002; Zsombok and Smith, 2009).

To begin to understand the effects diabetes has on synaptic connections of the DVC, the streptozotocin (STZ) model of Type 1 diabetes (T1-diabetes) was used in electrophysiological studies in the DMV. This model involves injecting

animals systemically with STZ, which kills the insulin-producing pancreatic β-cells and causing chronic hyperglycemia in conjunction with hypoinsulemia (Craighead, 1980). These studies revealed that DMV neurons of diabetic animals receive enhanced excitatory input. More specifically, this study revealed an increase in the spontaneous and miniature excitatory postsynaptic current (sEPSC and mEPSC) frequency in DMV neurons of T1-diabetic mice. No change phasic in spontaneous or miniature inhibitory post synaptic currents (sIPSCs or mIPSCs) was observed in these studies and suggested modulation specific to excitatory neurotransmission in T1-diabetic mice (Zsombok et al., 2011). An increase in the EPSC frequency suggests an increase in the probability of glutamate release presynaptically, from the presynaptic terminal and/or from presynaptic neurons. Glutamate is the principal excitatory neurotransmitter in the DVC and activates both NMDA and non-NMDA receptors (Bonham and Hasser, 1993; Seagard et al., 1999; Smith et al., 2002).

NMDA Receptors

Function and Pharmacology of NMDA Receptors

NMDA receptors are ionotropic receptors prominently thought to consist as tetrameric subunit assemblies (Paoletti and Neyton, 2007; Traynelis et al., 2010). Upon activation by glutamate and/or glycine, NMDA receptors typically contribute to cellular depolarization and Ca^{2+}-dependent signaling cascades by increasing the conductance of Na^{+} and Ca^{2+}. Under normal physiological conditions the presence of Mg^{2+}, and its permeation into the pore of the channel,

leads to a block of ionic flux (Mayer et al., 1984; Nowak et al., 1984). Both the extent of Mg^{2+} inhibition and Ca^{2+} permeation, however, are dependent on the subunit assembly of NMDA receptors (Traynelis et al., 2010).

Throughout the CNS seven NMDA receptor subunits have been identified, namely NR1, NR2A-D and NR3A/B subunits. While NR1 subunit incorporation is thought to be obligatory to form functional receptors, these subunits are not believed to assemble as homomers. Rather it is thought that NMDA receptors exist in a di- or tri-heteromeric state, but it is still unclear whether NR3 subunits are able to assemble with NR1 subunits in the absence of NR2 subunits (Paoletti and Neyton, 2007; Traynelis et al., 2010). This may be due to the functional significance of NR2 subunits have in assembly (Meddows et al., 2001).

Each subunit is composed of four domains, an N-terminal domain (NTD), an agonist binding domain (ABD), a transmembrane domain (TMD) and a C-terminus domain (CTD). The NTD is most critically involved in subunit assembly and contains the binding site for the allosteric NR2A-subunits inhibitor Zn^{2+} , as well as the allosteric NR2B-subunit inhibitor Ro-25-698, an ifenprodil-like compound (Meddows et al., 2001). The ABD binds the agonist glycine on NR1- and NR3-subunits and glutamate on NR2-subunits
Additionally, this domain binds competitive antagonists such as 2-amino-5-phosphonopentanoic acid (AP-5) (Paoletti and Neyton, 2007). The TMD lines the pore region of NMDA receptors where Mg^{2+} and channel blockers such as dizocilpine (MK-801) permeate to block channel conductance. Finally, the CTD is

located intracellularly and is important in protein interactions (Paoletti and Neyton, 2007).

As mentioned above, NMDA receptor subunit assemblies alter the pharmacokinetics of NMDA receptors (Paoletti and Neyton, 2007; Traynelis et al., 2010). NR2-subunit types, in particular, have a ~50 fold range of decay times in the order NR2A< NR2B<NR2C<NR2D, with decay time constants of NR1/NR2D lasting between 4-5 seconds (Cull-Candy and Leszkiewicz, 2004). Furthermore, Mg^{2+} sensitivities differ amongst the subunits and correlate with Ca^{2+} permeability and channel conductance. Consequently, NR2A/B subunits have higher conductance states and Ca^{2+} permeability, but show much higher Mg^{2+} sensitivity than NR2C and NR2D subunit containing receptors. While it remains unclear whether or not NR3 subunits form functional channels in the absence of NR2 subunits, expression systems have identified these receptors to lack Mg^{2+} sensitivity and are virtually impermeable to Ca^{2+} (Henson et al., 2010; Pachernegg et al., 2012).

NMDA receptor subunit regional and developmental expression profiles

Subunit distribution is both regionally and developmentally regulated. Being obligatory to functional NMDA receptors, the NR1 subunit is expressed throughout the brain at all stages of development. During early development, NR2B subunits are the primary subunits expressed throughout all brain regions, but its high level of expression is maintained only the forebrain areas throughout adulthood. NR2A receptor expression, on the other hand, progressively

increases to high levels of ubiquitous expression. The expression profiles of these subunits are established by postnatal day (P) 21 and are maintained into adulthood. NR2C and NR2D have a more restricted expression pattern. NR2C subunit expression increases at P7 into adulthood, but its strongly expressed only in the cerebellum. While NR2D expression occurs throughout the brain, expression drops dramatically throughout development and during adulthood remains limited to the brainstem and diencepehlon (Lujan et al., 2005; Monyer et al., 1994; Paoletti, 2011). NR3A subunit expression has been quite contradictory and may be region specific. In most nuclei studied to date, expression increases markedly to peak between P4-P10, when expression decreases again to a low level adult expression, although notably in the amygdala peak expression seems to occur in adult mice (Henson et al., 2010; Wong et al., 2002). NR3B subunits on the other hand progressively increase their expression, which they maintain throughout adulthood, and virtually everywhere in the CNS (Henson et al., 2010; Paoletti, 2011; Wee et al., 2008). Some of these expression changes have been shown to correlate with critical periods in development of the central nervous system. It has therefore been proposed that the differences in kinetic properties of the receptor subunits aid in establishing and maintaining neuronal circuits during early development and into adulthood, respectively (Paoletti P, Zhou, 2013). Neuronal activity patterns are thought to be a crucial determinant in these processes (Bellone and Nicoll, 2007). As a result, subunit expression changes have been studied in various disorders of the CNS, and such changes have been

identified in a wide array of diseases including diabetes (Di Luca et al., 1999; Lau and Zukin, 2007; Paoletti et al., 2013).

NMDA receptors in the context of synaptic plasticity

Synaptic plasticity is the process by which the central nervous system establishes and refines the circuitry between nuclei of the brain. Long-term potentiation (LTP) and long term depression (LTD), to strengthen and weaken synaptic contacts respectively, are two of the most widely studied mechanisms of synaptic plasticity (Bliss and Lomo, 1973; Citri and Malenka, 2008). These mechanisms are thought to underlie learning and memory processes (Bliss and Lomo, 1973).

Experimentally, high frequency stimulation (HFS) or pairing protocols were recognized to trigger the induction of LTP, while prolonged low frequency stimulation resulted in the induction of LTD. Both of these mechanisms were prevented through the inhibition of NMDA receptors (Collingridge et al., 1983; Dudek and Bear, 1992). The realization that both of these mechanisms, resulting in opposing levels of synaptic strength, were NMDA dependent intensified the search for the underlying mechanisms. It became apparent that NMDA receptors act as coincidence detectors as a result of their unique biophysical properties dependent on both ligand and voltage dependent gating. Consequently, a robust presynaptic stimulation, and concomitant glutamate release, is needed to activate postsynaptic α-Amino-3-hydroxy-5-methyl-4-isoxazolepropionic acid (AMPA) receptors and produce membrane depolarization conducive to Mg^{2+} expulsion from the pore of NMDA receptors. Permeation of Ca^{2+} through Ca^{2+}

permeable NMDA receptors were subsequently shown to underlie signaling mechanism essential to LTP and LTD. The Ca^{2+} concentrations and the temporal profile of Ca^{2+} flux is believed to underlie the reason distinct signaling pathways favoring either LTP or LTD are activated (Malenka et al., 1989). Whereas LTP requires Ca^{2+} flux above a critical threshold, LTD is triggered by a modest influx of Ca^{2+} (Cummings et al., 1996; Malenka and Nicoll, 1993). One of the established signaling molecules involved in triggering LTP is the Calcium/calmodulin (CaM)-dependent protein kinase II (CaMKII) (Barria et al., 1997; Fukunaga et al., 1995). The prominent opinion of LTD induction holds that it is dependent on phosphatase activity including that of calcineurin, subsequently acting on the protein kinase A and C (PKA and PKC) (Hrabetova and Sacktor, 1996; Kameyama et al., 1998; Lisman, 1989)

In LTP, these signaling cascades potentiate the insertion of AMPA receptors and their subunits into the postsynaptic density (PSD). The insertion and/or subunit exchange of AMPA receptors into the postsynaptic density can lead to both the strengthening and unsilencing of synaptic contacts (Durand et al., 1996; Malenka and Nicoll, 1997). As a result, the cell can respond more robustly to presynaptically released glutamate (Benke et al., 1998; Citri and Malenka, 2008). LTP induced AMPA insertion into the PSD is believed to occur within one hour of LTP induction, but LTP is also thought to initiate more long term changes that lead to the restructuring and stabilization of the newly organized synapse (Reymann and Frey, 2007; Thomas and Huganir, 2004). In

LTD, AMPA receptor removal leads to an overall weakening of the synapse (Citri and Malenka, 2008).

NMDA receptor-dependent receptor trafficking has established itself as an important process in synaptic plasticity. Receptor localization in relation to the PSD, and in effect presynaptic release sites, plays an important role in the level of glutamate available for binding. Synaptic receptors opposing the presynaptic terminal directly receive glutamate released preteriminally and consequently are more readily activated. Perisynaptic receptors are located just outside the PSD and are generally thought to be activated as a result of glutamate spillover from the PSD due to increased excitatory neurotransmission. The role of extrasynaptic NMDA receptors remains controversial. One argument is that they may serve as receptor reserve pools and aid in the trafficking of AMPA receptors. Additionally, other studies have identified that these receptors respond to ambient glutamate outside and maintain a tonic NMDA current (Lau and Zukin, 2007; Sanz-Clemente et al., 2013).

While NMDA receptors play a crucial role in synaptic plasticity during development, pathological insults can lead to dysfunctional NMDA receptor subunit expression, trafficking and localization. The disruption of these processes has been demonstrated in a wide array of pathologies including pain, Alzheimer's disease, Parkinson's disease and depression as well as diabetes (Artola et al., 2005; Paoletti et al., 2013). Long-term diabetes is associated with cognitive impairments as well as abnormalities in brain structure and their activation (Artola, 2008).

The link between cognitive decline and memory formation in the hippocampus spawned an interest in studying the effect diabetes and the ability to induce mechanism of synaptic plasticity such as LTP and LTD (Artola, 2008). Using the streptozotocin (STZ) model of Type 1 diabetes (T1-diabetes), it was originally thought that prolonged hyperglycemia may nearly abolish the ability to induce HFS or pairing dependent LTP while producing larger LFS dependent LTD (Chabot et al., 1997; Kamal et al., 1999). More recently, additional studies have revealed that both LTP and LTD are of comparable magnitude in T1-diabetic animals, but that the membrane threshold for their induction is shifted leftward in LTP and rightward in LTD (Artola et al., 2005). In this model the subunit composition of NMDA receptors has been shown to be altered along with expression of CaMKII (Di Luca et al., 1999). Overall, these studies provide compelling evidence that disruption in energy homeostasis can have profound influences on synaptic circuitry.

A large body of literature comes from the study of LTP and LTD in hippocampal circuits where the original studies into their mechanisms were conducted, but both forms of long-term synaptic plasticity have been identified in many other regions of the brain (Citri and Malenka, 2008). Additionally, non-NMDA dependent forms of long term synaptic plasticity, in particular metabotropic glutamate receptor (mGLUR) and endocanabanoid-mediated LTD (eCB-LTD) have been identified throughout the brain (Bolshakov et al., 1997; Gerdeman et al., 2002; Oliet et al., 1997). Studies of eCB-LTD identified a close

link between endocannabonoid and NMDA signaling, including presynaptically mediated mechanisms (Sjostrom et al., 2003).

Presynaptic NMDA Receptors

While NMDA receptors have classically been implicated in their involvement of postsynaptic membrane depolarization, their presence and significance on presynaptic terminal membranes has begun to emerge more recently. The first evidence of preterminal NMDA (preNMDA) came from immunohistochemical approaches that identified NMDA protein expression patterns consistent with their localization on the preterminal membrane in the hippocampus (Aoki et al., 1994). Following this discovery, their functional significance as facilitators of glutamate release at hippocompal synapses was established (Berretta and Jones, 1996). A newly found appreciation for NMDA receptors at the preterminal membrane spawned an interest in their functional significance in other regions of the CNS, which quickly lead to the identification in a number of other nuclei, including the visual cortex and spinal cord (Glitsch and Marty, 1999; Sjostrom et al., 2003). To date, NR2A, NR2B as well as NR3 subunits have been identified to be present on preNMDA receptors in various regions of the brain (Bidoret et al., 2009; Casado et al., 2002; Larsen et al., 2011; Yang et al., 2006). Some of these studies revealed that preNMDA receptors also act as heteroreceptors by facilitating the release of GABA (Glitsch and Marty, 1999).

In cerebellar nuclei, preterminal depolarizations can result from voltage-gated calcium channel activation elicited through electrotonic spread of NMDA-

mediated dendritic depolarization (Christie and Jahr, 2008), suggesting that postsynaptic NMDA receptor activation can elicit effects on presynaptic terminals. This view, however, is challenged not only by electrophysiological evidence but by light and electron microscopic imaging studies localizing NMDA receptors to axon terminals in several forebrain regions (Aoki et al., 1992; Aoki et al., 1994; Bidoret et al., 2009; Charton et al., 1999; Woodhall et al., 2001; Yang et al., 2006; Zhang et al., 2009).

Neurotransmitter release is Ca^{2+} dependent and short term facilitation is thought to be the result of residual Ca^{2+} that remains bound to release sites (Katz and Miledi, 1968, Kamiya, Zucker RS 1998, Bertram 1997). The hypothesis that the increase of preterminal Ca^{2+} through the influx of Ca^{2+}-permeable preNMDA receptors was experimentally confirmed by Chochilla and Alford (1999). These results have been expanded upon to show indirect activation through local depolarizations that open voltage-gated Ca^{2+} channels and potentiation of Ca^{2+}-dependent Ca^{2+} release via ryanodine receptors (Lanore et al., 2010).

As the functional significance of preNMDA receptors became solidified, their involvement in synaptic plasticity during development and in the context of pathological states was investigated. Not long after their discovery their involvement in epilepsy was identified, mediating an NR2B increase in the tonic facilitation of glutamate (Yang et al., 2006). NR3-subunit containing receptors established themselves as crucial players in developmental processes of the visual cortex while preNMDA mediate LTD induction in the cerebellum and neocortex (Casado et al., 2002; Larsen et al., 2011).

NMDA receptor and their physiological significance in the DVC

In the brainstem all of the known NMDA receptor subunits (except NR3As) have been shown to exist and undergo developmental expression pattern similar to those seen elsewhere in the brain (Liu and Wong-Riley, 2010). On a physiological level, NMDA receptors in the DVC have been linked to a variety of gastrointestinal responses. Specifically activation of NMDA receptors through the injection of NMDA or glycine, via bilateral guide cannulas implanted in the DVC, resulted in a decrease of gluconeogenesis (Lam et al., 2010). This agonist response could be inhibited though with NMDA receptor antagonists or vagotomy. Using this approach it was further identified that activation of NMDA receptors is necessary to process hypothalamically initiated signals to lower gluconeogenesis (Lam et al., 2011; Lam et al., 2010). Inhibition of NMDA receptors has also been shown to prevent the food intake reduction normally elicited by hormones such as cholecystokinin (Wright et al., 2011). These studies demonstrate the critical role NMDA receptors play in modulating energy homeostasis in the DVC and questions what role they play under pathological insults such as diabetes.

Glutamatargic neurons and their identification

The NTS is composed of a heterogeneous population of neurons, with inhibitory GABAergic and excitatory glutamatergic neurons as the two predominant populations (Lin and Talman, 2006; Travagli et al., 1991a). Vesicular release of glutamate requires vesicular glutamate transporters

(VGLUTs) that use a H^+ electrochemical gradient to transport glutamate from the cytoplasm into presynaptic vesicles (Santos et al., 2009). To date, three VGLUT isoforms, VGLUT 1-3, have been identified (Herzog et al., 2001; Herzog et al., 2004; Werner et al., 1998). These proteins differ in their localization throughout the central nervous system. For instance, in the NTS both VGLUT2 and VGLUT3 show significant expression in neurons and do not appear to co-localize (Lin et al., 2004; Lin and Talman, 2005). VGLUT1 expression is observed on afferent terminals and sub regions of the NTS, but its expression is much lower (Hermes et al., 2013; Lin, 2009) The expression of VLGUTs has been widely used as a marker for glutamatergic neurons (El Mestikawy et al., 2011; Fremeau et al., 2004; Santos et al., 2009). In the context of these studies VGLUTs are important for phenotypic identification of glutamatergic neurons.

Study Aims and Significance

Metabolic disorders, diabetes in particular, are posing an unprecedented societal burden throughout the developing world. The involvement and pathological effects on the central nervous system are becoming increasingly well established. The mechanisms underlying changes in the synaptic circuitry within the CNS of diabetics are only beginning to be elucidated; and it remains unclear whether or not these changes are reversible.

The DVC plays a critical role in energy metabolism, and has thus become a region of interest in the involvement in the development of metabolic disorders. Studies in this laboratory were previously conducted in STZ-induced T1-diabetic mice and revealed an increased excitatory drive to DMV neurons (Zsombok

2011). This study revealed that under conditions of chronic hyperglycemia and/or hypoinsulemia DMV neurons are hyperexcited. The previously observed increase in mEPSC and sEPSC frequency suggests that changes mediating hyperexcitability occurrs presynaptic to DMV neurons.

Presynaptically released glutamate activates AMPA- and NMDA-receptors on the postsynaptic membrane. A change in the frequency of EPSCs, in the absence of a change in amplitude, whole cell currents and/or decay time, is indicative of a presynaptic change of glutamate release. Presynaptic changes in glutamate release could be the result of changes in the number of synaptic contacts and/or changes in the probability of glutamate release.

Increases in sEPSCs target mechanisms to changes at the soma-dendritic and/or presynaptic terminal membrane of presynaptic neurons. Miniature excitatory post synaptic currents (mEPSCs) are action potential independent events dependent on the stochastic release of glutamate release (Kandel et al., 2000). The observed increase in mEPSC frequency in diabetic mice suggests that synaptic plasticity that changes the are at least in part due to changes occurring at terminals contacting DMV neurons.

NMDA receptors play an important role in glucose homeostasis in the DVC and are amongst the most widely studied receptors in the context of synaptic plasticity throughout the central nervous system (Lam et al., 2011; Traynelis et al., 2010). Thus, they are likely candidates to show functional modulation and contribute to the enhanced excitatory neurotransmission of the DMV in T1-diabetic mice.

Although preNMDA receptors and their involvement in mechanisms underlying physiological and pathological changes in synaptic plasticity have been identified in other regions of the CNS, their presence and functional significance to synaptic circuitry have never been explored in the DVC. Chapter 3 of this dissertation was aimed at identifying the presence and functional significance of preNMDA receptors on terminal contacts of DMV neurons.

Chapter 4 of this dissertation focuses on NMDA receptors in the DVC of T1-diabetic mice. The increase in sEPSC frequency in diabetic mice suggested that presynaptic neurons alter their function to enhance action potential dependent release. NTS neurons form functional glutamatergic connections with the DMV; and excitability in these neurons could trigger an increase in the release of glutamate. It was hypothesized that NMDA receptors are unregulated in presynaptic NTS neurons of T1-diabetic mice. Given that excitatory neurotransmission was altered in T1-diabetic mice, it was hypothesized that NMDA receptors were upregulated, particularly in the glutamatergic subpopulation of neurons. This hypothesis was tested by using single-cell PCR approaches to correlate NMDA-mediated electrophysiological responses to a glutamatergic phenotype (VGLUT2+ neurons).

The studies conducted throughout this dissertation were aimed at advancing the understanding of the rules governing neuronal excitatory, transmission between nuclei of the DVC and their ability to undergo synaptic plasticity in a model of T1-diabetes. An increase in this excitatory efferent output could serve as counter-regulatory mechanism to lower gluconeogenesis in

response excessive glucose concentrations induced by diabetes. Understanding the mechanisms involved in this process could eventually pave the road to developing therapeutic strategies for pathological perturbations of diabetes and other metabolic disorders.

Chapter 2: Materials and Methods

Animal Injections and monitoring

Adult (3-12 weeks) female and male CD-1 (Harlan Laboratories) or GIN mice (FVB-Tg (GadGFP) 4570Swn/J; The Jackson Laboratory) were used for all experiments. Experiments in Chapter 3 investigating the presence and functional significance of preNMDA receptors on terminal contacts to DMV neurons were conducted in male CD-1 mice exclusively. Experiments in Chapter 4 and 5 investigated changes in T1-diabetic mice also used both male and female GIN mice. The effects on T1-diabetic mice were observed specifically on excitatory neurotransmission presynaptic to DMV neurons. Consequently, mechanistic changes were hypothesized to occur in presynaptic glutamatergic neurons. A mouse strain expressing a fluorescent tag in glutamatergic neurons was unavailable to target recordings specifically to the glutamatergic NTS neuronal population. The best of alternative was to use the FVB-Tg (GadGFP) 4570Swn/J to prevent recording from the somatostatin expressing GABA neuron population. These neurons make up a large population of cells in the NTS and preventing recordings from this population increased the probability of recording from a glutamatergic neuron. As part of the studies conducted in Chapter 4 a glutamatergic phenotype was confirmed using single-cell PCR (see RNA isolation and Taq-Man PCR description). All animals were treated and cared for in accordance with National Institutes of Health guidelines, and all procedures

were approved by the Institutional Animal Care and Use Committee of the University of Kentucky.

Intra-peritoneal injections of 200mg/kg (either a single dose or in 5 doses of 40 mg/kg each over 5 days) of streptozotocin dissolved in saline (0.9% NaCl) were performed on normoglycemic mice. Prior to injections and/or fasting (saline injected animals were fasted for 4-6 hours) plasma glucose concentrations were measured using a Nova Max® PLUS glucometer. Based on the limitations of the glucometer, glucose levels could only be quantitatively determined up until blood glucose levels of 600 mg/dl and higher blood glucose concentrations were reported by the glucometer as high. The glucose levels table for diabetic animals (see appendix 2), therefore, are semiquantitative averages that designated all reading of high as 600 mg/dl and reported averages presumably are underestimations of the true average. Before and following fasting mice were provided food without restriction. Blood samples were obtained via tail prick and blood glucose measurements from saline and streptozotocin injected animals were taken daily until streptozotocin injected mice reached blood glucose levels of 300 mg/dL or above for at least three days. Mice with blood glucose levels of 300 mg/dL were considered T1-diabetic mice and animals that maintained hyperglycemic states for a minimum of 7 and up to 10 days were used for electrophysiological and molecular studies. Saline injected animals were never observed to reach blood glucose levels consistent with this level of hyperglycemia. The final glucose measurements were taken on the day mice were used sacrificed for experimental aims (animal treatments are outlined in

Table 1 of the Appendix). The weight of all mice was monitored and animals were excluded from further experiments if their weight dropped by more than 20% of their original body weight.

Brain stem slice preparation

Whole cell patch-clamp recordings were made using brainstem slices prepared from mice. Mice were deeply anesthetized by halothane inhalation to effect and then decapitated. The brain was removed and blocked on an ice-cold stand and the brainstem was glued to a sectioning stage using a small amount of crazy-glue® on a vibrating microtome (Vibratome Series 1000; Technical Products, St. Louis, MO). The entire brainstem was fully covered with ice-cold artificial cerebrospinal fluid (ACSF). Slices (300 µM) were cut at low vibrating microtome speed but high cutting amplitude. Transverse (i.e. coronal) brain stem slices (300 µm) from about 300 µm rostral to AP to the caudal edge of AP containing the DVC were made in cold (0–2°C), oxygenated (95% O_2-5% CO_2) ACSF using a vibrating microtome (Vibratome Series 1000; Technical Products, St. Louis, MO). The ACSF contained (in mM): 124 NaCl, 3 KCl, 2 $CaCl_2$, 1.3 $MgCl_2$, 1.4 NaH_2PO_4, 26 $NaHCO_3$, 11 glucose (pH 7.2–7.4; osmolality 290–315 mOsm/kg). Slices were then incubated for ≥1 h in warm (32–35°C) oxygenated ACSF.

Electrophysiological Recordings

For recording, a single brain slice was transferred to a chamber mounted on a fixed stage under an upright microscope (Model BX51WI; Olympus, Melville, NY), where it was continually superfused with warmed oxygenated ACSF.

Experimental drugs were added to perfusate via a pump. Prior to drug application the time to reach the bath chamber was measured in order to more accurately assess the time of drug activation.

Whole-cell voltage-clamp recordings were obtained in the DMV or NTS using recording pipettes pulled from borosilicate glass (open tip resistance of 3–5 MΩ; King Precision Glass Co., Claremont, CA). The pipette solution for most recordings contained (in mM): 130–140 Cs-gluconate , 10 HEPES, 1 NaCl, 1 $CaCl_2$, 3 CsOH, 5 EGTA, and 2 Mg^{2+}-ATP. Intracellular Cs^+ was used as the primary cation carrier in voltage-clamp recordings to block K^+ currents, including $GABA_B$ receptor-mediated currents in the recorded neuron. Neurons were targeted for recording under a 40x water-immersion objective (numerical aperture = 0.8) with infrared-differential interference contrast (IR-DIC). Electrophysiological signals were obtained using a Axopatch 200B or Multiclamp 700B amplifier (Molecular Devices, Union City, CA), low-pass filtered at 2 or 3 kHz, digitized and recorded onto a computer (Digidata 1440A, Molecular Devices) using pClamp 10.2 or 10.3 software (Molecular Devices). Seal resistance was typically 2–5 GΩ and series resistance, measured from brief voltage steps applied through the recording pipette (5 mV, 5 ms), was typically <25 MΩ and monitored periodically during the recording. Recordings were discarded if series resistance changed by >20% over the course of the experiment.

Electrical stimulation

Electrical stimulation was performed using a platinum-iridium concentric bipolar electrode (125 μm diameter, FHC, Bowdoinham, ME) placed in the medial NTS (Browning and Travagli, 2009; Glatzer et al., 2007). A minimum of 15 paired current pulses (2–100 μA; 300 μs; A.M.P.I., Jerusalem, Israel) at interpulse intervals of 30 ms and a cycle rate of 0.1 Hz were administered to the NTS, and responses in DMV neurons voltage-clamped at −80 mV were recorded and analyzed for current amplitudes before, during, and after the application of AP-5. The ratio of the second to the first response was measured to assess changes of paired-pulse ratios (PPr) in response to AP-5. Paired-pulse ratios can give an indication of the release probabilities of neurotransmitter release. Changes in PPr are indicative of a change in presynaptic release properties, with an increase in the ratio correlating to a decrease in the release probability (Debanne et al., 1996; Dobrunz et al., 1997; Dobrunz and Stevens, 1997). In connections in the DVC arising from the NTS and projecting to the DMV a paired pulse depression, consistent with high release probabilities, has been observed at inter-stimulus- intervals of 30-40 ms (Browning and Travagli, 2003; Williams et al., 2007). To measure current responses at membrane potential between -110 to +30 mV, voltage steps were applied at 10 mV increments. Steps were of 1 second duration to reach maximal current responses for each voltage measured. Incremental current step were made at inter-step-intervals of 400 ms. Current measurement were averages of four runs and were measured at each potential at the end of the voltage step. A current-voltage response graphs was

extrapolated from these measurements and compared between control and T1-diabetic mice.

Drugs used for electrophysiological recordings

The drugs and their respective concentrations, used for experiments were: Tetrodotoxin (TTX; 1-2 µM; Alomone Labs) DL-2-Amino-5-phosphonopentanoic acid (AP-5; 100 µM, Sigma), *N*-methyl-D-aspartic acid (NMDA; 15 µM; Sigma), Ro 25-6981 (1 µM; Tocris), $ZnCl_2$ (5 µM; MP Biomedicals), (-)-Bicuculline methiodide (Bic; 30 µM; Sigma) or picrotoxin (PTX; 100 µM, Sigma) d-tubocurarine chloride (DTC 10-20 µM; Sigma), Strychnine (1-2 µM; Tocris), Org 24598 (10 µM; Tocris), ALX-1393 (0.5 µM, Tocris), Glycine (30 µM,100 µM,300 µM,1000 µM, Fisher), 6-Cyano-7-nitroquinoxaline-2,3-dione (CNQX; 10 µM, Sigma), -(+)-5-Methyl-10,11-dihydro-5H-dibenzo[a,d]cyclohepten-5,10-imine hydrogen maleate (MK-801; 1mM, Sigma) and Bumetanide (10-20 µM; Tocris).

RNA isolation

Two to three brainstem slices (300-600 µm) were isolated as described for electrophysiological recordings. The DVC was carefully excised and tissue sample and suspended in 400-500 µL of TRIzol® and gently shaken periodically for 5-25 min. 100-250 µl of chloroform was added the tubes vortexed for 15 sec and maintained at 4ºC for 20 min or incubate them 2-3 min at RT and subsequently centrifuged at 12,000 rpm for 10-15 min at 4ºC. RNA supernatant was transferred into fresh 1.5 ml centrifuge tubes and suspended in 500 µL of ice-cold propanol. Resuspended samples were incubated at room temperature for 10 minutes and subsequently centrifuged at 12,000 rpm for 10 min at 4ºC.

Propanol was decanted and RNA was washed by resuspension in 500 µL 75% EtOH followed by centrifugation at 7500-12,000 rpm for 10 min at 4ºC. This wash step was repeated, the EtOH decanted. RNA samples were air-dried for 10-20 min. RNA samples were resuspended in 8-10 µL RNAse-free water and stored at -80 ºC or immediately reverse transcribed into cDNA. When obtaining single-cell mRNA the cytosol of the cell was aspirated into the recording pipette The recording pipette carefully pulled away from the cell and its contents were expelled into a sterile centrifuge tube. RNA was stored at -80 ºC or immediately reverse transcribed into cDNA.

TaqMan PCR

RNA samples were reverse transcribed in Reverse-Transcription Master Mix (1 µl random nonamers (50 uM) (Sigma), 5 µl MMLV RT buffer (5x) (Fisher), 5 µl dNTPs (10 mM) (ThermoScientific), 2 µl DEPC-treated H2O (Fisher), 1 µl Reverse Transcriptase (Fisher), and 1 µl RNAse Inhibitor (Fisher). For single-cell RT-PCR experiments, the cytosol was aspirated following electrophysiological recordings and suspended in RNA Reverse-Transcription Master Mix without enzymes and stored at -80 ºC until further use. Groups of cells were reverse transcribed after the addition of 1 µl Reverse Transcriptase (Fisher), and 1 µl RNAse Inhibitor (Fisher) in a thermocycler (Eppendorf Mastercycler) at 42ºC for 90 min followed by 5 min at 95ºC. For phenotype identification, positive controls (tissue samples) and single cells were probed for the presence of β-actin and VGLUT2. Primers and probes for β-actin were: fwd, CAGCAGGTACAGCATCACGG; rev, GCCATGTACGTAGCCATCC; probe,

CTGGTCGTACCACAGGCATTGTG; for VGLUT2: fwd, CCCGTCTACGCGATAATTGTT; rev, GTCATGACAAGGTGAGGGACT; Probe, ACTGCTCATCAGCCAGCTT and for GAD67: fwd, CCGTTCTTAGCTGGAAGCAG; rev, GTCTTGTGAGCGCCTTCAG; Probe, CCGGCGCACAGAGACCGACTTCT.

Mastermix containing 3 µl (β-actin) or 2 µl (VGLUT2) MgCl2 (25 mM), 2.4 µl PCR buffer (10x), 1 µl dNTPs (10 mM), 1 µl primers/probe (10 uM), 0.5 DNA polymerase and 14 µl was prepared and 3 µl of single cell or positive control RNA or RNAse free sterile H_2O (non-template control) loaded into optical tubes or a 96-well plate (Bio Rad). Samples were centrifuged for 2 min at 1000 RPM and placed in an ABI-Thermocylcer for PCR analysis. Samples were held at 95 ºC 2 min and cycled 50 times at 95 ºC for 30 s, 60 ºC for 15 s and at 72º C 15 s.

NanoString

To measure quantitative changes in mRNA expression between control and T1-diabetic mice, the NanoString® nCounter® system was used. The NanoString technology bridges the gap between measuring a few to a few dozens of genes using traditional qPCR and genome wide microarray studies by allowing the analysis of up to 800 genes. The multiplex capability of this technology allows genes to be assayed in a single reaction with as little as 100 ng of total RNA (Geiss et al., 2008; Kulkarni, 2011). The sensitivity achieved using the NanoString matches that of TaqMan based PCR and surpasses microarray sensitivity. NanoString does not require enzymatic amplification steps which can introduce experimental bias (Geiss et al., 2008; Malkov et al., 2009).

Sequences are detected though the use of 2 sequence specific probes (reporter and capture probe) for each gene detecting a total of around 100 contiguous base-pairs. The reporter probe carries a six-tiered barcode of non-overlapping fluorescent colors, each assigned to a gene of interest. RNA samples are mixed together with buffers and an excess of probes and the reaction is fully automated from this point forward. In short, the initial step allows the hybridization of probes to target sequences. Next, the capture probe, with its biotin labeled 3' end facilitates the capture and immobilization to streptavidin-coated slides. The excess probes are washed away and the color codes are counted (Kulkarni, 2011). More recently the technology has been adapted to allow detection at the single cell level and samples from paraffin embedded samples. To achieve a single cell detection sensitivity of 10 pg of total RNA an additional enzymatic amplification of RNA (Multiplexed Target Enrichment) step is added to the overall procedure.

A custom designed codeset was designed by and purchased from NanoString technologies (for complete list see Appendix 4). This codeset included the seven known NMDA receptor subunits (NR1, NR2A-D and NR3A-B) as well as four housekeeping genes (beta-actin, GAPDH, Hprt1, Ubc). The isolated RNA quality assessment and concentration determination was made at the University of Kentucky using the Agilent's Bioanalyzer 2100. The average RNA integrity number (RIN) for samples used in this study were 9.4 ± 0.07 (Range: 8.9-9.7). 100 ng of total RNA was used from each sample. Hybridization reaction using the custom designed codeset, and nCounter® master mix, was

performed according to protocol by the microarray facility at the University of Kentucky using the nCounter® from NanaString® Technology. The NanoSting probe identifiers for genes analyzed throughout this dissertation were: For NR1: NM_008169.2:492, for NR2A: NM_008170.2:4080, for NR2B: NM_008171.3:6340, for NR2C: NM_010350.2:2720, for NR2D: NM_008172.2:1201, for NR3A: NM_001033351.1:1332, for NR3B: NM_130455.2:2030, for beta-actin: NM_007393.3:1138, for GAPDH: NM_001001303.1:890, for Hprt1: NM_013556.2:30, for Ubc: NM_019639.4:21. For a more complete list of probes included in these analyses refer to Appendix 2. Normalization was performed using the nSolver™ software from NanoString® Technology. The nSolver® software normalizes to negative and positive controls to eliminate background noise and variability unrelated to samples. To calculate the normalization factor of these controls the geometric mean (geometric mean= $\sqrt[n]{x^1 x^2 \dots x^n}$) of each sample is obtained. Subsequently, to account for variability between samples the geometic mean of samples is taken. This average is divided by individual sample specific geometric means to calculate a normalization factor, which is multiplied by sample specific counts. Normalization of endogenous control genes, is subsequently conducted, on counts normalized to positive and negative controls using the same workflow of normalization used for positive and negative controls.

Western Blots

Brainstem slices (300-600 µm) were isolated as described for electrophysiological recordings. The DVC was isolated and sections were

immediately transferred to 40-60 µl of lysis buffer consisting of 0.15M NaCl, 5mM EDTA (pH 8), 1% Triton X-100, 10mM Tris-Hcl (pH 7.4), 10ul/ml of 100mM PMSF (174.2 mg/10ml in methanol), and 100ul/ml of 0.5M NaF (pH 10). Each sample was sonicated and centrifuged immediately at 12,000 RPM for 3 min. Supernatant was aspirated, aliquoted, and stored at -80 ºC until further use. Protein concentration was measured using a Bradford Protein Assay. For Western blots, 20 µg of protein was loaded per lane. The appropriate volume of sample together with equal amounts of loading buffer were boiled in water for 2 min. Samples and ladder were loaded into precast PDF gels in and subsequently the gel was electrophoresed at 50 mA for 45–80 min. Proteins were then transferred at 200 mA for 2 hrs onto polyvinylidene difluoride membranes for Western blot analysis. Membranes were blocked in 1:1 Odyssey blocking buffer/PBS/0.1% Tween 20 for 1 hr at room temperature. Due to well separated molecular weights of the NR1 (band at 105-120 kD) and β-actin (band at 40-45 kD) protein membranes could be cut in half to be incubated over-night at 4°C, with a rabbit monoclonal anti-NMDAR1 (1:1000; Abcam) and a rabbit monoclonal anti-β-actin (1:10000; Abcam) antibody in Odyssey blocking buffer/PBS/0.1% Tween 20. Membranes were washed with 4 times 5 min with PBS on a shaker. After the final wash membranes were scanned on a densitometer (Odyssey model 9120, Li-COR Biosciences) to quantify band density. Background density was subtracted from the NMDAR1 band density and normalized to β-actin, which was used as a loading control.

Statistical analysis

For electrophysiological recordings, an n was defined as an individual neuron that was recorded from. For some of the experimental groups within this dissertation, multiple neurons where recorded from a single animal. In all experimental groups at least three animals were used to validate that the observed responses were not due to an abnormal animal's response. The glycine transport inhibitor study of T1-diabetic mice is an exception. Since studies of potential preterminal glycine and NR3-subunit containing NMDA receptors were not completed the glycine transport inhibitor study was halted and included only two mice for preliminary results presented in this dissertation.

Spontaneous and miniature postsynaptic currents (PSCs) were analyzed with MiniAnalysis (Synaptosoft) to measure the peak amplitude, frequency, and decay time. Spontaneous or miniature synaptic events (minimum 65; typically 2-min continuous recording) were measured within a recording under each condition. Intra-assay analysis of drug-evoked changes in spontaneous and miniature PSC frequency and amplitude within a recording were assessed using a Kolmogorov-Smirnov test.

For electrical simulations, evoked responses were analyzed using pClamp. Peak amplitudes from a minimum of 15 evoked responses were averaged and measured for each treatment. To attain a paired-pulse response ratio, the ratio of the amplitude of the second to the first EPSC response to afferent stimulation was calculated. The primary effect was on the first amplitude

and paired-pulse recordings were therefore normalized to the amplitude of the second response.

Pooled results of single comparisons of drug effects (i.e., before and after a single drug treatment) were analyzed using a paired, two-tailed Student's *t*-test. When comparing pooled effects of a single variable between two animal groups (comparison between untreated controls or saline injected controls and streptozotocin injected mice) a homoscedastic two-tailed Student's t-test was used. In studies between animals, in which a variable based on a drug response was introduced, a two-way Anova was employed to test for statistical significance. Identifying percent changes as a function of drug application consolidated frequency responses into a single variable and a two-tailed homoscedastic Student's t-test could therefore be used to compare responses between animal groups. The nature of responses through western blot analysis and paired-pulse ratios did not produce normally distributed responses.
As a result, a non-parametric Wilcoxon signed-rank test was, therefore, used to test for statistical significance.

Statistical significance for all measures was set at $P < 0.05$. Statistical measurements were performed with Microsoft Excel (Microsoft, Redmond, WA) or Prism (GraphPad Software, La Jolla, CA). Numbers were expressed as means ± SE.

Chapter 3- Presynaptic NMDA receptor-mediated modulation of excitatory neurotransmission in the mouse dorsal motor nucleus of the vagus

Introduction

Studies conducted in this chapter were aimed at gaining a better understanding of the circuitry within the DVC; more specifically presynaptic modulation of excitatory and inhibitory neurotransmission on terminals contacting DMV neurons.

While NMDA receptors typically contribute to postsynaptic conductances, their role as presynaptic receptors that modulate neurotransmitter release from synaptic terminals is receiving increased attention, and various subunit combinations have been identified at preterminal receptors (Corlew et al., 2008; Engelman and MacDermott, 2004; Ma and Hargreaves, 2000; MacDermott et al., 1999). Presynaptic glutamate receptors, possibly including NMDA receptors, contribute to glutamatergic heterosynaptic facilitation of GABA release onto DMV neurons (Derbenev et al., 2006), but the sub-type of glutamate receptor mediating this enhanced release is not known. Metabotropic glutamate receptors have been identified previously to contribute to modulation of both excitatory and inhibitory neurotransmission in the DMV (Browning and Travagli, 2007).

These findings are consistent with the hypothesis that glutamate released in the DMV can regulate synaptic transmission by acting at receptors on afferent terminals. Presynaptic NMDA receptors, and their potential role in contributing to

facilitation of fast excitatory and/or inhibitory neurotransmission have not been adequately studied in the DVC.

This study aimed to identify the presence of presynaptic NMDA receptors in the DMV and their functional relevance as modulators of excitatory and/or inhibitory neurotransmission.

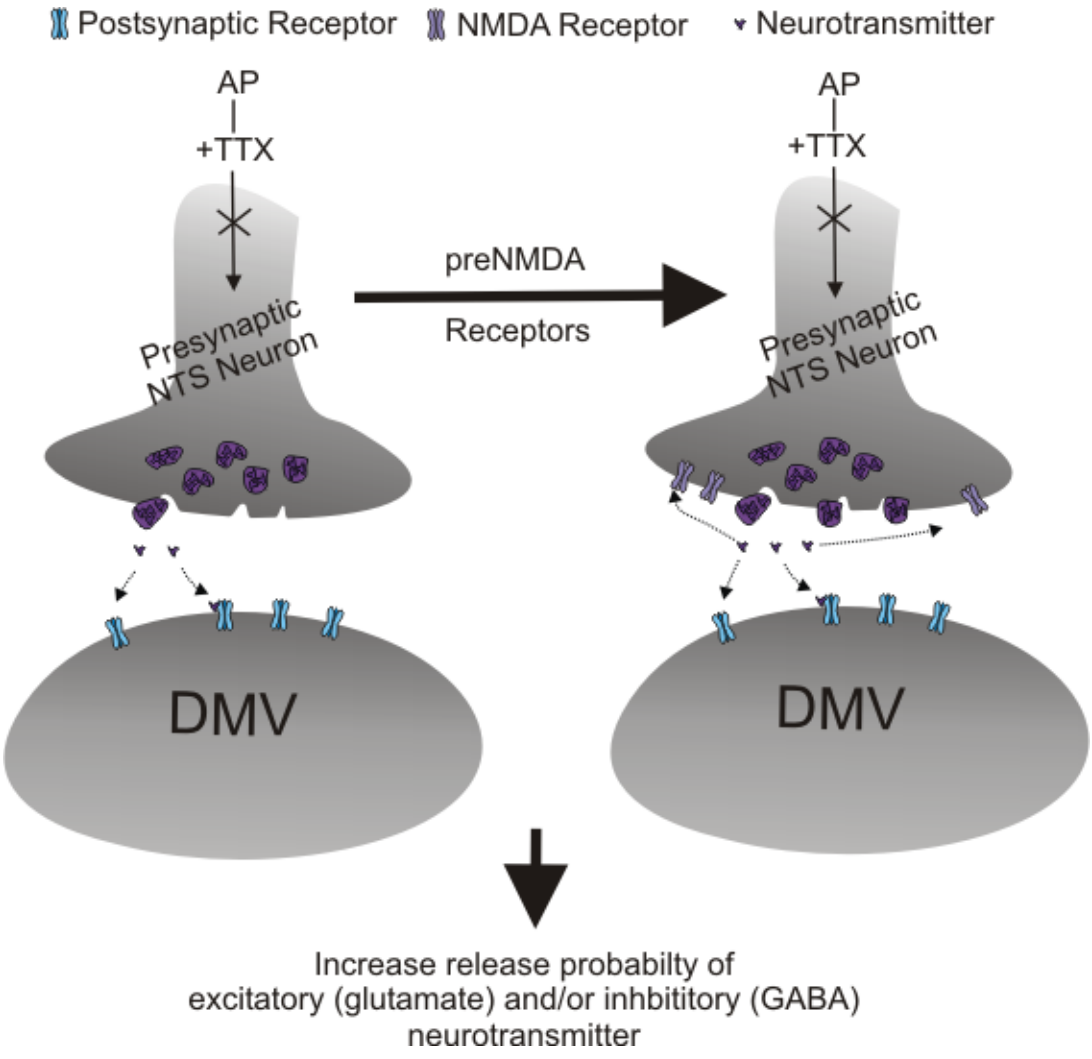

Figure 3. 1 Schematic representation of preNMDA mediated facilitation of neurotransmitter release of NTS terminals contacting DMV neurons.

Methods

Only methods and materials specific to this Chapter are restated here. To avoid redundancy refer to Chapter 2 of this dissertation, when indicated.

Animals

Male CD-1 mice (Harlan, Indianapolis, IN), 4–11 wk of age, were housed under a standard 14-h light 10-h dark cycle, with food and water provided without restriction. All animals were treated and cared for in accordance with National Institutes of Health guidelines and all procedures were approved by the Institutional Animal Care and Use Committee of the University of Kentucky.

Brain stem slice preparation- see general methods in Chapter 2

Electrophysiological recording- see general methods in Chapter 2 for complete methods. Seal resistance was typically 2–5 GΩ and series resistance, measured from brief voltage steps applied through the recording pipette (5 mV, 5 ms), was typically <25 MΩ (mean=13.03±0.86 MΩ) and monitored periodically during the recording. Recordings were discarded if series resistance changed by >20% over the course of the experiment.

Drugs used for electrophysiological recording- For specific experiments, DL-2-Amino-5-phosphonopentanoic acid (AP-5; 100 µM), *N*-methyl-D-aspartic acid (NMDA; 15 µM), Ro 25-6981 (1 µM), $ZnCl_2$ (5 µM), or picrotoxin (PTX; 100 µM; Sigma, Ellisville, MO) were added to ACSF. When indicated, -(+)-5-Methyl-10,11-dihydro-5H-dibenzo[a,d]cyclohepten-5,10-imine hydrogen maleate (MK-801; 1 mM) was added to the pipette solution to block postsynaptic NMDA receptors in the recorded cell. Inadvertent ejection of MK-801 during acquisition of patch-clamp recordings was unavoidable, and such leakage could result in inconsistent

blockade of receptors. Such blockade was predicted to affect responses to low levels of glutamate released endogenously in the slice, so MK-801 was added to the recording pipette for agonist application experiments only. Intracellular Cs^+ was used as the primary cation carrier in voltage-clamp recordings to block K^+ currents, including $GABA_B$ receptor-mediated currents in the recorded neuron.

Electrical Stimulation- Electrical stimulation was performed using a platinum-iridium concentric bipolar electrode (125 µm diameter, FHC, Bowdoinham, ME) placed in the medial NTS (Browning and Travagli, 2009; Glatzer et al., 2007). A minimum of 15 paired current pulses (2–100 µA; 300 µs; A.M.P.I., Jerusalem, Israel) at inter-pulse intervals of 30 ms and a cycle rate of 0.1 Hz were administered to the NTS and responses in DMV neurons voltage-clamped at -80 mV were recorded and analyzed for current amplitudes before, during, and after the application of AP-5.

Data analysis - For electrical stimulation, peak amplitudes from a minimum of 15 evoked responses were averaged and measured for each treatment using pClamp programs and analyzed using a paired, two-tailed Student's t-test. Paired-pulse response ratios, taken as the ratio of the amplitude of the second to the first EPSC response to afferent stimulation resulted in non-normal disctributed ratios. Based on the fact that these ratios incorporated two normally distributed populations of amplitudes (first and second amplitude) a non-

parametric statistical was deemed appropriate. Ratios were analyzed using a non-parametric Wilcoxon signed-rank test.

Results

Blocking NMDA receptors decreased tonic excitatory input to DMV neurons

Electrophysiological recordings were made in voltage-clamp mode in the presence of PTX (100 μM) and TTX (1-2 μM) using Cs^+ intracellularly to block K^+ currents. At a membrane potential of -80 mV, postsynaptic NMDA receptors in DMV neurons are under substantial voltage-dependent Mg^{2+} blockade, reducing the contribution to EPSCs of NMDA receptor activation. By also blocking fast IPSCs with PTX, action potential propagation with TTX, and K^+ channels with intracellular Cs^+, the effect of the NMDA receptor antagonist AP-5 was targeted to presynaptic effects of glutamate release acting on AMPA mediated mEPSCs. Bath application of AP-5 (100 μM) resulted in an average 31.1 ± 5.7% decrease in mEPSC frequency (n=9), from a baseline frequency of 12.4 ± 3.6 events/s to 8.3±2.5 events/s in AP-5 ($p<0.05$; Fig. 3.2). Application of AP-5 did not result in a significant change in amplitude (19.8 ± 1.8 pA baseline; 19.2±1.5 pA AP-5; $p=0.21$) or decay time constant (1.6 ± 0.1 ms baseline; 1.6 ± 0.9 ms AP-5; $p=0.43$) of mEPSCs. The decrease in mEPSC frequency in response to AP-5, in the absence of a change in amplitude or decay time, suggested that AP-5 inhibited glutamate release by acting at receptors located on presynaptic terminals.

In cortical neurons, NMDA receptors located on presynaptic terminals have been reported to contain NR2B subunits (Woodhall et al., 2001; Yang et al.,

2006). To test the hypothesis that NR2B-containing receptors modulated glutamate release in the DMV, the NR2B antagonist Ro 25-6981 (1 μM) was applied under conditions identical to those used for AP-5 experiments. No change was observed in frequency (14.5 ± 2.9 events/s baseline; 16.8 ± 3.7 events/s Ro 25-6981; p=0.10; n=11), amplitude (19.5 ± 1.8 pA baseline; 17.4 ± 2.3 pA Ro 25-698; p=0.28) or decay time (1.8 ms baseline; 2.0 ms Ro 25-6981; p=0.06; Fig. 2). Since NR2A subunit-containing NMDA receptors have also been identified at presynaptic terminals (Bidoret et al., 2009), we tested for the presence of this subunit using $ZnCl_2$. Application of $ZnCl_2$ (5 μM) resulted in a significant decrease in mEPSC frequency from 15.5 ± 2.9 events/s to 11.6 ± 2.2 events/s in the presence of $ZnCl_2$ (n=8; $p<0.05$). No change in amplitude (19.6 ± 1.6 pA baseline; 20.0 ± 2.3 pA $ZnCl_2$; p=0.48) or decay time constant (1.7 ± 0.2 ms baseline; 1.8 ± 0.2 ms $ZnCl_2$; p= 0.45) was observed (Fig. 3.3.)

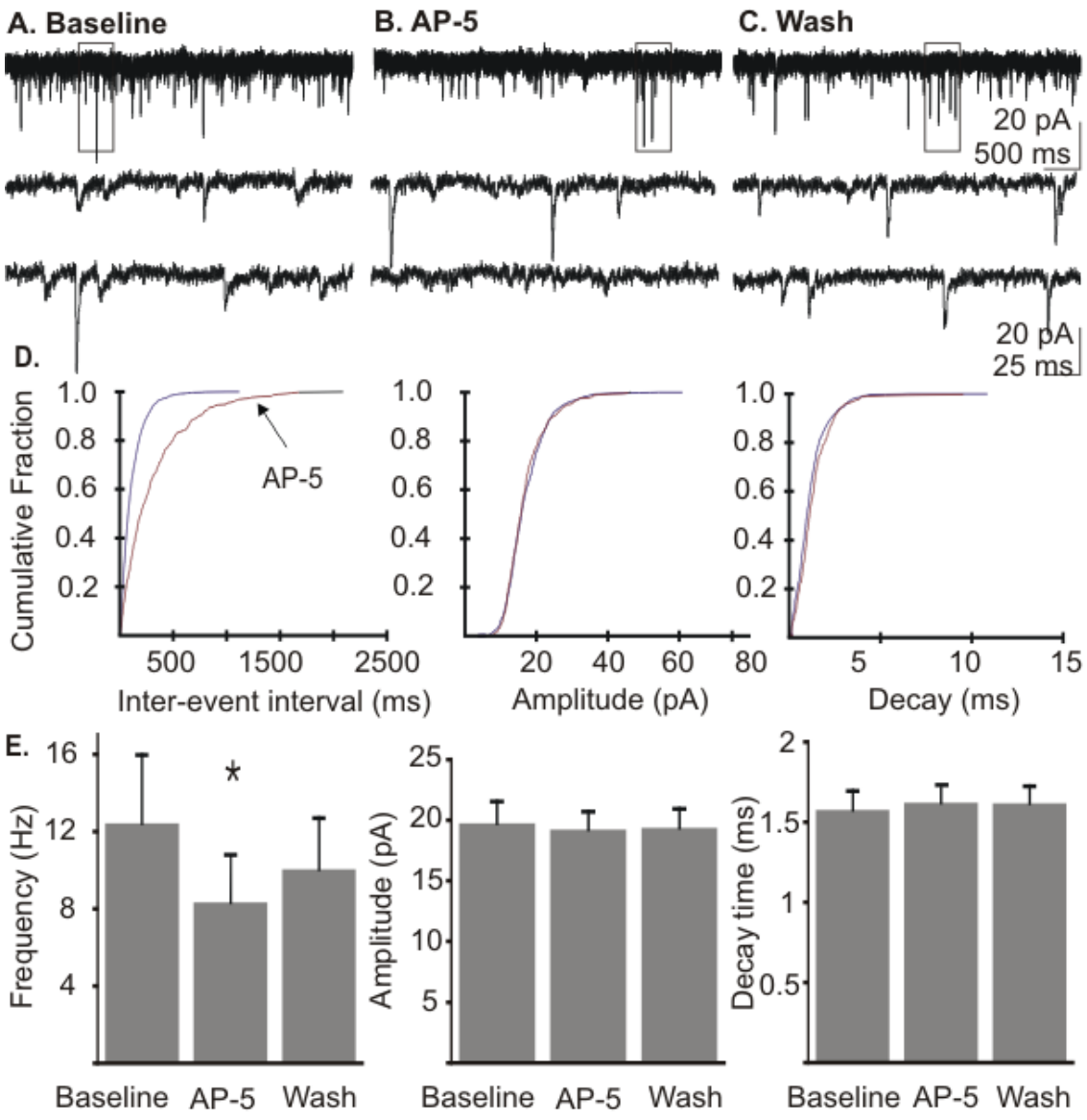

Figure 3. 2 Blockade of NMDA receptors decreased mEPSC frequency without changing amplitude or decay time constant.

A. Representative recording of mEPSCs in a DMV neuron. **B**. Recording of mEPSCs from the same neuron during the application of AP-5 (100 μM; 10 min application). **C**. Recording from the same neuron during wash of control ACSF (i.e., no AP-5). Boxed areas in **A**-**C** are shown expanded temporally below each

trace. **D**. Cumulative probability plots of mEPSC frequency, amplitude, and decay time constant for the neuron represented in **A-C**. **E**. Mean mEPSC frequency, amplitude and decay time constant before and during the application of AP-5 (n=9; asterisk indicates significant difference from control established through the use of a paired two-tailed Student's t-test; $p<0.05$).

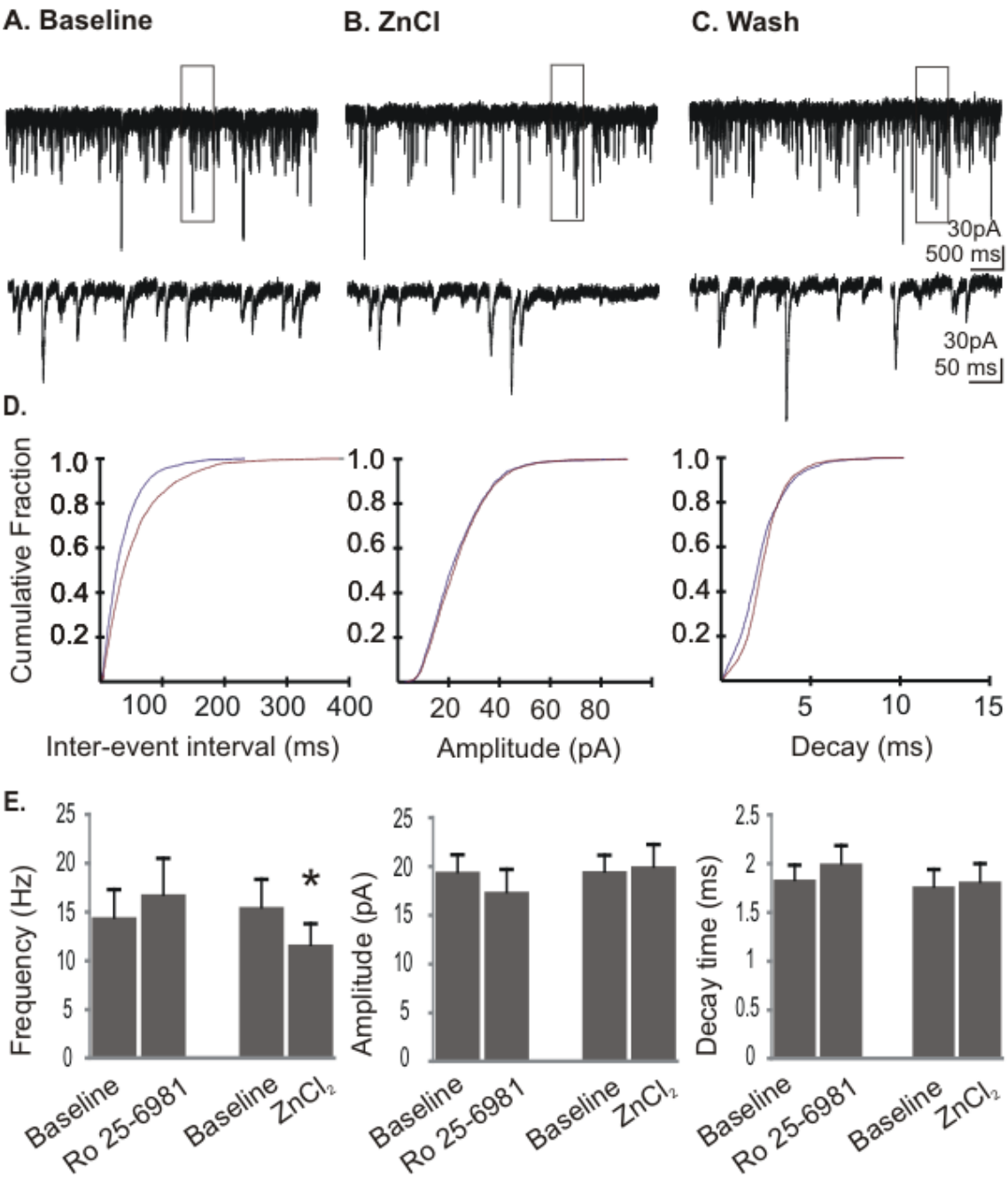
A. Baseline
B. ZnCl
C. Wash
30pA
500 ms
30pA
50 ms
D.
Cumulative Fraction
1.0
0.8
0.6
0.4
0.2
100 200 300 400
Inter-event interval (ms)
20 40 60 80
Amplitude (pA)
5 10 15
Decay (ms)
E.
Frequency (Hz)
Amplitude (pA)
Decay time (ms)
*
Baseline
Ro 25-6981
Baseline
ZnCl2

Figure 3. 3 Application of Ro 25-6981 did not change frequency, amplitude or decay time of mEPSC, while $ZnCl_2$ application decreased mEPSC frequency without changing amplitude or decay time constant.

A. Representative recording of mEPSCs in a DMV neuron. **B**. Recording of mEPSCs from the same neuron during the application of $ZnCl_2$ (5 μM; 15 min application). **C**. Recording from the same neuron during wash to control ACSF. Boxed areas in **A**-**C** are shown expanded temporally below each trace. **D**. Cumulative probability plots of mEPSC frequency, amplitude, and decay time constant for the neuron represented in **A-C**. **E**. Mean mEPSC frequency, amplitude and decay time constant before and during the application of $ZnCl_2$ (n=8) or Ro 25-6981 (1 μM; n=11); asterisk indicates significant difference from control using a paired two-tailed Student's t-test; $p<0.05$.

NMDA facilitates glutamatergic release onto DMV neurons

When bath applying the receptor agonist NMDA at the previously described concentration of 15μM, MK-801 was included in the intracellular solution in order to permeate and block postsynaptic NMDA receptors from within the cell (Berretta and Jones, 1996; Glitsch and Marty, 1999). Neurons were first depolarized to 0 mV for 5 min to facilitate blockade of the receptor pore (Berretta and Jones, 1996). Following this initial depolarization, the membrane was repolarized to a holding potential of -80 mV for recording EPSCs in the presence of PTX and TTX. Consistent with the MK-801 blockade of postsynaptic NMDA receptors, application of NMDA (15 μM) did not induce a significant changes to whole cell holding currents in response to AP-5 (-3.0± 5.1 pA in response to

NMDA), nor was mEPSC amplitude (20.0± 2.0 pA baseline; 20.1 ± 2.1 pA NMDA; p=0.87) or decay time (1.8± 0.2 ms baseline; 1.7± 0.2 ms NMDA; p=0.70) altered (Fig. 3.4). However, NMDA application resulted in a significant increase in mEPSC frequency (27±4.7%), from 10.8 ± 2.9 events/s before and 14.4 ±3.3 events/s during NMDA application (n=6; $p<0.05$; Fig. 3). The increase in mEPSC frequency in absence of a change in whole-cell current or mEPSC amplitude or decay time constant implied that NMDA augmented glutamate release by acting at presynaptic terminals.

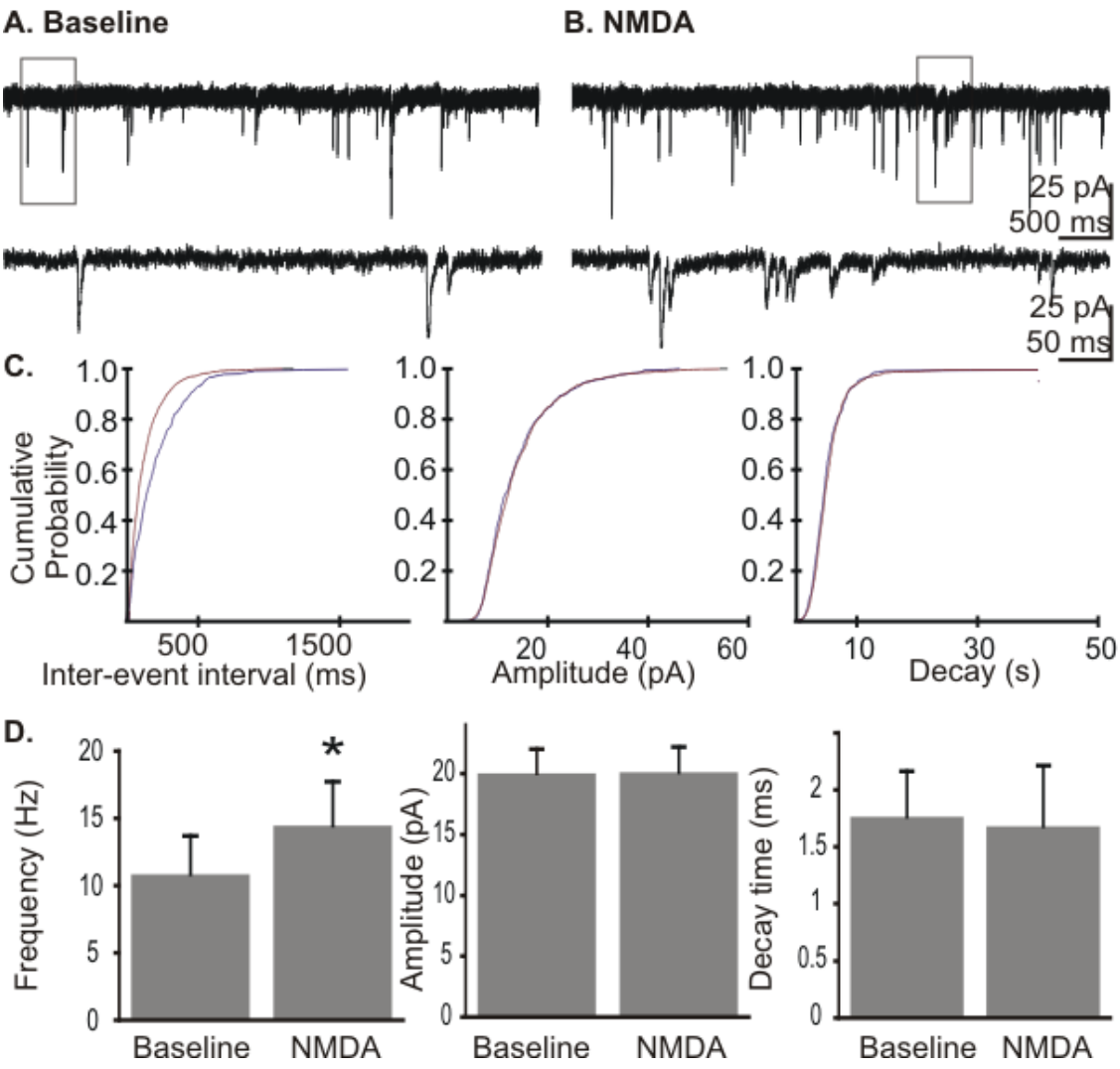

Figure 3. 4 NMDA application increased mEPSC frequency without changing amplitude or decay time.

A. Representative recording of mEPSCs in a DMV cell in control ACSF. **B**. Recording of mEPSCs during the application of NMDA (10 μM). Boxed areas in **A** and **B** are shown expanded below each trace. **C**. Cumulative probability plots of mEPSC frequency, amplitude, and decay time constant for the cell represented in A and B. **D**. Average mEPSC frequency, amplitude, and decay time constant before and during the application of NMDA (n=6; asterisk indicates

significant difference from control using a paired two-tailed Student's t-test; $p<0.05$). Pipette solution contained MK-801 (1 mM).

Electrical stimulation

Paired electrical stimuli (30ms interstimulus interval) were delivered to the NTS at 0.1 Hz and resulting paired evoked EPSC (eEPSC) amplitudes were recorded in DMV neurons in the presence of picrotoxin at -80 mV. Paired stimulation of the NTS resulted in eEPSCs that typically displayed prominent paired pulse depression of the second response. The average amplitude of the first eEPSC was significantly decreased following application of AP-5 (90 ± 10pA baseline; 51 ± 6 pA AP-5; $p<0.05$), without a significant change in the amplitude of the second response (61 ± 6 pA baseline; 53 ± 5 pA AP-5; $p=0.29$; Fig. 3.5). This greater relative effect on the first EPSC amplitude resulted in a decrease in paired-pulse depression, which was reflected in an increase in the paired-pulse ratio (PPr; 0.7 ± 0.1 baseline and 1.2 ± 0.3 in the presence of AP-5; $n=9$; $p<0.05$). The change in PPr induced by AP-5 was consistent with activity at receptors located on presynaptic terminals and suggested a reduction in the ongoing activity of endogenously activated NMDA receptors.

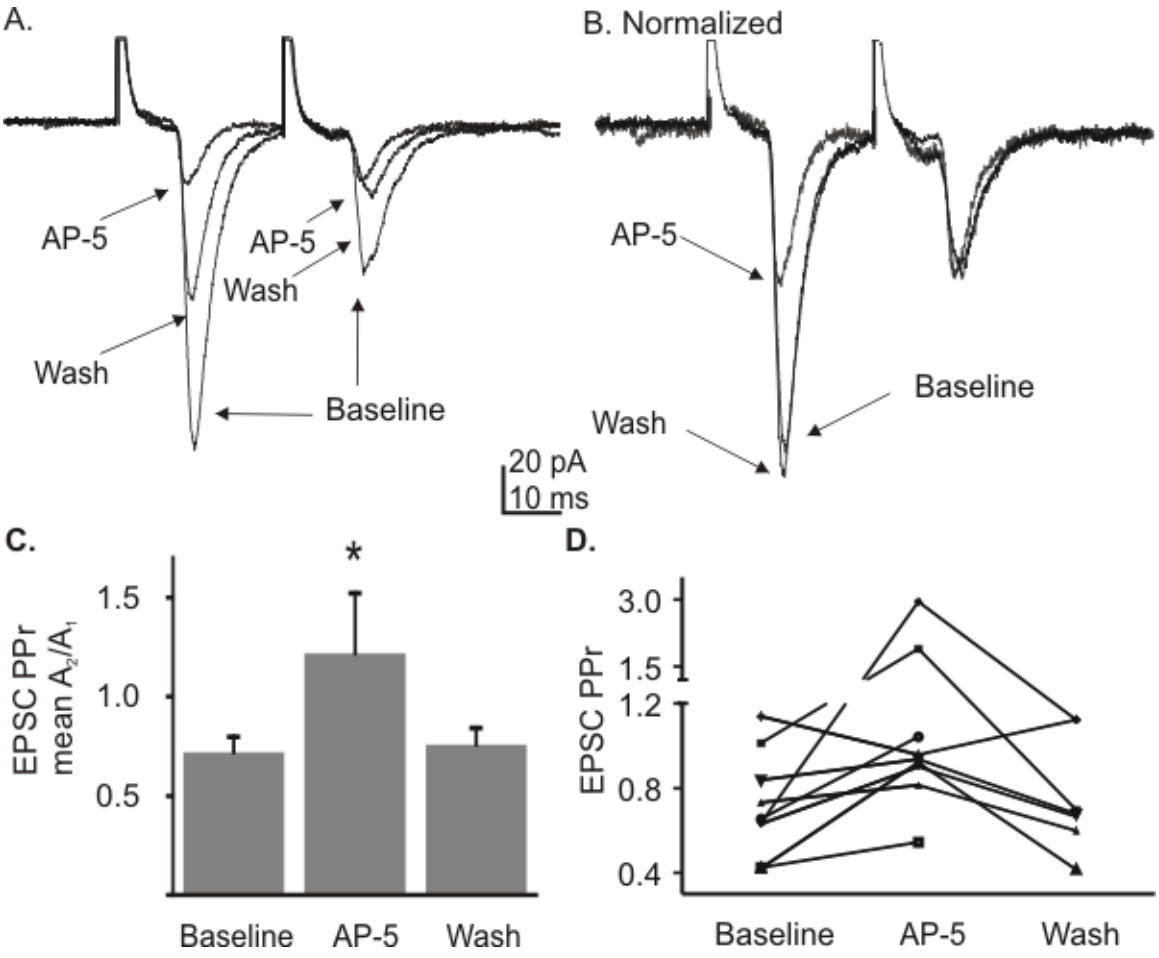

Figure 3. 5 NMDA receptor blockade induced a decrease in the amplitude of EPSCs evoked after NTS stimulation and an increase in PPr.

A. Paired electrical stimulation of the NTS in control ACSF, AP-5 (100 μM), and 15 min after removal of the antagonist indicated in a decrease in evoked EPSC amplitude during drug application. Averages of 15 responses are shown for each condition. **B**. Averaged evoked EPSCs (normalized to the amplitude of the second response in **A**) before, during, and after the application of AP-5 indicated the antagonist induced a greater decrease in the first response amplitude than the second. **C**. Mean paired-pulse ratio for control, AP-5, and wash indicates a

significant increase in PPr using a Wilcoxon signed-rank test (P>0.05; n=9). **D**. The PPr of individual cells shows the increase in PPr by AP-5 application in 8 out of 9 cells tested.

NMDA receptor modulation did not affect IPSCs

Activation of ionotropic glutamate receptors enhances GABA release from synaptic terminals in the DMV (Derbenev et al., 2006). The hypothesis that presynaptic NMDA receptor activation increases GABA release was tested by recording mIPSCs in voltage clamp mode at a holding potential of 0 mV in the presence of TTX and intracellular Cs^+. The mean mIPSC frequency (1.0 ± 0.3 events/s baseline; 1.0 ± 0.3 events/s NMDA; p=0.94), amplitude (26.1 ± 1.7 pA baseline; 25.2 ± 2.7 pA NMDA; p=0.95), and decay time constant (7.0 ± 0.6 ms baseline; 7.3 ± 0.6 ms NMDA; p=0.50) were not changed following the application of NMDA (15μM; n=7; 3.6.). Likewise, blockade of NMDA receptors with AP-5 (100 μM; n=7) did not alter mIPSC frequency (2.9 ±0.8 events/s baseline; 2.2 ± 0.8 events/s AP-5; p=0.922), amplitude (30.6 ± 2.7 pA baseline; 31.6 ± 3.2 pA AP-5; p=0.97), or decay time constant (8.6 ±0.7 ms baseline; 8.5 ±0.6 ms AP-5; p=0.94; Fig 3.7.). These results suggested that activation or blockade of NMDA receptors on GABA terminals did not consistently alter synaptic GABA release onto DMV neurons.

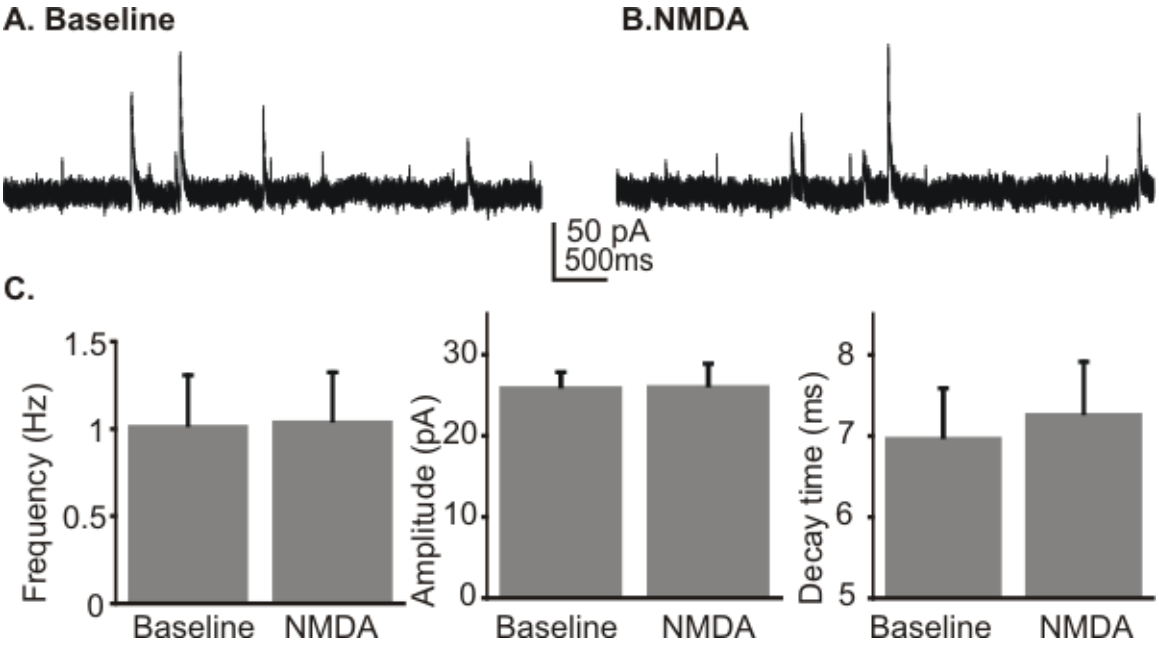

Figure 3. 6 Effect of NMDA application on mIPSCs was not significant.

A. Representative baseline recording of mIPSCs. **B**. Recoding of mIPSCs in the presence of NMDA (15 μM). **C**. Average frequency, amplitude, and decay time constant of mIPSCs in response to NMDA indicated no significant mean changes using a paired two-tailed Student's t-test ($P>0.05$; $n=7$). Pipette solution contained MK-801 (1 mM).

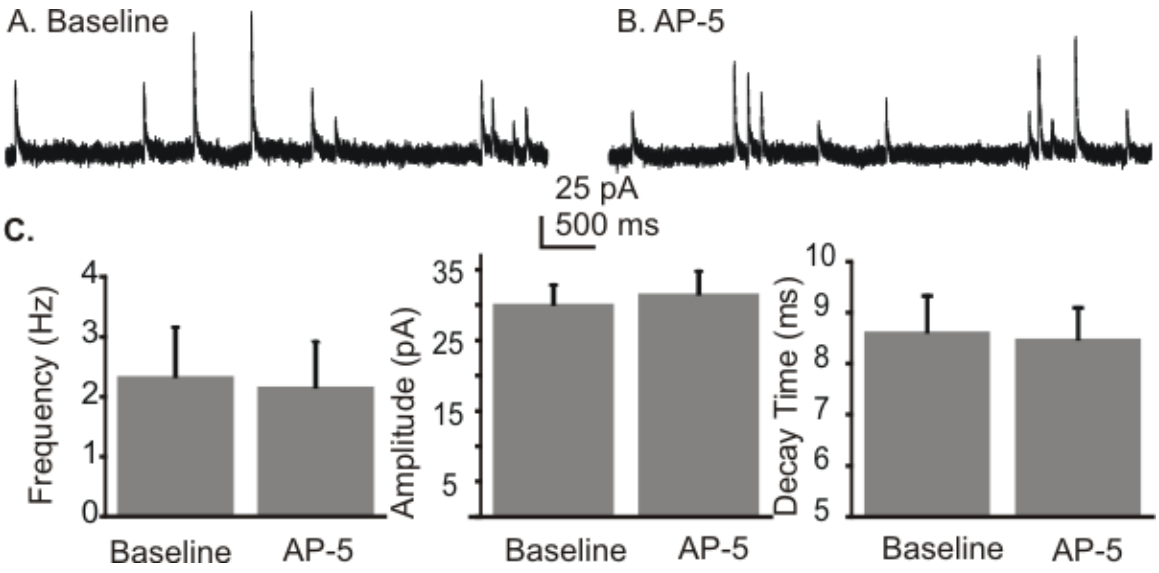

Figure 3. 7 NMDA receptor blockade was without effect on mIPSCs.

A. Representative baseline recording of mIPSCs. **B**. Representative recordings of mIPSCs in the presence of AP-5 (100 μM). **C**. Average frequency, amplitude and decay time constant of mIPSCs in response to AP-5 indicated no significant mean changes using a paired two-tailed Student's t-test ($P>0.05$; $n=7$).

Discussion

A goal of this study was to provide evidence supporting the presence and function of NMDA receptors on presynaptic terminals contacting DMV neurons in the DVC. In other brain regions, including the hippocampus and the neocortex, presynaptic NMDA receptors have been found to function as autoreceptors to facilitate the release of glutamate (Berretta and Jones, 1996; Brasier and Feldman, 2008), participating in increasing excitatory synaptic tone (Woodhall et al., 2001). Presynaptic NMDA receptors located on GABAergic terminals have

also been found to function as heteroreceptors to enhance the release of GABA (Duguid and Smart, 2004; Mathew and Hablitz, 2011; Sjostrom et al., 2003). Given these disparate functions of presynaptic NMDA receptors and the existing evidence for glutamatergic modulation of GABA release in the DVC (Browning and Travagli, 2007; Derbenev et al., 2006), this study was further aimed at identifying their putative function on synaptic activity in the DVC. Effects of NMDA receptor activation and antagonism on mEPSCs and paired evoked responses to afferent stimulation were consistent with the presence of NMDA receptors on glutamate terminals in the DMV.

A change in the frequency of action potential-independent (miniature) synaptic currents, in the absence of a change in the amplitude or decay time constant, suggests an NMDA receptor-mediated modulation of neurotransmitter release from presynaptic terminals. The decrease in mEPSC frequency in response to AP-5 or Zn^{2+}, in the absence of a change in mEPSC decay time constant or amplitude, suggests that presynaptic NMDA receptors are activated by ambient glutamate and tonically facilitate excitatory input to DMV neurons. Further, the increase in mEPSC frequency in response to applied NMDA suggests that the receptors are not fully saturated in the slice preparation. Consequently, an increase in presynaptic activity resulting in an increase in preterimal glutamate release could be maintained through preNMDA autoreceptors responses. Physiologically, preNMDA autoreceptors may therefore act as important mediators to facilitate spacio-temporal integration of disparate incoming inputs.

$ZnCl_2$ application resulted in a decrease in mEPSC frequency similar to that of AP-5, while the selective NR2B subunit containing receptor antagonist Ro 25-6981 failed to have an effect on parameters measured. While it remains possible that other subunits, are also present, these data suggest that NMDA receptors on glutamatergic presynaptic terminals in the DMV most likely contain NR2A, but not NR2B subunits, in young adult mice. NR2B and NR1 subunit-containing NMDA receptors are present at birth, but there is a progressive inclusion of NR2A subunits in the first 3-5 weeks of life, after which expression stabilizes (Quinlan et al., 1999; Sheng et al., 1994). Although relative subunit expression may influence NMDA receptor expression differently in immature animals, most animals used in the present study were >5 weeks of age, a time at which NMDA receptor expression is relatively stable.

Blockade of NMDA receptors can reduce the fidelity of synaptic currents evoked subsequent to stimulation of the NTS, and the change in PPr further suggests this occurs subsequent to modulation of NMDA receptors located on presynaptic terminals. The paired-pulse depression observed here and previously (Browning and Travagli, 2003; Browning and Travagli, 2009; Glatzer and Smith, 2005; Williams et al., 2007) suggests a synaptic connection with relatively high release probability, with the second response being of smaller-amplitude due to depletion of the readily-releasable primed pool during the first activated release (Debanne et al., 1996). A change in the PPr is often interpreted to indicate preterminal modulation of neurotransmitter release probability, with an increase in the ratio implicating a decrease in the probability of release (Debanne

et al., 1996; Dobrunz et al., 1997; Dobrunz and Stevens, 1997). Modulation of the amplitude of the first evoked EPSC by NMDA receptor blockade suggests that presynaptic NMDA receptors modulate terminal Ca^{2+} influx tonically. The absence of change in the second amplitude may imply that successive stimuli activate additional Ca^{2+}-permeable receptors, allowing further release of the available vesicular pool.

Tonic activation of presynaptic NMDA receptors to enhance excitatory synaptic input has been suggested in other regions of the brain (Berretta and Jones, 1996; Sjostrom et al., 2003). This autoreceptor-mediated facilitation may serve to enhance the overall gain of the glutamate response at particular synapse locations. As such, presynaptic NMDA receptor modulation could selectively enhance specific signals, for example those arriving from the NTS, as opposed to those arriving from other central areas. In the DMV, satiety signals from diencephalic brain areas converge with inputs arising from NTS neurons relaying specific mechanical or chemical visceral signals pertaining to physiological state, especially from digestive system organs. Modulation of feed-forward glutamate tone via presynaptic NMDA receptors would be expected to increase the gain at active synapses, contributing to both temporal and spatial integration of synaptic signals in the DMV. In effect, appropriately timed central and peripheral satiety signals could thus augment each other by affecting summated glutamate release along specific physiologically relevant synaptic pathways driving central parasympathetic output.

In addition to enhancing glutamate release, presynaptic NMDA receptors have also been found to enhance GABA release in some regions of the brain (Duguid and Smart, 2004; Glitsch and Marty, 1999; Mathew and Hablitz, 2011), and glutamate enhances GABA release in the DMV by acting at ionotropic and metabotropic receptors on presynaptic GABA terminals (Derbenev et al., 2006). GABA neurons are prominent in the medial NTS, which project inhibitory inputs to gastrointestinal-projecting regions of the DMV (Davis et al., 2004; Derbenev et al., 2004; Ferreira et al., 2001; Glatzer et al., 2007; Travagli RA, 1991). Inhibitory input to DMV cells has been found to be modulated through a variety of preterminal receptors, including those for monoamines, catecholamines, peptides, and lipids, in addition to glutamate receptors on GABA terminals (Browning and Travagli, 2007; Derbenev et al., 2006; Glatzer et al., 2007; Travagli and Gillis, 1995; Zsombok et al., 2011). Metabotropic glutamate receptors have been found to serve a complex integrative role to maintain both tonic tone of inhibitory neurotransmission and negatively modulate acitivity-dependent excitatory neurotransmission in synaptic connections between NTS and DMV neurons (Browning and Travagli, 2007). Failure to observe a consistent change in mIPSC frequency in response to NMDA or AP-5 suggests that the glutamatergic heteroreceptors participating in the response of DMV neurons to TRPV1 activation (Derbenev et al., 2006) are likely not predominantly NMDA receptors. It further suggests that glutamatergic terminals with presynaptic NMDA receptors are not in close proximity to heteroreceptors, since the increased glutamate released by presynaptic NMDA receptor activation might be expected

to “spill over” and activate glutamate heteroreceptors on GABA terminals, and consequently increase mIPSC frequency. This was not the case. It remains possible that presynaptic NMDA receptors exist on a subset of GABA terminals, but the absence of any predominant effect on GABA release suggests that presynaptic NMDA receptors are located preferentially on glutamatergic terminals, most likely including those arising from NTS afferents. Thus, activation of presynaptic NMDA autoreceptors may represent a spatially distinct means of selectively augmenting glutamate release in the DMV.

In cerebellar nuclei, preterminal depolarizations can result from voltage-gated calcium channel activation elicited through electrotonic spread of NMDA-mediated dendritic depolarization (Christie and Jahr, 2008), suggesting that postsynaptic NMDA receptor activation can elicit effects on presynaptic terminals. This view, however, is challenged not only by electrophysiological evidence but by light and electron microscopic imaging studies localizing NMDA receptors to axon terminals in several forebrain regions (Aoki et al., 1992; Aoki et al., 1994; Bidoret et al., 2009; Charton et al., 1999; Woodhall et al., 2001; Yang et al., 2006; Zhang et al., 2009). The present results are consistent with the hypothesis that NMDA receptors located at presynaptic terminals regulate synaptic glutamate release in the DMV, since NMDA effects on mEPSCs persisted when the postsynaptic channels were blocked from inside the cell. However, the possibility that NMDA receptors located on dendrites contribute to presynatic modulation via a retrograde signal (e.g., electrotonic depolarization) remains to be explored. In summary, the results obtained in this study suggest

that NMDA receptors are present on presynaptic terminals and their activation positively modulates glutamate release onto DMV neurons, with little effect on GABA release. The presence of presynaptic NMDA receptors on GABAergic terminals cannot be entirely excluded, but if present their physiological function relative to synaptic regulation of DMV neurons is unclear. Presynaptic NMDA receptors on glutamate terminals facilitate the release of glutamate tonically, providing a means of downregulating as well as upregulating glutamate release, depending on ongoing synaptic activity. Their activation may serve to augment specific excitatory synaptic contacts in an autoregulatory fashion, acting to enhance specific inputs in a spatially and temporally distinct manner.

Chapter 4: NMDA receptor modulation of excitatory neurotransmission in the dorsal vagal complex of Type 1 Diabetic mice

Introduction

Chapter 3 of this dissertation established the presence and function of NMDA receptors on terminals contacting DMV neurons to tonically facilitate the release of glutamate, but not GABA, onto this nucleus (Bach and Smith, 2012).

Activating NMDA receptors in the DVC results in decreased gluconeogenesis, while their inhibition suppresses food intake (Lam et al., 2011; Ritter, 2011). NMDA receptor function in the DVC is, therefore, critical for homeostatic regulation of vagal activity and visceral function. Synaptic input to DMV neurons is altered in disease states affecting visceral function, underscoring the importance of understanding synaptic control of these neurons (Zsombok et al., 2011). A tonic elevation in glutamate release was observed previously in the DMV of T1-diabetic mice (Zsombok et al., 2011; Zsombok and Smith, 2009), suggesting a chronic alteration in synaptic regulation of vagal activity. The mechanism/s of this modulation remains to be elucidated. NMDA receptors have been extensively studied for their involvement in modulating synaptic plasticity under physiologic as well as pathologic states.

Changes in NMDA sensitivity in central vagal circuits could contribute to elevated glutamate release in the DVC and subsequent modulation of visceral function associated with diabetes. The hypothesis that plasticity of NMDA receptor function in the DVC of T1-diabetic mice leads to the observed increase

in excitatory neurotransmission was tested. Figure 4.1 shows a schematic illustration of the potential sites of NMDA receptor modulation.

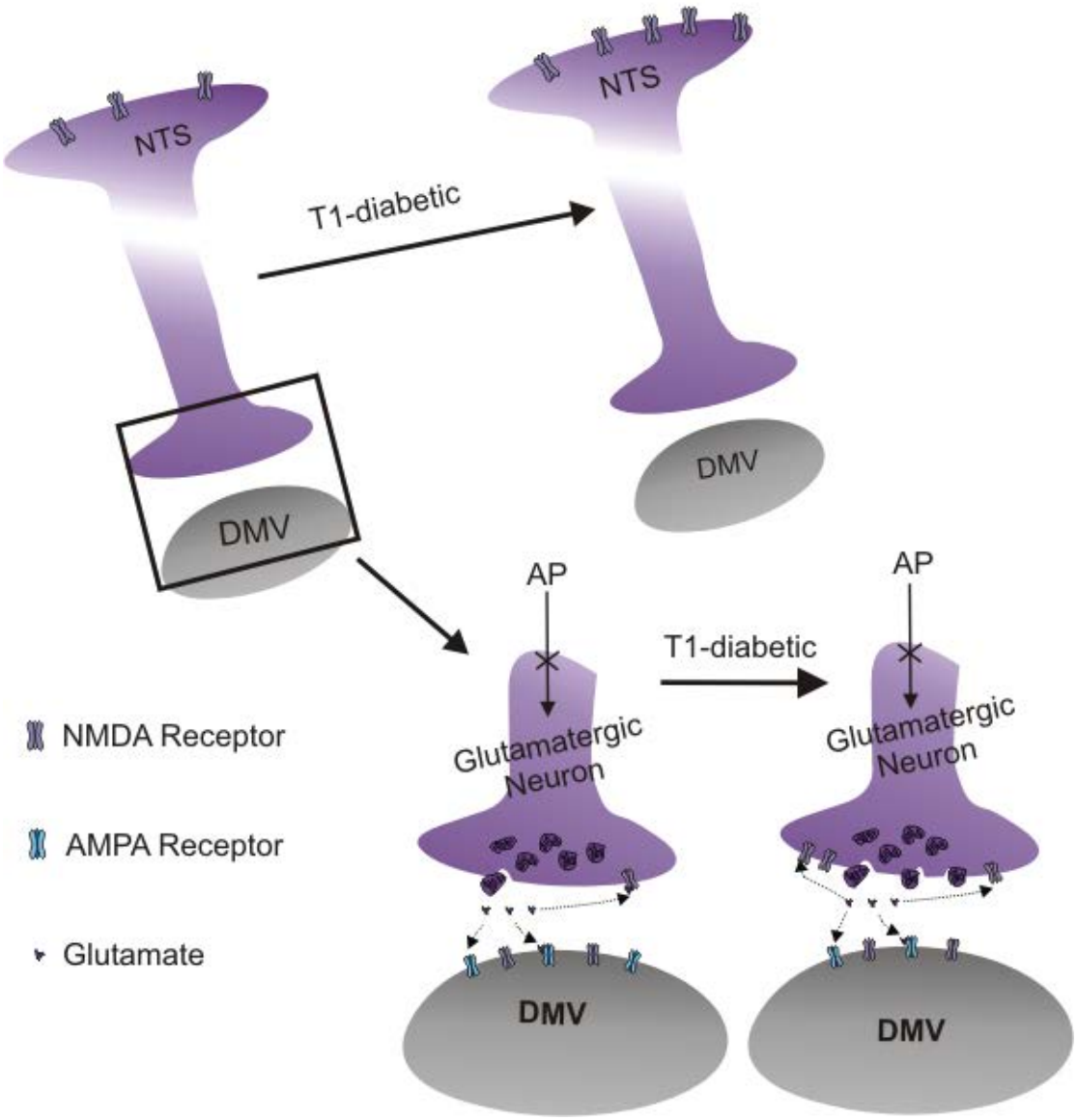

Figure 4.1 Schematic illustration of potential sites of presynaptic NMDA receptor modulation to enhance excitatory neurotransmission to DMV neuron of T1-diabetic mice.

Material and Methods

Animals

Male and female mice CD-1 (Harlan, Indianapolis, IN) and GIN mice (FVB-Tg (GadGFP) 4570Swn/J; The Jackson Laboratory) 4–11 wk of age, were housed under a standard 14-h light/10 h dark cycle, with food and water provided without restriction. All animals were treated and cared for in accordance with National Institutes of Health guidelines and all procedures were approved by the Institutional Animal Care and Use Committee of the University of Kentucky.

Animal Injections

Mice were given intra-peritoneal injections of 200mg/kg (either a single dose or in 5 doses of 40 mg/kg each over 5 days) of streptozotocin. Controls were either injected with saline (0.9% NaCl) or untreated. No differences in electrophysiological parameters were observed between normoglycemic saline-injected and untreated mice. They were therefore pooled and considered as a single control group. Systemic glucose levels were measured prior to injections and monitored daily. Animals were used for electrophysiological recordings and molecular analyses after 7-10 days of persistent hyperglycemia (blood glucose level of above 300mg/dl).

Brain stem slice preparation- refer to general methods of Chapter 2.

Electrophysiological recording- refer to general methods of Chapter 2**.**

The drugs, and their respective concentrations, used for experiments specific to this chapter were: Tetrodotoxin (TTX; 1-2 µM; Alomone Labs) DL-2-Amino-5-phosphonopentanoic acid (AP-5; 100 µM, Sigma), *N*-methyl-D-aspartic acid (NMDA; 15 µM; Sigma), picrotoxin (PTX; 100 µM, Sigma), d-tubocurarine chloride (DTC 10-20 µM; Sigma), Strychnine (1-2 µM; Tocris), 6-Cyano-7-nitroquinoxaline-2,3-dione (CNQX; 10 µM, Sigma). To measure current responses at membrane potentials of at membrane potential of -110 to +30 mV, voltage steps were applied at 10 mV increments. Steps were of 1 second duration to reach maximal current responses for each voltage measured. Incremental current step were made at inter-step-intervals of 400 ms. Current measurement were averages of four runs and were measured at each potential at the end of the voltage step. A current-voltage response graphs was extrapolated from these measurements and compared between control and T1-diabetic mice.

RNA isolation

Two to three brainstem slices (300-600 µm) were isolated as described for electrophysiological recordings. The DVC was carefully excised and tissue sample and suspended in 400-500 µL of TRIzol® and gently shaken periodically for 5-25 min. 100-250 µl of chloroform was added the tubes vortexed for 15sec and maintained at 4ºC for 20 min or incubate them 2-3 min at RT and subsequently centrifuged at 12,000 rpm for 10-15 min at 4ºC. RNA supernatant was transferred into fresh 1.5 ml centrifuge tubes and suspended in 500 µL of

ice-cold propanol. Resuspended samples were incubated at room temperature for 10 minutes and subsequently centrifuged at 12,000 rpm for 10 min at 4ºC. Propanol was decanted and RNA was washed by resuspension in 500 µL 75% EtOH followed by centrifugation at 7500-12,000 rpm for 10 min at 4ºC. This wash step was repeated, the EtOH decanted. RNA samples were air-dried for 10-20 min. RNA samples were resuspended in 8-10 µL RNAse-free water and stored at -80 ºC or immediately reverse transcribed into cDNA. When obtaining single-cell mRNA the cytosol of the cell was aspirated into the recording pipette using. Negative pressure was removed and the recording pipette carefully removed and its contents were then expelled into a sterile centrifuge tube. RNA was stored at -80 ºC or immediately reverse transcribed into cDNA

TaqMan PCR

RNA samples were reverse transcribed in Reverse-Transcription Master Mix (1 µl random nonamers (50 uM) (Sigma), 5 µl MMLV RT buffer (5x) (Fisher), 5 µl dNTPs (10 mM) (ThermoScientific), 2 µl DEPC-treated H2O (Fisher), 1 µl Reverse Transcriptase (Fisher), and 1 µl RNAse Inhibitor (Fisher). For single-cell RT-PCR experiments, the cytosol was aspirated following electrophysiological recordings and suspended in RNA RNA Reverse-Transcription Master Mix without enzymes and stored at -80 ºC until further use. Groups of cells were reverse transcribed after the addition of 1 µl Reverse Transcriptase (Fisher), and 1 µl RNAse Inhibitor (Fisher) in a thermocycler (Eppendorf Mastercycler) at 42ºC for 90 min followed by 5 min at 95ºC. For phenotype identification, positive

controls (tissue samples) and single cells were probed for the presence of beta-actin and VGLUT2. Primers and probes for beta-actin were: fwd, CAGCAGGTACAGCATCACGG; rev, GCCATGTACGTAGCCATCC; probe, CTGGTCGTACCACAGGCATTGTG; and for VGLUT2: fwd, CCCGTCTACGCGATAATTGTT; rev, GTCATGACAAGGTGAGGGACT; Probe, ACTGCTCATCAGCCAGCTT. Mastermix containing 3 µl (beta-actin) or 2 µl (VGLUT2) MgCl2 (25 mM), 2.4 µl PCR buffer (10x), 1 µl dNTPs (10 mM), 1 µl primers/probe (10 uM), 0.5 DNA polymerase and 14 µl was prepared and 3 µl of single cell or positive control RNA or RNAse free sterile H2O (non-template control) loaded into optical tubes or a 96-well plate (Bio Rad). Samples were centrifuged for 2 min at 1000 RPM and placed in an ABI-Thermocylcer for PCR analysis. Samples were held at 95 ºC 2 min and cycled 50 times at 95 ºC for 30 s, 60 ºC for 15 s and at 72º C 15 s.

NanoString® gene expression

A custom designed codeset was designed by and purchased from NanoString technologies (for complete list see Appendix 4). This codeset included the seven known NMDA receptor subunits (NR1, NR2A-D and NR3A-B) as well as four housekeeping genes (beta-actin, GAPDH, Hprt1, Ubc). The isolated RNA quality assessment and concentration determination was made at the University of Kentucky using the Agilent's Bioanalyzer 2100. The average RNA integrity number (RIN) for samples used in this study were 9.4 ± 0.07 (Range: 8.9-9.7). 100 ng of total RNA was used from each sample. Hybridization

reaction using the custom designed codeset, and nCounter® master mix, was performed according to protocol by the microarray facility at the University of Kentucky using the nCounter® from NanaString® Technology. The NanoSting probe identifiers for genes analyzed throughout this dissertation were: For NR1: NM_008169.2:492, for NR2A: NM_008170.2:4080, for NR2B: NM_008171.3:6340, for NR2C: NM_010350.2:2720, for NR2D: NM_008172.2:1201, for NR3A: NM_001033351.1:1332, for NR3B: NM_130455.2:2030, for beta-actin: NM_007393.3:1138, for GAPDH: NM_001001303.1:890, for Hprt1: NM_013556.2:30, for Ubc: NM_019639.4:21. For a more complete list of probes included in these analyses refer to Appendix 2. Normalization was performed using the nSolver™ software from NanoString® Technology. The nSolver® software normalizes to negative and positive controls to eliminate background noise and variability unrelated to samples. To calculate the normalization factor of these controls the geometric mean (geometric mean= $\sqrt[n]{x^1 x^2 \dots x^n}$) of each sample is obtained. Subsequently, to account for variability between samples the geometic mean of samples is taken. This average is divided by individual sample specific geometric means to calculate a normalization factor, which is multiplied by sample specific counts. Normalization of endogenous control genes, is subsequently conducted, on counts normalized to positive and negative controls using the same workflow of normalization used for positive and negative controls.

Western Blots

Brainstem slices (300-600 μm) were isolated as described for electrophysiological recordings. Slices were immediately transferred to 40-60 μl of lysis buffer consisting of 0.15M NaCl, 5mM EDTA (pH 8), 1% Triton X-100, 10mM Tris-Hcl (pH 7.4), 10ul/ml of 100mM PMSF (174.2 mg/10ml in methanol), and 100ul/ml of 0.5M NaF (pH 10). Each sample was sonicated and centrifuged immediately at 12,000 RPM for 3 min. Supernatant was aspirated, aliquoted, and stored at -80 ºC until further use. Protein concentration was measured using a Bradford Protein Assay. For Western blots, 20 μg of protein was loaded per lane. The appropriate volume of sample together with equal amounts of loading buffer were boiled in water for 2 min. Samples and ladder were loaded into precast PDF gels in and subsequently the gel was electrophoresed at 50 mA for 45–80 min. Proteins were then transferred at 200 mA for 2 hrs onto polyvinylidene difluoride membranes for Western blot analysis. Membranes were blocked in 1:1 Odyssey blocking buffer/PBS/0.1% Tween 20 for 1 hr at room tremparature. Due to well separated molecular weights of the NR1 (band at 105-120 kD) and β-actin (band at 40-45 kD) protein membranes could be cut in half to be incubated over-night at 4°C, with a rabbit monoclonal anti-NMDAR1 (1:1000; Abcam) and a rabbit monoclonal anti-β-actin (1:10000; Abcam) antibody in Odyssey blocking buffer/PBS/0.1% Tween 20. Membranes were washed with 4 times 5 min with PBS on a shaker. After the final wash membranes were scanned on a densitometer (Odyssey model 9120, Li-COR Biosciences) to quantify band density. Background density was subtracted from the NMDAR1 and β-actin band density and normalized to β-actin, which was used as a loading control.

Data analysis- see general methods of chapter 2.

Results

Glutamate release in the DMV of T1-diabetic mice is increased

Whole-cell patch-clamp recordings were made from DMV neurons from control and T1-diabetic mice, voltage-clamped at -80 mV in the presence of the GABA-A receptor blocker picrotoxin to isolate AMPA-mediated synaptic currents. To record mEPSCs tetrodotoxin (1-2 μM) was added to the ACSF. The frequency of both sEPSCs (control: 11.80 ± 1.46 Hz, n=16; T1-diabetic: 26.05 ± 5.44 Hz, n=20) and mEPSCs (control: 12.98 ± 1.43 Hz, n=55; T1-diabetic: 24.34 ± 4.53 Hz, n=20) was greater in in T1-diabetic mice when compared to control animals ($p<0.05$; Figure 4.2C). No change in amplitude was observed for sEPSCs (Figure 4.2D). Consistent with previous reports, glutamate release was enhanced in the DMV of T1-diabetic mice (Zsombok et al., 2011; Zsombok and Smith, 2009).

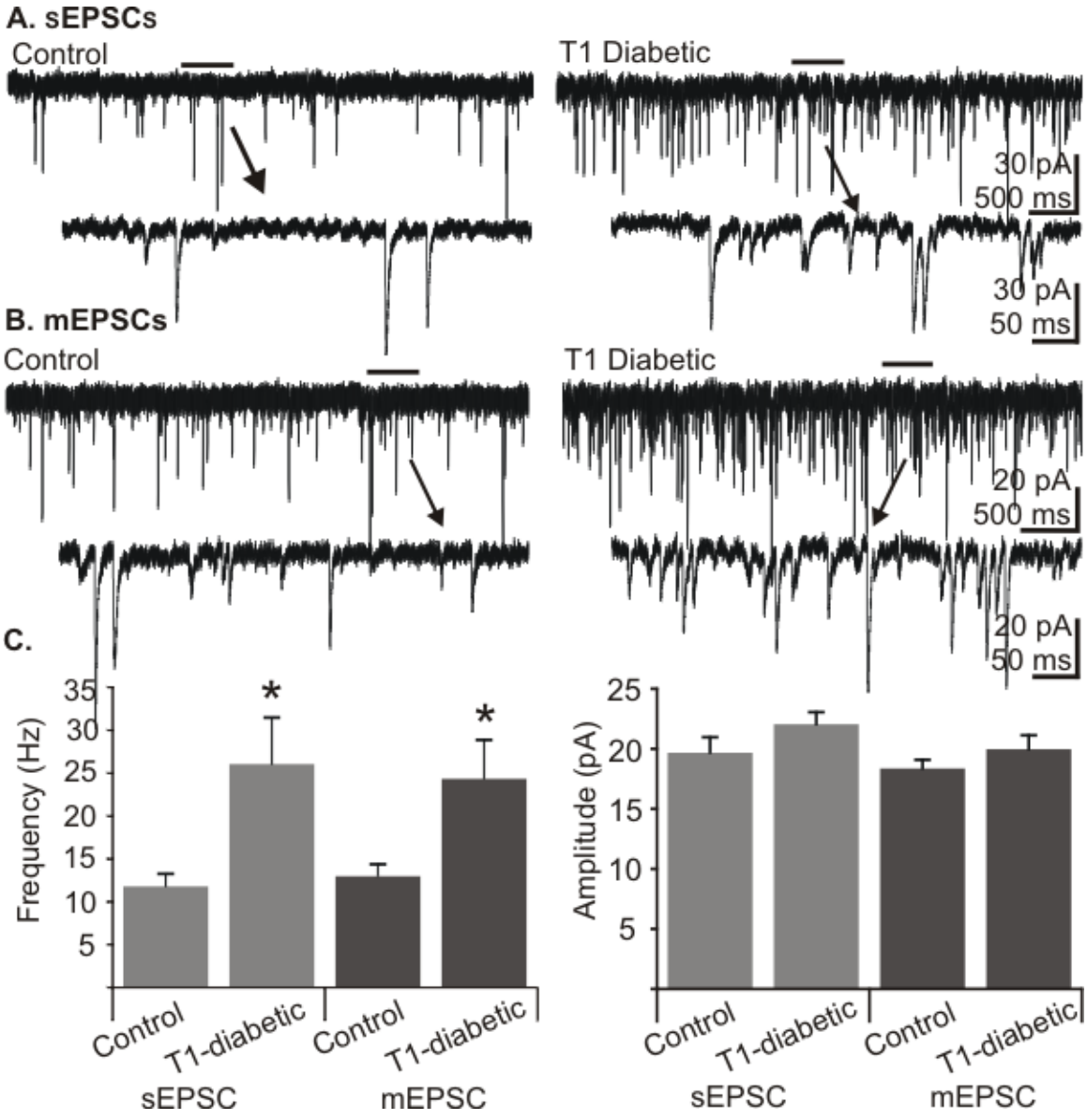
A. sEPSCs
Control
T1 Diabetic
30 pA
500 ms
30 pA
50 ms
B. mEPSCs
Control
T1 Diabetic
20 pA
500 ms
20 pA
50 ms
C.
Frequency (Hz)
35
30
25
20
15
10
5
*
*
Control
T1-diabetic
Control
T1-diabetic
sEPSC
mEPSC
Amplitude (pA)
25
20
15
10
5
Control
T1-diabetic
Control
T1-diabetic
sEPSC
mEPSC

Figure 4.2 Comparison of sEPSC and mEPSC in control and T1-Diabetic mice in the presence of picrotoxin confirmed an increase in the frequency without a change in amplitude. **A.** Representative trace of sEPSCs in a control and T1 Diabetic mouse. **B.** Representative of mEPSCs in a control and T1 Diabetic mouse. **C.** Group frequencies and amplitudes in control and T1 Diabetic mice. Underlined sections indicate regions expanded below. A significant increase in sEPSC and mEPSC was observed in T1-diabetic mice using a homoscedastic Student's t-test and * indicates significance of $p<0.05$.

NMDA receptor-mediated modulation of glutamate release in the DMV is increased in diabetic mice.

Tonically active NMDA receptors (i.e., activated by ambient glutamate in the slice) located on glutamatergic terminals were described previously in the DMV (Bach and Smith, 2012). The hypothesis that sensitivity of these receptors was enhanced in T1-diabetic mice, resulting in increased glutamate release was tested. The response to the NMDA receptor antagonist AP-5 was compared between normoglycemic and hyperglycemic T1-diabetic mice to reveal tonically activated NMDA receptors. DMV neurons were voltage clamped at -80 mV, to diminish the effect of postsynaptic NMDA receptor activation and concentrate resultant effects on presynaptically mediated mechanisms. Application of AP-5 resulted in a significant decrease in the frequency of sEPSCs in both normoglycemic mice, decreasing sEPSC frequency from a baseline of 13.42 ±

2.81 Hz to 10.08 ± 1.89 Hz during application of AP-5 (n=5; $p<0.05$). Similarly, application of AP-5 also diminished sEPSC frequency in hyperglycemic, T1-diabetic mice from a baseline of 16.85 ± 4.68 Hz to 10.42 ± 3.46 Hz during application of AP-5 (n=6; $p<0.05$; Figure 4.3C). No change in amplitude was observed in control (baseline 18.822 ± 1.93 pA and 18.83 ± 1.59 pA during application of AP-5) or T1-Diabetic mice (baseline 20.46 ± 2.02 pA and 18.47 ± 2.11 pA during the application of AP-5). There was a significantly greater percent decrease in the frequency of T1-diabetic than normoglyemic mice (23.78 ± 1.74 % change in controls (n=5), 40.65 ± 1.98 % change T1-diabetic mice (n=6); $p<0.05$; Figure 3D). This result suggested that NMDA receptors exert a greater tonic enhancement of glutamate release in the DMV of T1-diabetic than in normoglycemic mice.

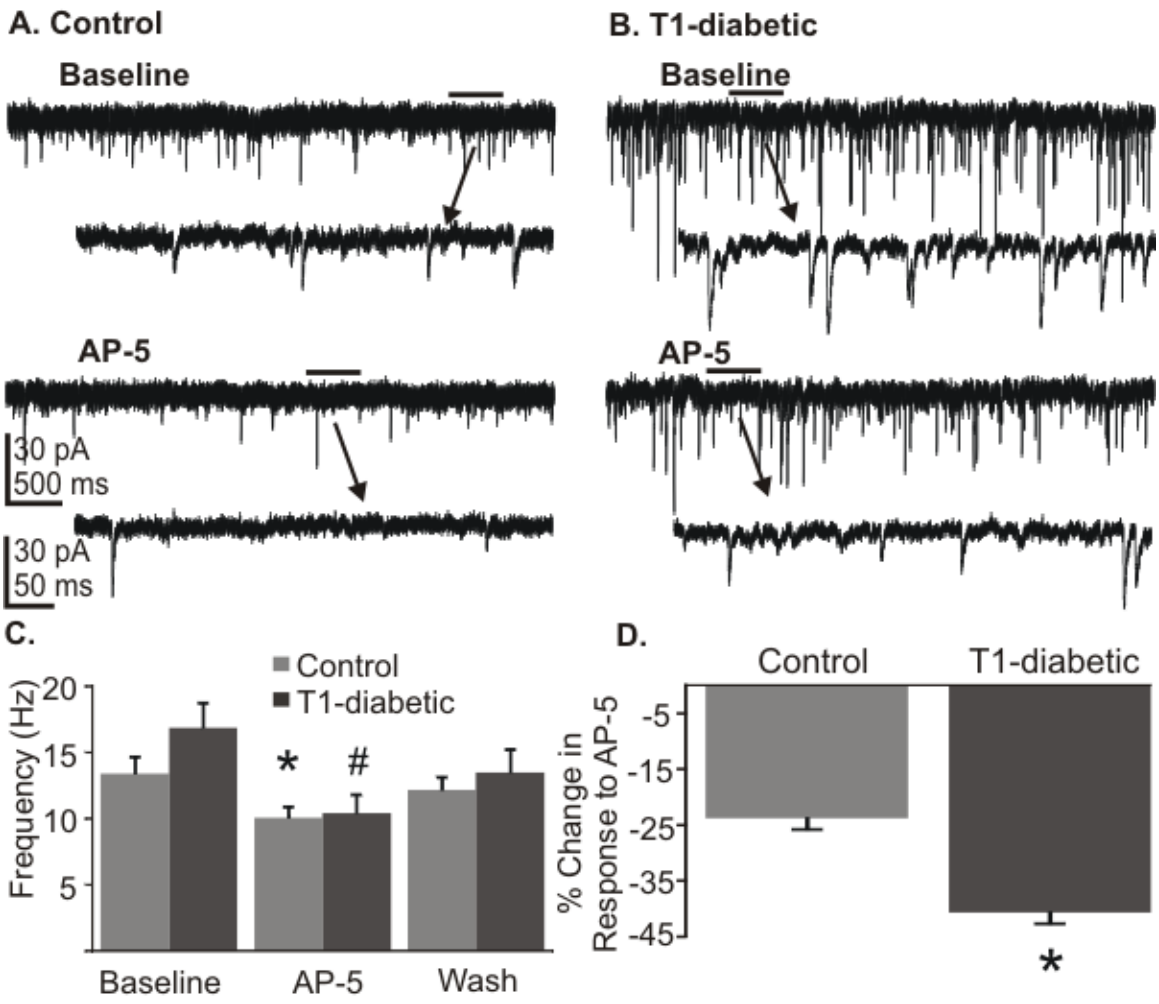

Figure 4.3 AP-5 application on sEPSCs revealed a greater relative effect on the frequency in T1-Diabetic than control mice **A.** Representative trace showing sEPSCs in a slice from a control mouse under baseline conditions and following the application of AP-5. **B.** Representative trace from an T1 Diabetic mouse under baseline conditions and following the application of AP-5. **C.** Average group sEPSC frequency in control and STZ-treated mice before, during and after the application of AP-5. **D.** Average group percent decrease in sEPSC frequency following application of AP-5 in control and T1 Diabetic mice. Line above indicates section expanded below. * and # indicate significance from intragroup

responses to AP-5 application using a paired two-tailed Student's t-test of $p<0.05$. Intergroup differences were analyzed using a two-way Anova.

Preterminal NMDA receptors tonically modulate glutamate release in both normoglyemic and T1-diabetic mice

Since sEPSCs reflect both action potential-dependent and -independent glutamate release, NMDA receptor-mediated differences in sEPSC frequency between control and T1-diabetic mice could result from changes in receptors located on terminals contacting DMV neurons and/or soma-dendritic receptors on presynaptic neurons. Preterminal NMDA receptors were previously identified in normoglycemic mice, which function to enhance glutamate release tonically in the DMV (Bach and Smith, 2012). In the presence of PTX and TTX, application of AP-5 (100 μM) decreased mEPSC frequency in DMV neurons from a baseline of 12.84 ± 3.58 Hz to 8.97 ± 2.48 Hz in AP-5 ($n=10$; $p<0.05$). No change in amplitude (19.75 ± 1.83 pA versus 19.23 ± 1.51 pA) or decay time (1.74 ± 0.13 ms versus 1.68 ± 0.15 ms in AP-5; $p=0.44$) was observed. Application of AP-5 in of T1-diabetic mice also resulted in a significant decrease in the frequency of mEPSCs in DMV neurons (15.53 ± 4.96 Hz baseline and 9.70 ± 3.28 Hz during the application of AP-5; $n=10$; $p<0.05$; Figure 4.4 C). Neither mEPSC amplitude (20.04 ± 1.74 pA versus 19.28 ± 1.43 pA in AP-5) nor decay time (1.58 ± 0.12 ms versus 1.62 ± 0.09 ms in AP-5) was altered (Figure 4.4 C). The relative effect on mEPSC frequency of AP-5 in control (31.12 ± 5.67% decrease; $n=9$) versus T1-diabetic animals (31.90 ± 6.04% decrease; $n=10$) was not different ($p>0.05$; Figure 4.4D). This result suggests that preterminal NMDA receptors tonically

modulate glutamate release in the DMV of T1-Diabetic mice to a similar degree as in normoglycemic controls. Since baseline mEPSC frequency was elevated in the DMV of T1-diabetic mice, effects of AP-5 as a function of baseline mEPSC frequency were determined. No correlation was detected, however, between baseline mEPSC frequency and relative AP-5-mediated response in control (R^2= 0.02) or T1-diabetic (R^2= 0.09) mice. Although AP-5 was effective in reducing mEPSC frequency in both groups, the relative effect of blocking preNMDA receptors on glutamate release was similar for normoglycemic and T1-diabetic mice. These results, therefore, were not consistent with altered function of preNMDA receptors in mediating the observed differences in NMDA receptor-mediated modulation of glutamate release in the DMV of T1-diabetic mice.

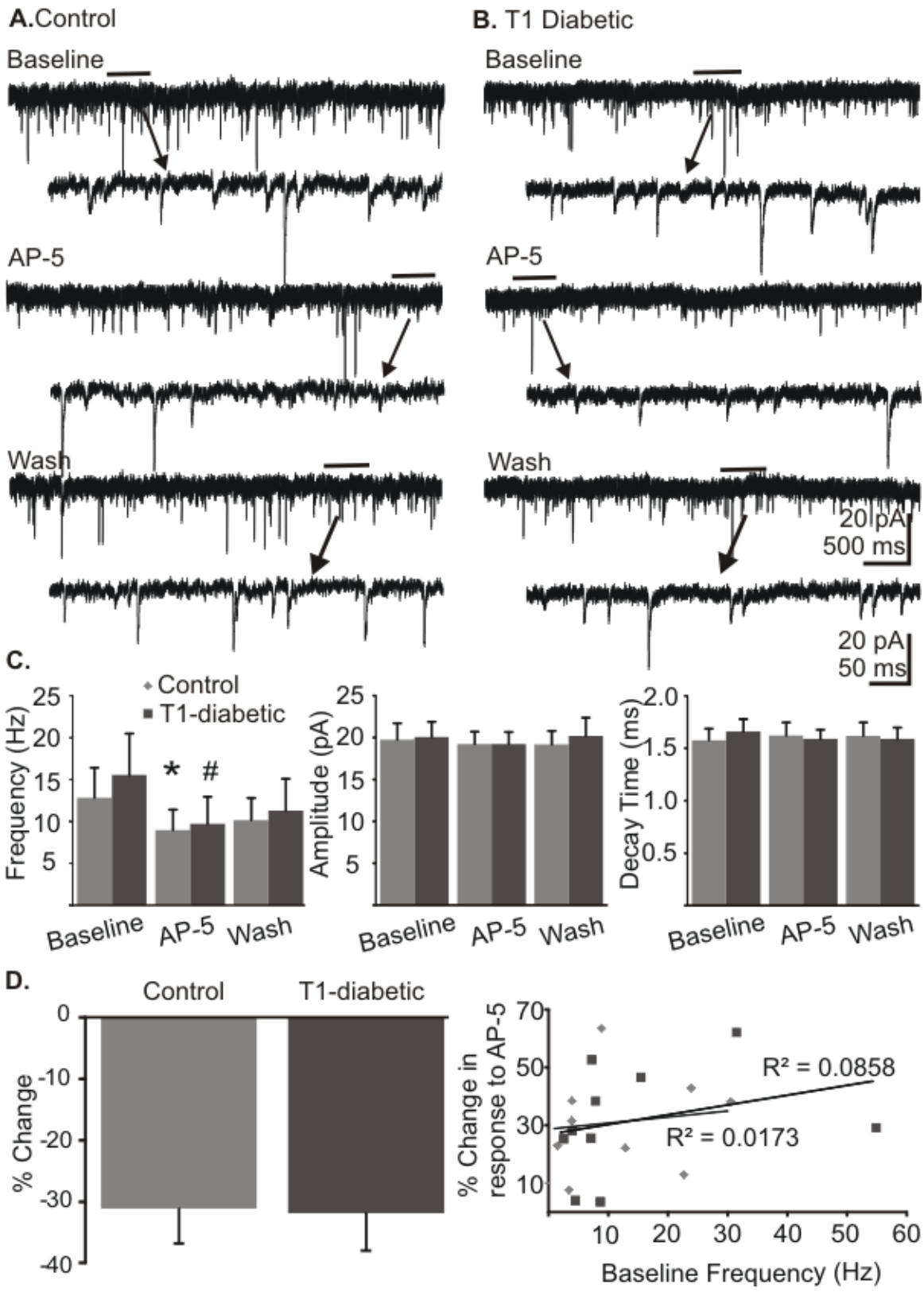
A.Control
B. T1 Diabetic
Baseline
AP-5
Wash
20 pA
500 ms
20 pA
50 ms
C.
Control
T1-diabetic
Frequency (Hz)
Amplitude (pA)
Decay Time (ms)
*
#
Baseline
AP-5
Wash
D.
Control
T1-diabetic
% Change
% Change in response to AP-5
R² = 0.0858
R² = 0.0173
Baseline Frequency (Hz)

Figure 4.4 The tonic inhibition of mEPSC frequency in response to AP-5 was similar T1-diabetic and control mice. **A.** Representative traces showing mEPSCs in a slice from a control mouse before, during and after the application of AP-5. **B.** Representative traces from an T1 Diabetic mouse before during and after the application of AP-5. **C.** Average group mEPSC frequency, amplitude and decay times in control and T1 Diabetic mice before, during and after the application of AP-5. **D.** Average group percent decrease in mEPSC frequency following application of AP-5 in control and T1 Diabetic Mice. **E**. Correlation of baseline frequency and percent change of frequency in response to AP-5. Line above traces indicate section expanded below. * and # indicate significance from intragroup responses to AP-5 application using a paired two-tailed Student's t-test of $p<0.05$. Intergroup differences were analyzed using a two-way Anova.

NMDA receptor-mediated whole-cell currents in NTS neurons were enhanced in T1-diabetic mice

To determine if sensitivity of afferent neurons to NMDA was increased in T1-diabetic mice, whole-cell currents were recorded in NTS neurons in response to applied NMDA. To isolate NMDA receptor-mediated responses, all recordings were made with a Cs^+-gluconate-based internal solution to block K^+ currents and in the presence of TTX (1-2 µM), PTX (100 µM), strychnine (1-2 µM), DTC (20 µM), and CNQX (10 µM) to block action potentials, GABA-A, nicotinic, and AMPA receptors, respectively. When applying 300 µM NMDA to NTS neurons

recorded while voltage-clamped at a holding potential of -30 mV, T1-diabetic mice exhibited significantly greater whole-cell current responses were observed in neurons from T1-diabetic mice (259 ± 31 pA; n=22) than controls (175 ± 25 pA; n=21; $p<0.05$). To account for cell size, current densities were calculated by normalizing each cell to cell capacitance, which did not differ between animal groups (14.2 ± 0.84 pF controls, 13.2 ± 1.06 pF T1-diabetic; p=0.45). When normalized to cell capacitance, NTS neurons from T1-diabetic mice had significantly greater NMDA-evoked current density (21.4 ± 3.2 pA/pF) than controls (12.5 ± 1.2 pA/pF; $p<0.01$; Figure 4.5B). Using TaqMan based single cell RT-PCR, a subset of neurons from both groups was identified as glutamatergic (i.e., expressed VGLUT2; Figure 4.5D). When NMDA-evoked whole-cell currents and current densities were compared in this glutamatergic subpopulation of NTS cells, both whole-cell current (75.4 ± 24.3 pA controls; 258 ± 18.6 pA T1-diabetic; $p<0.01$) and current density (6.7 ± 2.2 pF controls, 18.1± 2.4 pF T1-diabetic; $p<0.01$), were significantly greater in T1-diabetic (n=5) than control (n=5) mice. This result suggests that NMDA receptor activation was enhanced in glutamatergic NTS neurons from diabetic mice and this enhancement could account for the greater relative increase in glutamate release in the DMV of diabetic mice in response to AP-5 application.

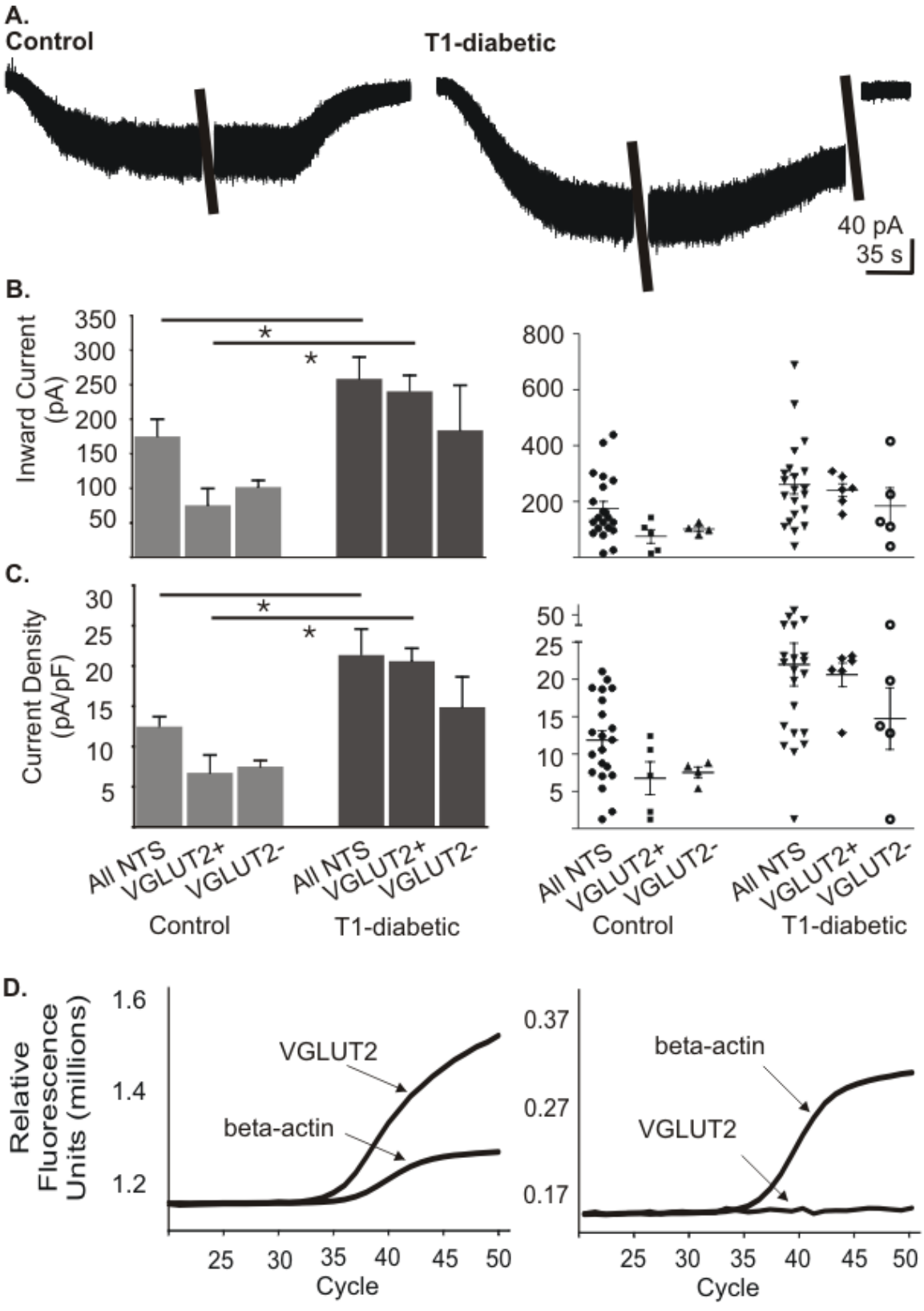
A.
Control
T1-diabetic
40 pA
35 s
B.
Inward Current (pA)
350
300
250
200
150
100
50
800
600
400
200
C.
Current Density (pA/pF)
30
25
20
15
10
5
50
25
20
15
10
5
All NTS
VGLUT2+
VGLUT2-
Control
T1-diabetic
D.
Relative Fluorescence Units (millions)
1.6
1.4
1.2
VGLUT2
beta-actin
0.37
0.27
0.17
25 30 35 40 45 50
Cycle

Figure 4.5 NMDA mediated whole cell current (WCC) responses and current densities in NTS neurons of control and T1-diabetic mice. **A.** Representative traces of NMDA (300 µM) mediated WCC responses in control and T1-diabetic mice. **B.** Average NMDA mediated WCC in control and T1-diabetic of the total (n=21 controls, n=22 T1-diabetics) and the VGLUT2+ (n=5 controls, n=5 T1-Diabetics) NTS neurons population (asterisk indicates significant difference from control, $p<0.05$). **C.** Average NMDA mediated current densities in control and T1-diabetic of the total (n=21 controls, n=22 T1-diabetics) and the VGLUT2+ (n=5 controls, n=5 T1-diabetics) NTS neuron population (asterisk indicates significant difference from control, $p<0.05$). **D.** Example of a VGLUT2+ neuron.

Voltage-dependence of soma-dendritic NMDA Receptors in NTS neurons

Responses to NMDA were determined in neurons voltage-clamped at -30 mV, a potential presumed to reveal maximal NMDA receptor-mediated responses (Mayer et al paper; Smith et al., 1998). To determine if the voltage-dependence of the NMDA induced responses differed between NTS neurons of control and diabetic mice, a voltage step protocol was applied in a subset of neurons and currents evoked by NMDA application (300 µM) were examined at voltages between -80 and 30 mV. NMDAR responses were recorded in the presence of PTX, TTX, strychnine, DTC and CNQX. The current-voltage relationship was determined during the maximal NMDA receptor- mediated response. When comparing the NMDA receptor-mediated current, calculated as the current density at each voltage in NMDA minus the current density at each respective baseline voltage, there was a significant increase in the current

density in NTS neurons from T1-diabetic (n=21) versus control (n=12) mice at all voltages between -40 to 0 mV ($p<0.05$; Figure 4.6A).

Maximal activation of the NMDA receptor is thought to occur near -30 mV due to Mg^{2+} dependent block (Mayer et al., 1984), and our experimental results are therefore in agreement with this response being NMDA-mediated. There was no significant difference between the baseline holding current responses of the two animal groups (Figure 4.6B). The observed responses exhibited a nonlinear current-voltage relationship consistent with a voltage-sensitive response. Most importantly, at the theoretical maximum response to NMDA (-30 mV) there was a greater NMDA-mediated current density in T1-diabetic than control mice (-8.8 ± 1.47 pA/pF control, n=12; -17.1 ± 1.99 pA/pF T1-diabetic, n=21); $p<0.05$) (Figure 4.6A). The NMDA response was reversible (n=8 controls; n=11 T1-diabetic; Figure 4.6.C and D) and the NMDA receptor specificity was confirmed using AP-5 (which blocked the response) in a subset of cells (n=3; Figure 4.6.E).

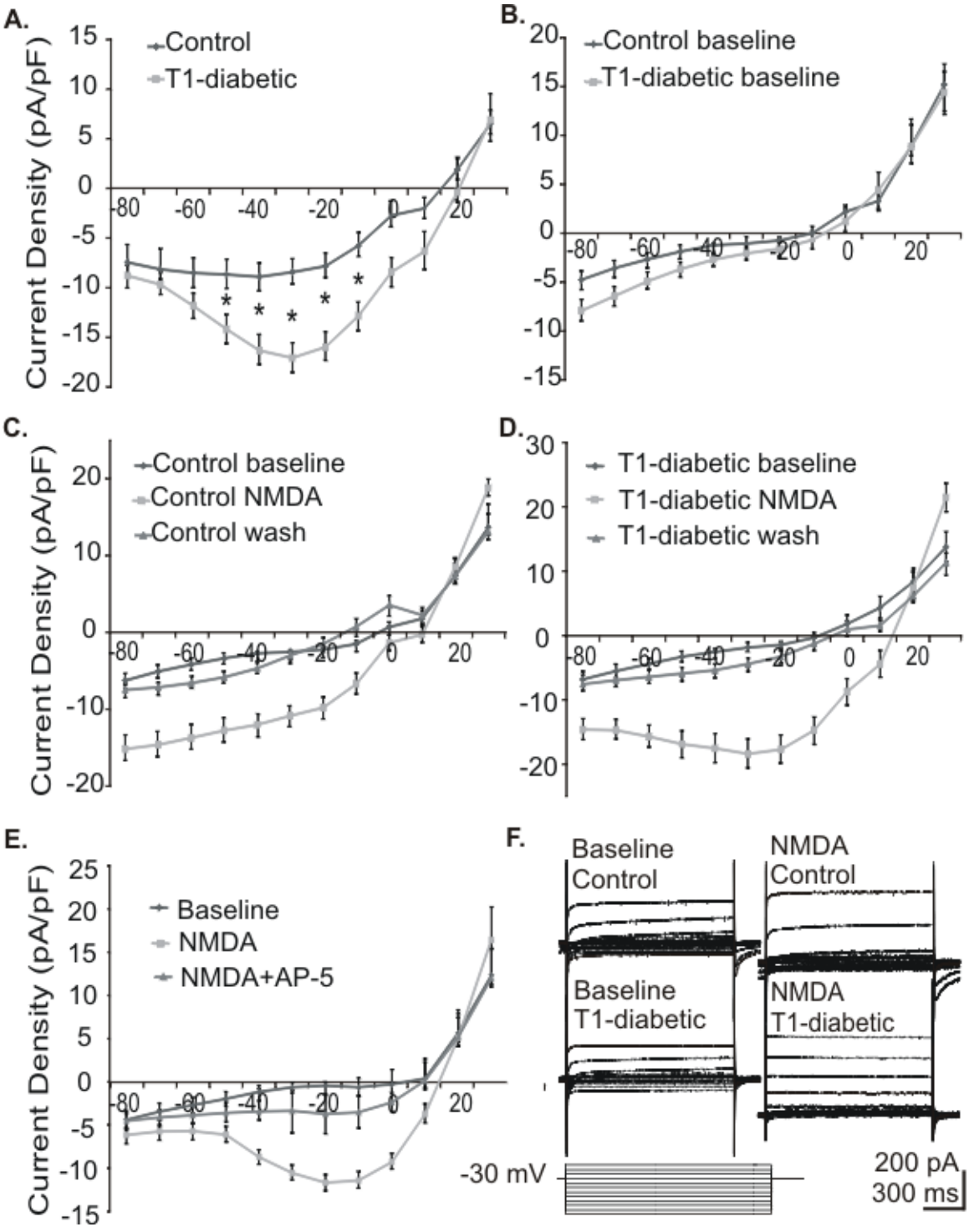
A.
Control
T1-diabetic
Current Density (pA/pF)
B.
Control baseline
T1-diabetic baseline
C.
Control baseline
Control NMDA
Control wash
Current Density (pA/pF)
D.
T1-diabetic baseline
T1-diabetic NMDA
T1-diabetic wash
E.
Baseline
NMDA
NMDA+AP-5
Current Density (pA/pF)
F.
Baseline
Control
NMDA
Control
Baseline
T1-diabetic
NMDA
T1-diabetic
-30 mV
200 pA
300 ms

Figure 4.6 Current-voltage responses in control and T1-Diabetic mice. **A.** NMDA (300 µM) mediated current-voltage responses in control (n=12) and T1-Diabetic (n=21) mice. **B.** Baseline current-voltage responses in control and T1-Diabetic mice (asterisk indicates significant difference from control, $p<0.05$). **C.** Current-voltage responses of reversible NMDA mediated responses in control (n=8) mice. **D.** Current-voltage responses of reversible NMDA-mediated responses in T1-Diabetic (n=11) mice. **E.** Current-voltage responses of AP-5 dependent reversible NMDA-mediated WCC (n=3). **F.** Representative examples of current-step responses before and during the application of NMDA in control and T1-Diabetic mice and stimulus waveform used in these studies. * indicates $p<0.5$ using a two-sample equal variance two-tailed Student's t-test.

Western Blot analysis of NR1 Subunits

The NR1 subunit is an obligatory NMDAR subunit (Traynelis et al., 2010). An NR1 antibody raised against this subunit was used to examine protein levels as a measure of possible differences in the number of NMDA receptors between control (n=6) and T1-Diabetic (n=6) mice (Fig. 4.7). A discrete band at 105-120 kD was observed that was consistent with the NR1 protein. Band density was normalized to that of β-actin. No statistically significant difference between the relative expression of the NR1 subunit between control and T1-diabetic mice was observed (100 ± 22 % controls and 126 ± 13 % T1 diabetic mice; p=47).

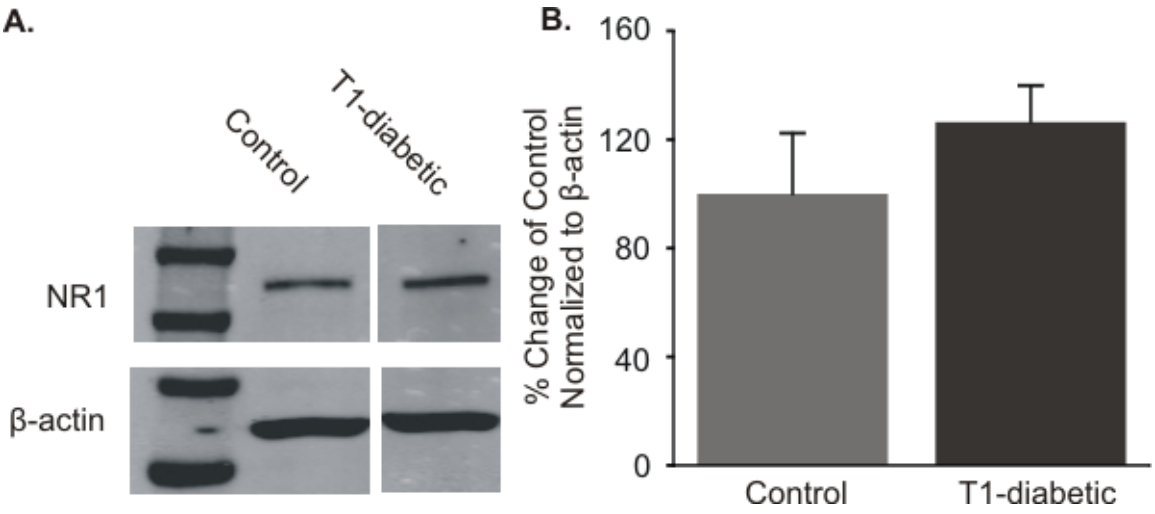

Figure 4.7 Protein expression of the NR1 subunit in control and T1-diabetic mice. **A.** Representative examples of NR1 subunit and ß-actin protein expression in the DVC of control (n=6) and T1-diabetic (n=6) mice. **B.** Average NR1 protein expression in the DVC of control and T1-diabetic mice. Statistical significance was analyzed using a Wilcoxon signed-rank test.

NMDA receptor subunit RNA abundance

The RNA expression of the seven NMDA receptor subunits was quantitatively using the nCounter NanoString technology. All genes were normalized to positive and negative internal controls. Genes of interest were subsequently normalized to the four control genes, beta-actin, GAPDH and Hprt1. No differences in RNA abundance was detected in any of the seven NMDA receptor subunits were observed between control and T1-diabetic mice (Fig 4.8). The average RNA abundance for each NMDA receptor subunit is expressed in Table 4.1. below.

Table 4.1. NMDA receptor subunit mRNA abundance

Gene	Control	T1-diabetic
NR1	1562 ± 60	1585 ± 96
NR2A	561 ± 61	456 ± 71
NR2B	704 ± 22	714 ± 49
NR2C	132 ± 8	132 ± 6
NR2D	323 ± 19	329 ± 31
NR3A	1451 ± 44	1567 ± 33
NR3B	39 ± 7	45 ± 6

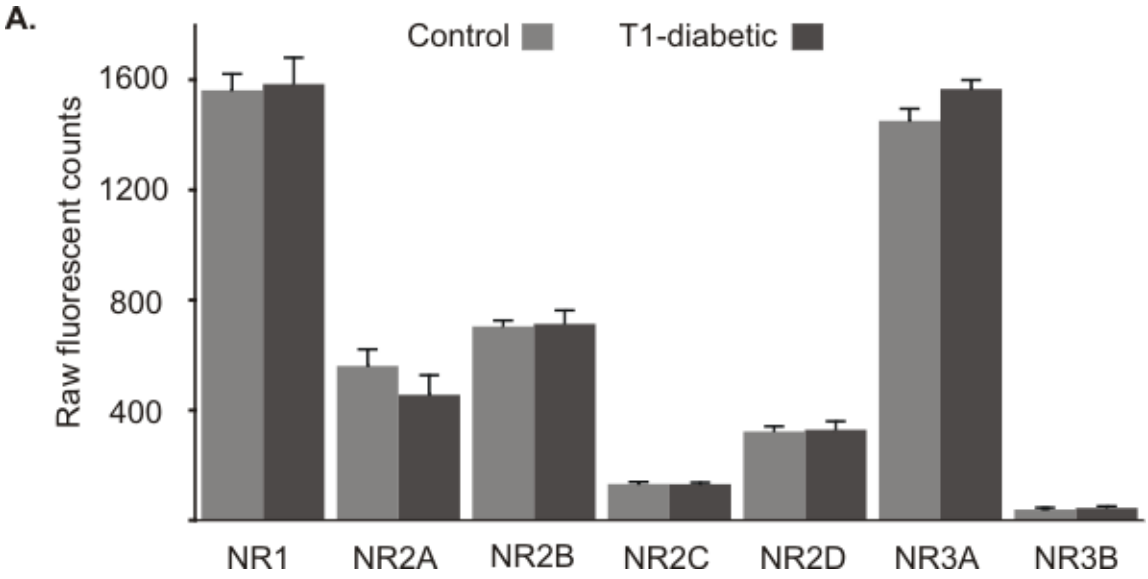

Figure 4.8 NMDA receptor subunit RNA abundance in normal and T1-diabetic mice. Intergroup differences in gene expression were analyzed using a two-tailed two-sample equal variance Student's t-test.

Discussion

In this study, mechanisms underlying increased mEPSC and sEPSC frequency of DMV neurons inT1-diabetic mice were investigated This study confirmed the increase in mEPSC and sEPSC frequency in T1-diabetic mice first observed by Zsombok et al.(Zsombok et al., 2011). The frequencies reported here were observed in the presence of a GABA-A antagonist to mitigate against possible network effects that might influence glutamate release in the DMV (Derbenev et al., 2006; Glatzer and Smith, 2005; Smith et al., 1998; Williams et al., 2007). Additionally, unlike previously, animals were maintained hyperglycemic for at least 7 and up to ten days before being used for electrophysiological and or molecular experiments and recordings were performed with 2 mM CaCl rather than 1.3 mM. All of these factors could contribute to the slightly larger enhancement of glutamate release versus that observed previously, but do not detract from the primary conclusion that excitatory input to DMV neurons is increased in T1-diabetic mice. The absence of an amplitude change suggests that excitatory neurotransmission is altered presynaptically, either at the terminal or on the presynaptic neuron.

NMDA receptors have been studied extensively for their involvement in enhancing excitatory neurotransmission under pathological conditions (Yang et

al., 2006). Antagonism of NMDA receptors in acute brainstem slices resulted in a greater relative decrease in sEPSC frequency, without an amplitude change, in T1-diabetic mice. This result established the involvement of NMDA receptors in circuitry changes of the DVC resultant to T1-diabetes. The AP-5-induced decrease in the frequency suggested a decrease in the probability of glutamate release at the presynaptic terminal and/or the soma-dendritic membranes of intact presynaptic neurons (Figure 4.1). An increase in sEPSC and mEPSC frequency (observed in this and previous studies by Zsombok et. al) in the absence of a change in amplitude of T1-diabetic mice posed NMDA as a probable mechanistic player in mediating the enhanced excitatory drive onto DMV neurons.

Activation of NMDA receptors located on presynaptic glutamate terminals was previously identified as a means of modulating glutamate release in the DMV (Bach and Smith, 2012). To determine if changes in NMDA receptors located on glutamatergic synaptic terminals contacting DMV neurons accounted for the relative differences in NMDA-dependent modulation of glutamate release, action-potential independent responses were isolated through the use of TTX. PreNMDA receptors were active tonically in both control and diabetic mice. When comparing the two animal groups, however, the relative contributions of NMDA receptors located on presynaptic terminals to tonic facilitation were similar. This result argues against preNMDA receptors contributing directly to the enhanced mEPSC frequency observed in T1-Diabetic mice.

To explain the greater relative NMDA effect on sEPSC frequency in T1-diabetic mice, soma-dendritic NMDA receptor responses of putative presynaptic neurons in the NTS were compared between groups. Functional glutamatergic synaptic connections between NTS and DMV neurons are maintained in the brainstem slice preparation used in this study (Davis et al., 2004; Davis et al., 2003; Derbenev et al., 2004). NMDA-mediated whole-cell current amplitude and current density was increased in NTS neurons of T1-diabetic mice relative to controls. The differences between groups were consisted in glutamateric (i.e., VGLUT2-expressing) NTS neurons, indicating that increased NMDA enhanced excitatory drive of glutamatergic NTS neurons represents a hallmark feature in T1-diabetic mice. Whereas NMDA sensitivity differences between groups was detected across the global NTS neuronal population, the range of responses exhibited considerable overlap between groups. In contrast, the response amplitude in identified VGLUT2+ neurons in T1-diabetic mice was consistently greater than in controls. The NTS includes a number of prominent phenotypes in addition to glutamate, including GABAergic, noradrenergic, and a variety of peptides. With respect to fast synaptic transmission to the DMV, glutamate and GABA predominate (McDougall and Andresen, 2012; McDougall and Andresen, 2013). The frequency of GABAergic IPSCs, however, was not altered in T1-diabetic mice. This suggests that tonic activity of GABAergic neurons does not contribute substantially to modulation of DMV function in T1-diabetic mice and also implies minimal contribution of altered tonic NMDA activation in NTS GABA cells to DMV neuron function in these mice. Although more direct assessment of

NMDA activity in GABA cells is required to be definitive, the consistently greater effect of NMDA in identified glutamate neurons from T1-diabetic mice may reflect phenotype-selective alteration of NMDA-dependent regulation of glutamate neurons in the NTS that project the DMV.

Although specificity of the increased NMDA sensitivity to glutamate neurons could not be determined conclusively, the relative sensitivity of this population is consistent with enhanced NMDA receptor-mediated activation of glutamatergic NTS neurons and is consistent with the enhanced glutamate release seen in T1-diabetic mice. The increased NDMA sensitivity in glutamatergic NMDA neurons is consistent with the increase increased sEPSC frequency in downstream DMV neurons.

NMDA receptor modulation of whole-cell current responses in NTS neurons could be due to changes in the number of receptors present, reorganization of receptor subunits, and/or receptor trafficking (Collingridge et al., 2004; Traynelis et al., 2010). The total number of receptors should be reflected by the expression of the NR1 subunit, since incorporation of this subunit is obligatory for functional NMDA receptor assembly (Paoletti et al., 2013). When protein expression of the NR1 subunit was compared between control and T1-Diabetic mice, no statistically significant differences were observed. The lack of significance may reflect, at least in part, the lack of phenotype specificity of the method used to detect protein differences in a heterogeneous cell population. This sensitivity in cell population may also account for the failure to observe significant changes in gene expression of the NMDA receptor subunits.

Additionally, expression changes between specific cell populations may be altered differentially, with some cell populations showing increased expression and others showing a decrease in expression. All these factors may account for the failure to identify protein expression and mRNA expression changes in NMDA receptor subunits and argues for the need to more specifically target distinct populations of cells, possibly through the use of transgenic animals that allow fluorescent genotypic identification. Finally, receptor trafficking may account for changes in NMDA-mediated electrophysiological measures and could be independent of expression changes (see Chapter 6 for more extensive discussion).

Neurons in the vagal complex respond to altered glucose concentrations and also influence blood glucose content. Subsets of dorsal vagal complex neurons and synaptic terminals are glucose-sensitive (Balfour et al., 2006; Balfour and Trapp, 2007; Ferreira et al., 2001; Wan and Browning, 2008), consistent with longstanding evidence that glucose-sensing neurons in this region regulate both feeding and blood glucose concentrations (Ritter et al., 1981; Ritter et al., 2000). Acutely, injection of glucose into the vagal complex inhibits gastric motility and increases intragastric pressure, most likely by inhibiting activity of DMV neurons (Ferreira et al., 2001). Vagally-mediated visceral function can also be compromised in chronically hyperglycemic animal models or human patients with either type 1 or type 2 diabetes (Ahren et al., 1996; Pocai et al., 2005b; Saltzman and McCallum, 1983; Undeland et al., 1998). Decreased parasympathetic visceral tone resulting from vagal atonia leads to a

number of outcomes detrimental to maintenance of metabolic homeostasis, including elevated hepatic gluconeogenesis and diabetic gastroparesis (diabetic gastropathy). A greater sensitivity of NMDA receptors in glutamatergic projections to the DMV could serve as a mechanism to counter the inhibitory effects of hyperglycemia on vagal output by increasing excitatory synaptic input to preganglionic parasympathetic motor neurons. In addition to insulin-dependent receptor trafficking (Zsombok et al., 2011), synaptic glutamate release in the DMV is persistently increased the STZ-treated mouse. DMV motor neurons are 'pacemakers' that fire action potentials tonically (Browning and Travagli, 1999). Their activity is tightly regulated by synaptic inputs, largely arising from GABA and glutamate neurons of the adjacent NTS (Davis et al., 2003; Glatzer et al., 2007; Travagli et al., 1991a; Williams et al., 2007). Normally, GABAergic input from the NTS to DMV neurons dominates the tonic regulation of vagal output, whereas glutamatergic regulation is thought to be more phasically active (Browning and Travagli, 2011) A sustained increase in glutamatergic, excitatory synaptic drive to DMV motor neurons in diabetic mice would be expected to enhance the tonic influence of glutamate in the DMV and increase vagal output, leading to diminished hepatic gluconeogenesis and/or enhanced output to the exocrine pancreas, as well as attenuation of diabetic gastroparesis (Ahren et al., 1996; Saltzman and McCallum, 1983). Significant, sustained modulation of excitatory synaptic function in the DMV of T1-diabetic mice thus involves a fundamental change in the balance of synaptic input to vagal motor neurons. In this sense, the altered synaptic balance may be an attempt by the system to

homeostatically compensate for putatively excessive inhibition of vagal activity in chronic hyperglycemia by increasing DMV neuron excitability. NMDA sensitivity in glutamatergic NTS neurons is increased in T1-diabetic mice and at least a portion of the chronically-enhanced glutamate release seen in these animals may be due to tonically enhanced NMDA-dependent modulation of NTS neurons. Chronic dysregulation of visceral autonomic control may contribute to development of insulin resistance and type 2 diabetes (Carnethon et al., 2003). NMDA receptor plasticity might represent a compensatory response to chronic hyperglycemia associated with diabetes and may therefore provide clues to re-establishing autonomic control in diabetic patients.

Chapter 5: Preterminal Glycine Receptor modulation of glutamate release in the dorsal vagal complex

Introduction

Glycine receptors (GlyRs) are pentameric, ionotropic chloride receptors activated by glycine. Although they are found throughout the central nervous system, their expression level is particularly high in the spinal cord and brainstem. Structurally they are members of the cys-loop receptor family, all of which are arranged in a symmetrical ring structure around a central ion-conducting pore. Like other ligand-gated ion channels, GlyRs consist of an N-terminal, a transmembrane, an extracellular domain and an intracellular loop that connects the four transmembrane segments (Lynch, 2009). Glycine binds in the extracellular domain and alternative splicing in this domain can alter glycine efficacy (Dutertre et al., 2012).

GlyRs can consist of heteromeric arrangements of α- and β-subunits or homomeric arrangements of α subunit isoforms. There are four α-subunit isoforms, namely α1- α4 and a single β-subunit. Functional changes resulting from subunit arrangements, are poorly understood due to the lack of pharmacological agents available to target specific receptor isoforms. Homomeric β-subunits do not appear to assemble into functional receptor channels (Lynch, 2009). Embryonic neurons express primarily homomeric α-subunit GlyRs, but these are gradually replaced to make α- and β-subunit heteromeric GlyR predominant by the third postnatal week in rats (Lynch, 2009). Co-assembly of α- and β-subunits not only results in a reduced picrotoxin

sensitivity, but also reduces single channel chloride conductance (Beato et al., 2004; Burzomato et al., 2004; Lynch, 2009; Pribilla et al., 1992).

GlyRs have long been studied for their contribution to the postsynaptic membrane potential. More recently, however, their effects on the probability of neurotransmitter release at the presynaptic terminal has been investigated (Turecek and Trussell, 2001). In the visual neocortex, the auditory brainstem, spinal cord, and a few other regions of the brain, preterminal glycine receptors (preGlyRs) have been identified to tonically increase the release of glutamate as well as GABA (Ye et al., 2004). The enhancement of neurotransmitter release by glycine receptor activation was shown to be dependent on Ca^{2+} entry through voltage-gated Ca^{2+} channels (VGCCs) (Jeong et al., 2003; Kunz et al., 2012; Turecek and Trussell, 2001).

Chloride conductance through GlyRs can be either hyperpolarizing and depolarizing, depending on the membrane potential relative to the Cl^- equilibrium. Two pumps, namely the Na^+- K^+-Cl^- co-transporter 1 (NKCC1) and K^+-Cl^- co-transporter 2 (KCC2), are pivotal players in establishing the Cl^- equilibrium potential which dictates the effect Cl^- influx imparts on the cell membrane potential. While NKCC1 transports chloride into the cell to increase the Cl^- equilibrium potential (i.e., makes E_{Cl^-} more depolarized), KCC2 transports Cl^- out of the cell and consequently lowers the Cl^- equilibrium potential (Payne et al., 2003). Throughout development the two transporters show opposing expression patterns, with NKCC1 expression being high in early development when KCC2 expression is low. As NKCC1 moves towards its low adult

expression levels, KCC2 expression increases. As a result, the increased KCC2 to NKCC1 ratio causes Cl^- flux through GlyRs to become progressively more hyperpolarizing (Song et al., 2006; Turecek and Trussell, 2001; Ye et al., 2004)

Glycine is removed from the synaptic cleft through Na^+/K^+-ATPase co-transport coupling of glycine transporters (GlyTs) (Mayor et al., 1981). Two GlyTs, namely GlyT1 and GlyT2, have been identified. These two transporters differ in their co-transport stoichiometry and more controversially in their subcellular localization (Aragon et al., 1987; Cubelos et al., 2005; Poyatos et al., 1997; Zafra et al., 1995). GlyT1 co-transportation has a stoichiometry of 2 Na^+:K^+:glycine, while GlyT2 maintains a 3 Na^+:K^+:glycine stoichiometry (Aragon et al., 1987; Betz et al., 2006). Differences in GlyTs cellular localization is thought to play an important role in dictating the effect these transporters have on glycine availability within the synaptic cleft (Berger et al., 1998; Bergeron et al., 1998). GlyT1 is thought to be localized primarily in astrocytes and in a small subpopulation of neurons, while GlyT2 is thought to colocalize specifically with glycinergic neurons (Poyatos et al., 1997; Zafra et al., 1997b). This localization specificity is believed to result in opposing functions of the two transporters, with GlyT1 clearing glycine form the synaptic cleft and GlyT2 leading to more efficient glycine recycling (Zafra et al., 1997a). Recent studies in various areas of the CNS, however, have challenged the cellular localization specificity of GlyTs (Cubelos et al., 2005; Raiteri et al., 2008). In the spinal cord, experimental evidence suggests co-localization of the two transporters on gliosomes and synaptosomes, and GlyT1 expression has been found on both GABAergic and

glutamatergic terminals, as well as in interneurons (Cubelos et al., 2005; Menger et al., 1998; Raiteri et al., 2008).

GlyR and GlyTs have been implicated for their role in pathological conditions (Eulenburg et al., 2005; Harvey et al., 2008). The availability of glycine is normally regulated partially by GlyTs and abnormal functions of GlyTs results in a variety of pathologies. GlyT2, for example, has been well established for its role in hyperekplexia, a neurological disorder characterized by pronounced startle responses and hypertonia. Mutations of GlyR, particularly the α-subunit, have been shown to suppress hyperexcitability during seizure activity (Chattipakorn and McMahon, 2003; Kirchner et al., 2003). Overall these studies establish a role of glycine receptors and modulators of glycine availability in disorders of neuronal hyperexcitability.

In this study the presence and the physiological function of GlyRs at preterminal contacts in the DMV was assessed. Their relevance in modulating neurotransmitter release and altered function during a disease state presented them as a potential mechanism of underlying changes in the release probability of glutamate in T1-diabetic mice. Consequently, changes in GlyR function were also investigated for their possible role in counterbalancing hyperexcitability in DMV neurons of T1-diabetic mice.

Methods

Only methods and materials specific to this Chapter are restated here. To avoid redundancy refer to Chapter 2 of this dissertation, when indicated.

Animals

Male and female GIN mice (FVB-Tg (GadGFP)4570Swn/J; The Jackson Laboratory)4–11 wk of age, were housed under a standard 14-h light/10 –h dark cycle, with food and water provided without restriction. All animals were treated and cared for in accordance with National Institutes of Health guidelines and all procedures were approved by the Institutional Animal Care and Use Committee of the University of Kentucky.

Animal Injections

Mice were given intra-peritoneal injections of 200mg/kg (either a single dose or in 5 doses of 40 mg/kg each over 5 days) of streptozotocin. Controls were either injected with saline (0.9% NaCl) or untreated. Systemic glucose levels were measured prior to injections and monitored daily. Animals were used for electrophysiological recordings and molecular analyses after 7-10 days of persistent hyperglycemia (blood glucose level of above 300mg/dl).

Brain stem slice preparation- see general methods in Chapter 2

Electrophysiological recording- see general methods in Chapter 2 for complete methods.

Drugs used for electrophysiological recording- The drugs, their respective concentrations, used for specific experiments in this chapter were: DL-2-Amino-5-phosphonopentanoic acid (AP-5; 100 µM; Sigma), picrotoxin (PTX; 100 µM;

Sigma), Tetrodotoxin (TTX; 1-2 µM; Alomone Labs), d-tubocurarine chloride (DTC; 10-20 µM; Sigma), Strychnine (1-2 µM), Org 24598 (10 µM; Tocris), ALX-1393 (0.5 µM; Tocris), Glycine (30 µM,100 µM,300 µM,1000 µM; Fisher), 6-Cyano-7-nitroquinoxaline-2,3-dione (CNQX; 10 µM; Sigma), (-)-Bicuculline methiodide (Bic; 30 µM; Sigma), Bumetanide (10-20 µM; Tocris).

Data analysis- see general methods in Chapter 2

Results

Strychnine antagonism increased mEPSC frequency

Whole-cell recordings were made from DMV neurons at a holding potential of -80 mV in the presence of TTX and picrotoxin to record mEPSCs. Cells were allowed to equilibrate and were monitored for a minimum of five minutes before baseline recordings were taken. Strychnine was subsequently bath applied for 10 minutes, and effects of strychnine on mEPSCs were assessed. Strychnine has been shown to serve as a potent antagonist of nicotinic α4β2 as well as α7 acetylcholine receptors (Matsubayashi et al., 1998). In the DVC, both α7 and non- α7 nicotinic acetylcholine receptors facilitate presynaptic glutamate release (Kalappa et al., 2011). This lack of strychnine specificity necessitated the use of the nicotinic receptor blocker 10-20 µM d-tubocurarine chloride (DTC) when examining strychnine-sensitive responses. Initially, DTC was omitted from the baseline solution. To avoid inadvertent responses on nicotinic acetylcholine receptors, DTC was included in all subsequent recordings. Strychnine-sensitive changes in mEPSC frequency did not differ between neurons pre-incubated with

or without DTC (14.3 ± 0.04 % without DTC, n=6; 14.8 ± 0.04% increase in mEPSC frequency in response to DTC, n=5; p=0.93). As a result these populations were combined. In control animals bath application of strychnine resulted in a small but significant increase in mEPSC frequency (20.79 ± 5.56 Hz baseline, 23.11 ± 6.25 Hz in response to 1-2 μM strychnine; n=11 $p<0.05$). The amplitude of the events also exhibited a small but statistically significant change (16.42 ± 1.74 pA baseline, 15.05 ± 1.69 pA in response to strychnine; $p<0.05$).

To additionally test inadvertent effects of NMDA receptor potentiation through increased glycine availability, the NMDA receptor blocker AP-5 was bath applied. Inadvertent actions on putative NR3 subunit containing receptors could not be prevented using this approach (see discussion). In control animals, the application of strychnine resulted in a small but significant increase in the frequency of mEPSCs (17.82 ± 4.5 Hz baseline, 21.15 ± 4.4 Hz in response to strychnine $p<0.05$; n=5 ; Figure 5.1 C). No change in mEPSC amplitude was observed (21.17 ±1.66 pA baseline, 21.15 ± 1.74 pA in response to strychnine p=0.99; Figure 5.1 C). Similarly, In T1-diabetic mice an increase in mEPSC frequency was observed in response to strychnine (22.90±5.8 Hz baseline, 34.70±5.5 Hz response to strychnine; $p<0.05$; n=3; Figure 5.1 C). No change in amplitude was observed (21.17±1.66 pA baseline, 21.15 ± 1.74 pA in response to strychnine p=0.13). Strychnine therefore increased mEPSC frequency in the DMV of normal and T1-diabetic mice.

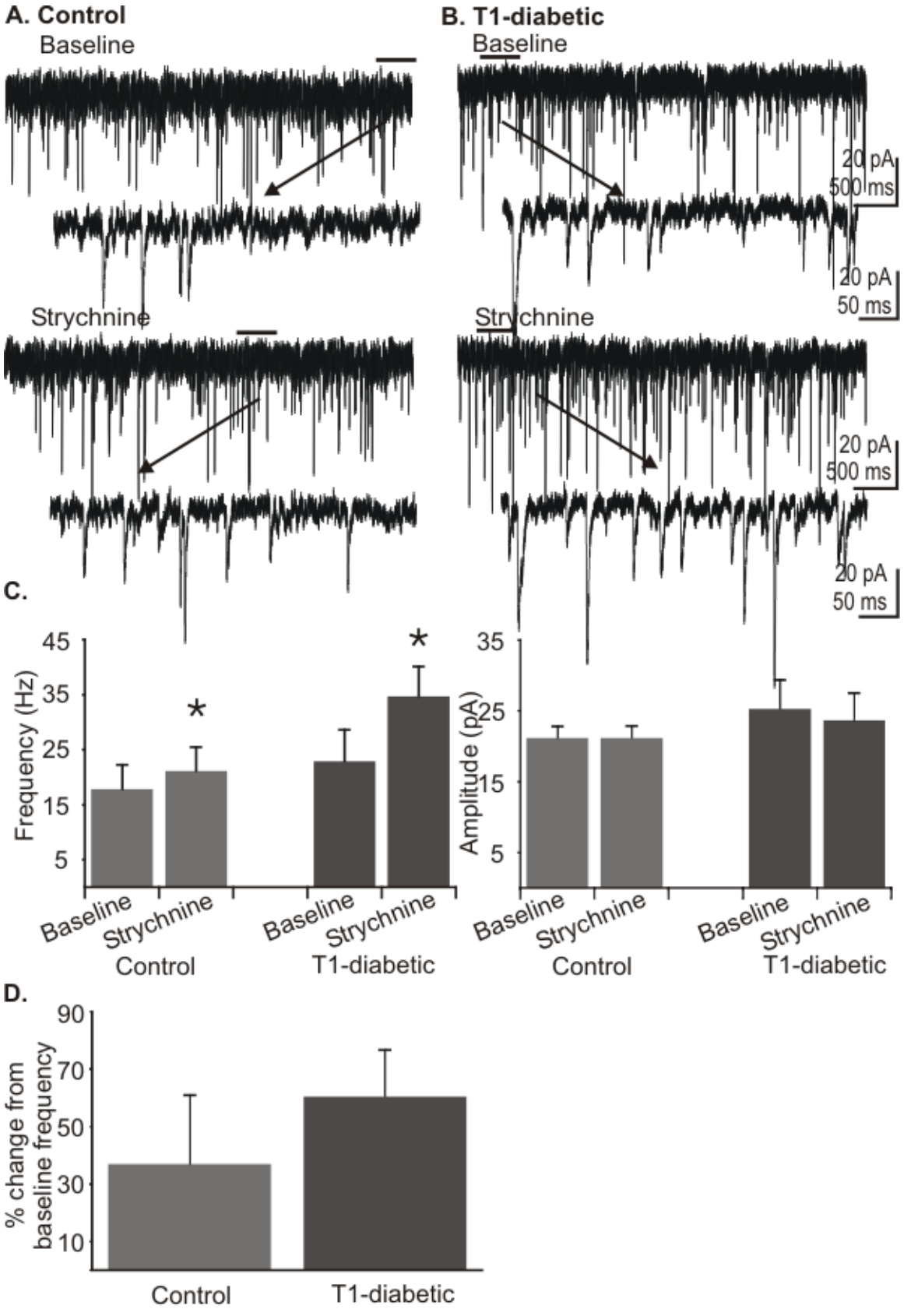
A. Control
Baseline
Strychnine
B. T1-diabetic
Baseline
Strychnine
20 pA
500 ms
20 pA
50 ms
20 pA
500 ms
20 pA
50 ms
C.
Frequency (Hz)
45
35
25
15
5
*
*
Baseline
Strychnine
Baseline
Strychnine
Control
T1-diabetic
Amplitude (pA)
35
25
15
5
Baseline
Strychnine
Baseline
Strychnine
Control
T1-diabetic
D.
% change from baseline frequency
90
70
50
30
10
Control
T1-diabetic

Figure 5.1 Strychnine antagonism resulted in an increase in mEPSC frequency. **A .** Representative recording of mEPSCs in control mice at baseline, in the presence of PTX, TTX, DTC and AP-5, (upper two traces) and in response to addition of 1-2μM strychnine (lower two traces) (n=5). **B.** Representative recording of mEPSCs in T1-diabetic mice at baseline, in the presence of PTX, TTX, DTC and AP-5, (upper two traces) and in response to 1-2μM strychnine (lower two traces) (n=4) **. C.** Average group frequency and amplitude of mEPSCs in response to strychnine. Asterisks (*) indicate significant effects of strychnine ($p<0.05$); paired two-tailed Student's t-test). **D.** Group average percent change from baseline frequency in response to strychnine ($p<0.05$; paired, two-tailed Student's t-test.

Bumetanide did not alter mEPSC frequency or inhibit the Strychnine mediated increase in mEPSC frequency

To investigate the involvement of NKCC1 in maintaining the chloride equilibrium potential at the preterminal membrane, the response of mEPSCs to the NKCC1 inhibitor bumetanide (10 μM, applied for at least 20 min) was assessed. Bumetanide application did not change the frequency or amplitude of mEPSCs recorded at -80 mV in the presence of PTX, TTX, DTC and AP-5 (9.41±3.8 Hz baseline and 10.00±3.6 Hz in bumetanide, $p=0.11$; 16.94±1.6 pA baseline and 16.12±1.5 pA in bumetanide, $p=0.20$; n=7; Figure 5.2 A, B and D). When strychnine was subsequently bath applied, the strychnine mediated increase in mEPSC frequency persisted (13.53±5.06 Hz at baseline and 15.40±5.2 Hz in

response to Strychnine, $p<0.05$; n=6; Figure 5.2 C and D). The amplitude of these events was unaffected by strychnine (17.41±0.9 pA at baseline and 17.36±0.9 pA in response to strychnine, p=0.88).

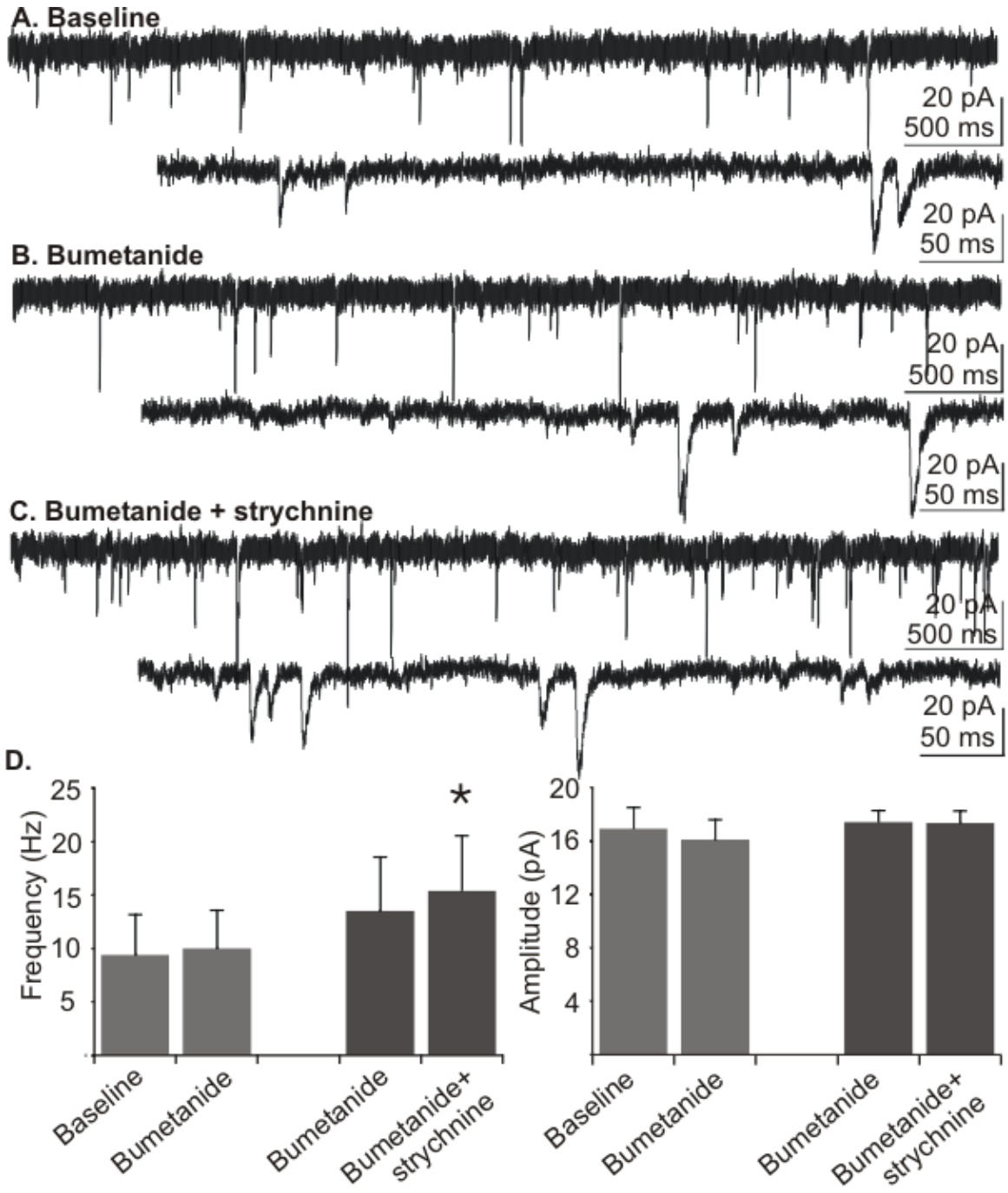

Figure 5.2 NKCC1 inhibition did not alter mEPSC frequency or inhibit the Strychnine mediated increase in mEPSCs in control mice. **A.** Representative recording of mEPSCs at baseline in control mice in the presence of PTX, TTX, DTC and AP-5 **B.** Representative recording of mEPSCs during the application of 10μM bumetanide (n=7). **C.** Representative recording of mEPSCs during the application of 1-2 μM strychnine (n=6). **D.** Average group frequency and amplitude of mEPSCs in response to bumetanide and strychnine. Statistical significance of drug application was assessed using a paired two-tailed Student's t-test. * indicates $p<0.05$.

Glycine has differential concentration effects on mEPSCs

Glycine at concentrations of 30, 100, 300 and 1000 μM were applied to neurons recorded at -80 mV in the presence of PTX or Bic, DTC, TTX and AP-5. In response to 30 μM there was a small but significant increase in the frequency of mEPSCs (14.53 ± 4.95 Hz baseline, 16.03 ± 4.41 Hz in the presence of 30 μM glycine $p<0.05$ n=5; Figure 5.3 A and C). The amplitude of these events was not changed by glycine (19.02 ± 2.64 pA baseline, 19.74± 3.16 pA in the presence of 30 μM glycine $p=0.33$). Increasing the concentration of glycine to 100 μM resulted in a decrease of mEPSC frequency (16.14 ± 2.73 Hz baseline 14.52 ± 2.25 Hz in the presence of 100 μM glycine $p<0.05$; n=5; Figure 5.3 B and C), with no effect on mEPSC amplitude (18.56 ± 3.87 pA baseline 18.33 ± 3.44 pA in the presence of 100 μM glycine $p=0.73$). While 300 μM (12.54 ± 3.98 Hz baseline 10.65 ± 3.53 Hz in the presence of 300 μM glycine; n=6; $p=0.13$) and 1000 μM

(12.92 ± 6.24 Hz baseline 7.74 ± 4.46 Hz in the presence of 1000 μM glycine; n=3; p=0.33) showed a non-significant trend toward decreasing frequency, these higher concentrations also resulted in whole-cell currents and mEPSC amplitude changes that interfered with interpretation of presynaptic changes. As a result, these higher concentrations were not further explored. The effect of glycine application was not assessed in T1-diabetic mice.

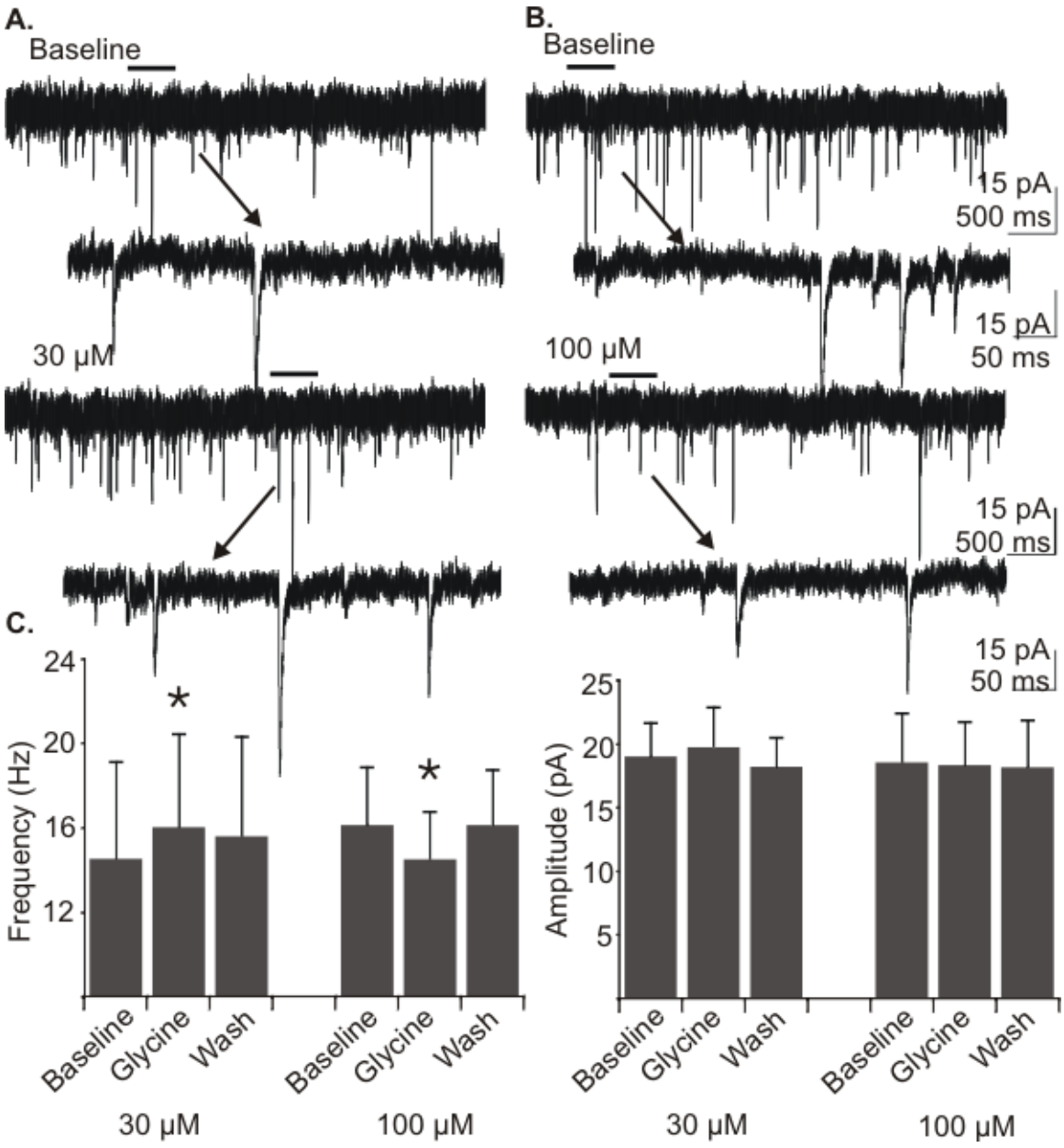

Figure 5.3 Glycine has differential concentration effects on mEPSC frequency. **A.** Representative trace of mEPSCs at baseline in the presence of PTX or Bic, DTC, TTX and AP-5 (upper two traces) and in response to 30 µM glycine (n=4) (lower two traces). **B.** Representative trace of mEPSCs at baseline in the

presence of PTX or Bic, DTC, TTX and AP-5 (upper two traces) and in response to 100 μM glycine (n=5) (lower two traces). C. Average mEPSC group frequency and amplitude in response to 30 and 100 μM glycine in the presence of PTX or Bic, DTC, TTX and AP-5 Statistical significance of drug application was assessed using a paired two-tailed Student's t-tests and * indicates $p<0.05$.

Glycine transport inhibitors did not change mEPSC parameters

Availability of glycine is partly controlled by GlyTs on neurons as well as on glial cells. Both of the two known glycine transporters have been identified in the DVC (Batten et al., 2010; Zafra et al., 1995). To test whether or not the inhibition of these transporters would result in glycine-mediated activation of glycine receptors, mEPSCs were measured in response to glycine transport inhibitors in normoglycemic controls and T1-diabetic mice. Recordings of mEPSCs were made at a holding potential of -80 mV in the presence of PTX, TTX, DTC and AP-5 prior to and following the application of the GlyT1 inhibitor, Org 24598 lithium salt (10 μM), and the GlyT2 inhibitor, ALX 1393 (0.5 μM). In normoglycemic mice, application of these receptors did not result in a significant change in mEPSC frequency (21.97±4.3 events/s baseline, 18.59±3.78 Hz in response to combined GlyT Inhibitors $p=0.08$; n=6; Figure 5.4 A and C). No change in the amplitude of mEPSCs was observed in response to GlyT Inhibitors (23.95±4.2 pA baseline, 19.31±3.1 pA in response combined GlyT Inhbitors $p=0.10$). As in control mice, the mEPSC frequency and amplitude of T1-diabetic

mice in response to GlyT1 and 2 inhibitors did not change (32.29±9.3 Hz baseline, 27.59±9.3 Hz in response GlyT Inhibitors , p=0.16 and 20.11+3.5 pA baseline, 22.16+4.6 pA in response to Org 24598 and ALX 1393 p=0.54; n=3; Figure 5.4 B and C).

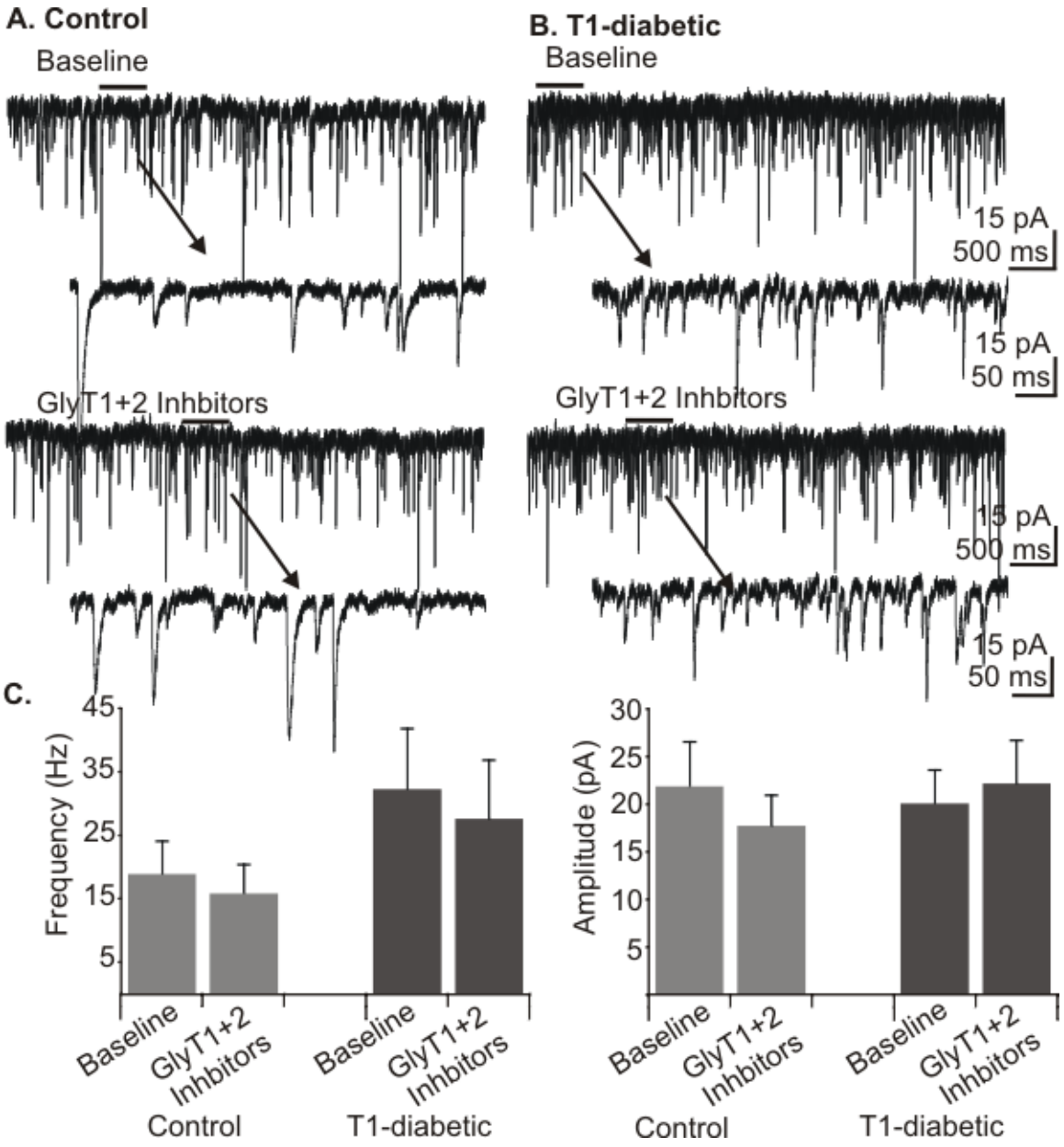

Figure 5.4 GlyT1+2 inhibitors did not change mEPSC parameters. **A.** Representative recording of mEPSCs in control mice at baseline, in the presence of PTX, TTX, DTC and AP-5, (upper two traces) and in response to 1-2μM GlyT1+2 inhbitors (lower two traces) (n=6) **B.** Representative recording of mEPSCs in T1-diabetic mice at baseline, in the presence of PTX, TTX, DTC and AP-5, (upper two traces) and in response to GlyT1+2 inhibitors (lower two traces) (n=3) **C.** Average group frequency and amplitude of mEPSCs in response to bumetanide and strychnine. **D.** Group average percent change from baseline frequency in response to strychnine. A paired two-tailed Student's t-test was used to assess statistical significance of intragroup drug application.

Org 24598 alone did not change mEPSC parameters

GlyT1 is thought to be primarily located on glial cells to prevent glycine removal from the synaptic cleft (Eulenburg et al., 2005). The GlyT1 inhibitor Org 24598 was used to measure the effect of GlyT1 on glycine availability at the synaptic cleft. Recordings were taken at -80 mV in the presence of PTX, TTX, DTC and AP-5 prior to and in the presence of Org 24598. Application of Org 24598 did not result in a change of mEPSC parameters (24.08±6.4 Hz baseline, 24.21±5.0 Hz in response to Org 24598 p=0.96 and 20.00 +2.6 pA baseline, 18.1+1.7 pA in response to Org 24598 p=0.19; n=4; Figure 5.5). Potential changes in mEPSC parameters were not measured in T1-diabetic mice.

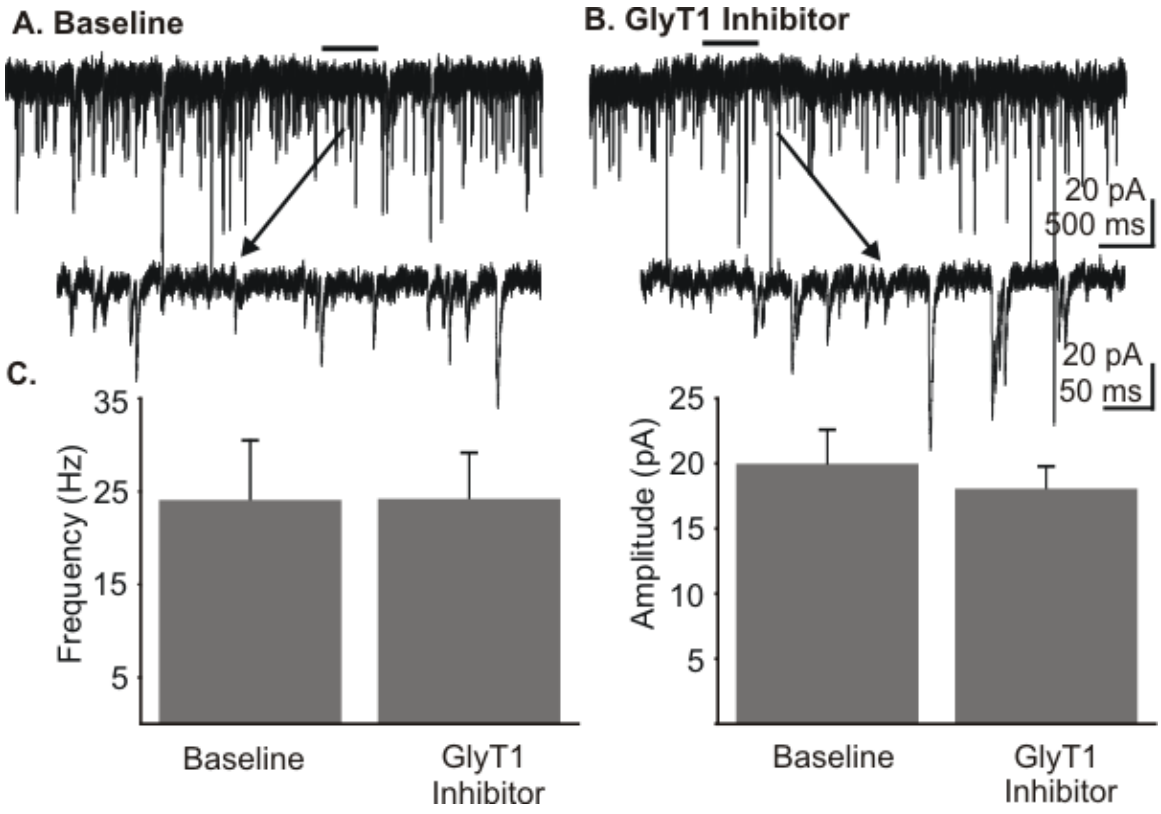

Figure 5.5 GlyT 1 inhibition by Org 24598 did not change mEPSC parameters. **A.** Representative recording of mEPSCs in control mice at baseline, in the presence of PTX, TTX, DTC and AP-5. **B.** Representative recording of mEPSCs in control mice, in response the GlyT1 inhibitor, Org 24598, in the presence of PTX, TTX, DTC and AP-5 C. Average frequency and amplitude of mEPSCs in response to GlyT1 inhibitor (n=4). A paired two-tailed Student's t-test was used to assess statistical significance.

Discussion

PreGlyR have been identified in other regions of the brain, and their activation has been linked to the tonic enhancement of excitatory and inhibitory neurotransmission (Kunz et al., 2012; Turecek and Trussell, 2001). In studies that identified a preGlyR activation mediated increase in release probability, this effect was found to be dependent on NKCC1 as a result of NKCC1's function to maintain a preterminal equilibrium potential conducive to a depolarizing influence of Cl^- influx (Kunz et al., 2012).

The result of this study using the GlyR receptor antagonist strychnine suggested the presence of preterminal glycine receptors. The increase in mEPSC frequency in the absence of a change in amplitude in response to strychnine suggested that glycine receptors are tonically active to lower glutamate release probability at terminals contacting DMV neurons. This result, therefore, would argue against a conventional role of preGlyRs in the DVC (in other regions of the brain preGlyRs inhibition causes a decrease in release probability of neurotransmitters).

The results of this study showing an increase in mEPSC frequency (suggesting and increase in the release probability of glutamate) led to hypothesis that preterminal Cl^- influx through preGlyR would hyperpolarize the preterminal membrane. To understand the differences in preGlyR function between previous studies and the present one, the effect of NKCC1 inhibition and subsequent strychnine inhibition was investigated. The NKCC1 inhibitor, bumetanide, did not have an effect on mEPSC frequency or amplitude. The strychnine-dependent

increase in mEPSC frequency persisted despite the presence of bumetanide. In previous studies, the effect of strychnine was abolished in the presence of the NKCC1 inhibitor bumetanide (Kunz et al., 2012). The results of this study argue that NKCC1 does not modulate preGlyR-dependent effects and are consistent with preGlyR underlying alternative rules of engagement.

Further experiments will need to be conducted to investigate such mechanisms. One possible player may be the potassium K^+-Cl^- co-transporter 2 (KCC2), which transports chloride outwardly and maintains a lower Cl^- equilibrium potential. As a result, during its developmental increase, it shifts chloride flux on postsynaptic currents from depolarizing to hyperpolarizing (Kunz et al., 2012; Payne et al., 1996; Stil et al., 2009). A future study examining the effect of KCC2 on strychnine-mediated effects would seem like a next logical experimental step.

Additionally, in previous studies the preGlyR was linked to a voltage-dependent calcium channel (VDCC) (Kunz et al., 2012; Turecek and Trussell, 2001). A future study addressing this link between preGlyR and VDCC would also be of interest in the context of preGlyR at terminals contacting DMV neurons. Therefore, Cd^+ could be used to study the Ca^{2+} dependence of preGlyR function.

Based on previous studies, it was hypothesized that blocking GlyTs would result in an increase in the amount of glycine available to bind to preterminal receptors. Strychnine antagonist studies suggested an increase in the release probability through the inhibition of preGlyRs. It was therefore reasoned that a GlyT inhibition-mediated increase in ambient glycine concentration, should enhance

activation of preGlyR and subsequently decrease glutamate release probability. This negative result argues that these transporters do not cause a sufficient increase in glycine to change its saturation level at preGlyRs. Alternatively, the excess glycine made available by GlyT inhibition also binds to NR3-subunit containing NMDA receptors to counterbalance the effects of glycine on GlyR (see further discussion below).

A localization of GlyT2 specific to glycinergic neurons would be expected to prevent the recycling of glycine, decreasing its vesicular release and ultimately making less glycine available. The specificity of GlyT1 and Glyt2 on glial cells and glycinergic neurons, respectively, has been challenged for some regions in the brain (Aroeira et al., 2013; Cubelos et al., 2013). The effect of GlyT1 inhibition alone was measured to rule out that GlyT2 localization on glycinergic neurons counterbalances the GlyT1 function, and mask the effects of GlyT1. (Zafra et al., 1995; Zafra et al., 1997b). The GlyT1 inhibitor Org 24598 lithium salt, however, had no effect on mEPSC parameters measured in DMV neurons from control mice. This result argues that GlyT1 does not have a significant impact on the availability of glycine on preGlyR in the DVC. Responses to Org 24598 were not measured in T1-diabetic mice. An upregulation of these transporters could be tested in T1-diabetic mice.

It remains possible that when applying exogenous glycine in the presence of a GlyTs the inability to uptake glycine would lead to a potentiation of glycine mediated preGlyR response. A comparison between the glycine mediated effect

in the presence and absence of GlyT inhibitors could be tested to better ascertain the physiological relevance mediated by these transporters. A glycine response curve to exogenously applied glycine, in the absence of inhibitors, would be necessary.

Experiments were conducted to establish an agonist response curve for glycine, but the results could not differentiate clearly between pre- and postsynaptic GlyRs and possible confounding effects mediated by NR3 subunit-containing NMDA receptors. NR3 subunit-containing diheteromeric NMDA receptors can be activated by glycine alone, in the absence of other agonists, and are not blocked by NR2 subunit-containing receptor antagonists such as AP-5 and/or MK-801 (Low and Wee, 2010; Paoletti and Neyton, 2007). Pharmacological manipulation of the NR3 subunit remains limited and further experiments would be necessary to determine whether or not these subunits are involved in mediating the small but significant increase in mEPSC frequency observed at a low glycine concentration (30 μM). Glycine induced a significant decrease in mEPSC frequency, without whole-cell current induction or amplitude change, at a concentration of 100 μM. The higher concentrations tested, 300 and 1000 μM caused a significant inward whole-cell current.

It has been argued that glycine is in the extracellular space surrounding of the synaptic cleft to allow constitutive activation and co-activation of glycine and NMDA receptors, respectively. This notion, however, has been challenged with the argument that glycine is readily cleared from the extracellular space and the

synaptic cleft through GlyTs (Berger et al., 1998; Bergeron et al., 1998). These clearing mechanisms have produced estimates of glycine concentrations around transporter microdomains that fall below saturation levels of NMDA receptors. NR3-containing NMDA receptors, therefore, create a potential confounding factor in glycine mediated effects. These subunits can be solely activated by glycine and do not show the AP-5 sensitivity seen in NR2 subunit-containing NMDA receptors. The presence of NR2-lacking NMDA receptors in the brain, however, has not been conclusively demonstrated.

The increase in mEPSC frequency at a low glycine concentration (30 μM) may be the result of NR3 subunit-containing NMDA receptor activation. Based on the current study, glycine might be predicted to have opposite effects on the membrane potential by acting at preGlyR and NR3-subunit containing preNMDA receptors. While glycine acting on NR3-subunit containing preNMDA receptors would be expected to facilitate glutamate release, glycine acting on preGlyR would be expected to lower glutamate release probability. These opposing effects may mask the significance of either receptor and cannot be appreciated from the studies conducted. Picrotoxin was used throughout most of these studies. Since picrotoxin blocks GlyR co-assembled as α- and β-subunits, their effect on preterminal glutamate cannot be appreciated by these studies and changes in subunit distribution could account for the differences in the percent change of frequency in response to strychnine in T1-diabetic mice.

The pharmacological approaches to address this question remain limited. An NR3 subunit specific antagonist that allows expression of AMPA-mediated postsynaptic EPSCs, which were used as primary outcome measures, is not available (Paoletti and Neyton, 2007). The agonist glycine could be used in the presence of strychnine and/or GlyT inhibitors to investigate the action of glycine on NR3 subunit containing preNMDA receptors. D-serine is endogenously biosynthesized enantiomer of the amino acid serine that binds to the NMDA receptor glycine binding sites (Mothet et al., 2000). D-serine is not thought to be transported by glycine transporters or to activate GlyR (Betz et al., 2006; Supplisson and Bergman, 1997). It could therefore be used in conjunction with glycine to confirm NR3 subunit-mediated glycine effects and provide a better understanding the two GlyTs may have on glycine availability. Specific agonists for GlyR are lacking and limit the understanding of their endogenous saturation state. A cross-talk between NR3-subunit containing and GlyR on preterminal membranes could be important in regulating glutamate release more tightly. Understanding the role this potential cross-talk plays on glutamate release would be interesting both in a physiological as well as pathological context (for more elaborate discussion see general discussion in Chapter 6).

The mEPSC frequency percent change in normoglycemic mice in response to strychnine was 36.97±24.1% while it was 60.05±16.2% in T1-diabetic mice. Increasing the number of neurons studied for these groups could reveal whether or not these differences are statistically significant. For a more complete

discussion on possible interpretations of significance in this result see general discussion in Chapter 6.

Chapter 6: General Discussion

Review of major findings

Preterminal NMDA receptors were previously established to be present in other regions of the brain, but their existence and functional significance of neurotransmitter release had not previously been looked at in the DVC (Aorti 1994; Berretta 1996, Marty and Glitsch 2002). Chapter 3 of this dissertation establishes the presence of preNMDA receptors on terminal contacts to the DMV, and their functional contribution to the tonic release of glutamate onto neurons within this nucleus. While their presence facilitated glutamate release, results within this dissertation argue against their presence on GABAergic terminals and functional significance to the release of GABA.

It was hypothesized that augmented facilitation by these receptors, possibly through increasing their expression, may lead to the enhanced glutamate release and excitatory drive onto DMV neurons (mEPSCs frequency increase) occurring in T1-diabetic mice.

NMDA receptors, including preNMDA receptors, were explored for their potential participation in pathological network changes in T1-diabetic mice in Chapter 4. Previous findings by Zsombok, showing an increase in mEPSC and sEPSC frequency in the absence of a change in amplitude, of T1-diabetic mice could be confirmed. NMDA dependent mechanisms underlying these changes in the release probability of glutamate were explored in Chapter 4.

Electrophysiological recordings of the DMV revealed that when NMDA receptors were blocked in the DVC of control and T1-diabtic mice, T1-diabtetic mice had a greater relative decrease in the frequency of sEPSCs. This result suggested a greater NMDA receptor mediated effect of glutamate release. The decrease in frequency in the absence of amplitude changes was consistent with a presynaptic modulation of NMDA receptors and supported their involvement in the underlying mechanisms of pathological changes in T1-diabetic mice.

The hypothesis that preNMDA receptors mediated augmented glutamate release onto DMV neurons of T1-diabetic mice could not be confirmed. While excitatory neurotransmission in both animal groups was tonically facilitated by preNMDA receptors, the relative contribution was not altered in T1-diabetic mice.

Consequently, postsynaptic NMDA receptor responses on presynaptic (NTS) neurons were investigated. An increase in the NMDA-induced whole-cell current and current density was observed and the current voltage steps revealed that this increase in whole-cell current and current density of T1-diabetic mice occurred at voltage potentials consistent with NMDA mediated responses.

Using single-cell PCR, an upregulation of NMDA subunit transcripts in a subpopulation of glutamatergic neurons could be demonstrated. Responses in these neurons showed a decrease in standard error of whole-cell current responses and current densities. When eliminating the identified VGLUT2+ neurons from the total NTS population, there was a significant difference between the current densities of control animals between the VGLUT2+ population and the total population.

These data, however, were not presented independently, because single-cell PCR was unsuccessful on many of these neurons. Their phenotype is therefore not known and they could be VGLUT2+ neurons especially since this population was biased towards non-GABA neurons by using GIN mice. GIN mice were used and electrophysiological recordings were typically targeted to those of non-GABA neurons. These neurons make up a large population of cells in the NTS.

NTS neurons are known to make direct glutamatergic synaptic connections to the DMV neurons. This result is therefore consistent with an NMDA mediated response eliciting an enhanced excitatory drive in NTS neurons. Given that the NTS and DMV form a direct functional glutamatergic connection, this increase in the excitatory drive would further be predicted to enhance excitatory neurotransmission on DMV neurons and is consistent with an the observed increase in sEPSCs observed on DMV neurons (Travagli 2011).

NMDA receptor modulation of whole-cell current (WCC) responses could be due to changes in the number of receptors present, reshuffling of receptor subunits, and/or receptor trafficking (Collingridge et al., 2004; Traynelis et al., 2010).

The total number of receptors should be reflected by the expression of the NR1 subunits, as this is the necessary receptor subunit for functional NMDA receptors (Traynelis et al., 2010). Protein expression of the NR1 subunit between control and T1-diabetic mice but was not statistically significant although we were able to observe trend towards an increase in NR1 expression in T1-diabetic

mice. Gene expression changes were analyzed for all seven NMDA receptor subunits, but no differences between control and T1-diabetic mice were observed in any of these subunits. This result likely reflects a more global problem in identifying changes between groups of animals in a heterogeneous population of cells (but see discussion below).

Preterminal mechanisms in control and T1-diabetic mice

The experiments conducted throughout this dissertation were unable to identify changes in synaptic plasticity at the presynaptic terminal suggested by the increase in mEPSC frequency of T1-diabetic mice. Nonetheless, the function of preNMDA receptors to facilitate glutamate release onto DMV neurons remains intact. Consequently, it could be conceivable to identify and manipulate such specific preterminal mechanisms. With the prediction that enhanced vagal output leads to a physiological response of lowering blood glucose concentrations, by extension, the NMDA-mediated enhancement of excitatory neurotransmission would serve as counter-regulatory mechanism in T1-diabetic mice. If this is indeed the case, driving this process may serve as a potential site to pharmacologically interfere with this process during acute states of hyperglycemia that can lead to a number of different complications. Therefore gaining a better understanding about the specific mechanisms involved in preterminal facilitation would be valuable.

PreNMDA receptor subunits effects in the DVC

Pharmacological limitations did not allow a full profile of preNMDA receptors to be made, but the use of Zn^{2+} suggested that NR2A subunits are most likely involved in the tonic modulation of glutamate release mediated by NMDA receptors (Paoletti et al., 1997). NR2C/NR2D or NR3 subunit specific antagonists are not currently available. NR3 subunits are not inhibited by AP-5 or activated by NMDA although triheteromeric receptors are thought to be affected by both (Paoletti and Neyton, 2007).

PreNMDA receptors containing NR2C and NR2D or NR3-subunit are less permeable to Ca^{2+} than NR2A and NR2B subunit containing receptors with NR3-subunit containing nearly completely lack Ca^{2+} permeability (Cull-Candy and Leszkiewicz, 2004; Henson et al., 2010; Paoletti and Neyton, 2007). The subunit identity is of particular interest for understanding the mechanisms for eliciting an increase in the probability of glutamate release. Therefore, these subunits and in particular the NR3-subunit at the preterminal membrane, that mediate this change towards indirect modulation of Ca^{2+} influx. The lack of Mg^{2+} sensitivity make them a likely NMDA-receptor subunit to be involved in tonic modulation of glutamate release and their presence in preNMDA receptors has been shown (Larsen, Philpot, Corlew 2011). Due to their concomitant lack of Ca^{2+} influx, it would be predictable that when searching for mechanistic underpinnings of glutamate release to look at more indirect increases in the level of Ca^{2+}. A local depolarization of the preterminal membrane could subsequently activate VDCC channels.

Cross-talk of preNMDA- and preGlyR receptors in the DVC in the context of development and synaptic plasticity

While antagonist approaches remain limited, the agonist glycine can activate these receptors and has therefore presented itself as an agonist to be used in studies of preNMDA NR3-subunit receptors (Henson, Philphot 2011). The prominent opinion holds that D-serine acts as an agonist on this receptor subunit, although some controversy regarding this opinion has been sparked (Nilsson, Sundstrom 2007; Yao and Mayer 2006, Chatterton, Zhang, 2002). Consequently studies looking into NR3-subunit containing receptors used glycine as an agonist. The GlyR specific antagonist strychnine was used in these studies to prevent potential interference of results underlying preGlyR activation. This experimental approach revealed a strychnine sensitive response suggesting the presence of preGlyR. These results were particularly interesting for further exploration, because they suggested a cross talk at the preterminal membrane between preGlyR and preNMDA receptors.

Understanding the role of NR3A-subunit containing receptors is of particular interest due to their high expression levels in the DVC as identified by mRNA expression using NanoSting®. While the subunit expression was not altered in T1-diabetic mice, it showed the highest expression levels of any of the subunits other than the obligatory NR1 subunit. In other regions of the brain the primary consensus holds that this subunit undergoes a developmental increase

in expression until P4-P10, but then drops to low levels in adulthood (Henson et al., 2010). In the amygdala, however, highest expression of this subunit is observed at adulthood (Wong et al., 2002). It cannot be assumed that NR3 expression is highest at the adult stages measured throughout these experiments. It does provide justification to look at expression changes for this subunit throughout development. Regardless of its developmental profile, its high adult gene expression argues that this subunit plays a prominent role in the DVC. Preliminary results obtained from presynaptic studies suggest that this subunit may potentially be located at preterminal membranes to facilitate glutamate release (see Chapter 5).

As prior, pharmacological limitations of NR3 antagonists and specific glycine receptor agonists makes studying these receptors in isolation limited (see Chapter 5 discussion for additional pharmacological approaches). The role of these receptors and the role GlyTs play in maintaining an appropriate excitatory and inhibitory balance under physiological as well as pathological states presents itself as an interesting question.

Preterminal results suggest that GlyR inhibition of preterminal glutamate may be enhanced in T1-diabetic mice (greater percent change of mEPSC frequency). It has recently been established that glycine and glutamate are colocalized in presynaptic terminals. Excitatory stimulation elicits a release of stored glycine and has suggested that glycine and glutmate are coreleased (Muller, Bergeron, 2013). If present in the DVC, this form of corelease could present itself as a form of preterminal balance between inhibitory preGlyR and

excitatory preNMDA receptor function. Modulating this balance could thus be the function of glycine-activated preNMDA receptors and preGlyR moving closer or further away from one another. Their proximity to each other may significantly affect the preterminal consequence of circulating glycine and underlie a compensatory mechanism or exacerbate preterminal hyperexcitability seen in T1-diabetic mice. Modulation of GABAergic release was not tested as part of these studies, but should be conducted in the future form a more complete picture of a preterminal excitatory-inhibitory balance as a function of preGlyR and preNMDA receptor cross-talk. Similarly, these cross-talks may balance excitatory and inhibitory neurotransmission at postsynaptic membrane receptors in the DVC.

Beyond the pharmacological approaches and limitations discussed as part of Chapter 5, ultrastructural and/or knock-out studies, may aid in shedding light on these hypotheses. It would be interesting whether these two receptors diffuse across the membrane in a manner that allows them to move closer or further apart from one another and therefore potentially alter the effective concentration of glycine observed at each receptor. This in turn could alter the balance of glutamate release at the terminal. The use of electron microscopy could, therefore, not only support the presence of these two receptors on glutamatergic preterminal membranes, but may detect concerted trafficking as a function of T1-diabetes induced synaptic plasticity.

NMDA receptors on NTS neurons of normal and T1-diabetic mice

While the results of this study establish enhanced NMDA-mediated whole-cell currents and current densities, they open up a large array of questions that remain to be explored further. Changes in NMDA receptor mediated responses could be due to changes in the number of receptors present, reorganization of receptor subunits, and/or receptor trafficking (Collingridge et al., 2004; Traynelis et al., 2010).

The total number of receptors should be reflected by the expression of the NR1 subunits, as this is the necessary receptor subunit for functional NMDA receptors (Traynelis et al., 2010). Protein expression of the NR1 subunit between animal groups but was not statistically significant difference although we were able to observe a trend towards an increase in NR1 expression in T1-diabetic animals.

Limitation of whole slice analysis in the of subpopulation specific changes

What must be taken into consideration, however, are experimental limitations of isolating solely the NTS region of the DVC. Tissue extracts typically also contained other areas including the DMV and the area postrema (AP) along with other prominent connections to the NTS. No recordings were conducted in the AP, and evidence for or against NMDA receptor changes between control and T1-diabetic animals cannot be discussed.

Electrophysiological recordings in the DMV did not suggest changes of postsynaptic receptors based on changes in amplitude or decay time, although

no conclusive studies to test this hypothesis were conducted. In all experiments, voltage clamp recordings of EPSCs were made at -60 or -80 mV. At these potentials Mg^{2+} dependent voltage block of NMDA receptor would remain largely intact (unless diheteromeric NR3-subunit containing NMDA receptors make up a substantial NMDA receptor population) and prevent interpretation of postsynaptic receptors. Based on the enhanced presynaptic excitatory neurotransmission an increased expression of NMDA receptors, possibly as a consequence of LTP_{NMDA} and LTD_{NMDA} –like mechanisms, on these neurons would not be surprising (Paoletti et al., 2013).

In the context of a failure to observe changes in NR1 expression levels, however, a lack of increased expression in the DMV and the AP could limit the needed sensitivity to observe changes specific only to NTS regions of the DVC.

Additionally, the NTS consists of a heterogeneous population of cells and NR1 expression was hypothesized only to be enhanced in the glutamatergic population (no change in IPSCs between control and T1-diabetic mice). Given that only a subpopulation of neurons in the NTS are of the VGLUT2+ phenotype, limitations of sensitivity to protein expression in the total NTS neuron population would persist. It could even be possible that other NTS phenotypic populations' exhibit decreased NMDA expression patterns.

Addressing the correlation of NMDA expression in other phenotype and between animal groups could be interesting both in a physiological and pathological context. Overall the identification of increased whole-cell currents argues for a greater NMDA mediated component of excitatory

neurotransmission, which would, in the presence of sufficient glutamate, be expected to lead to more prolonged membrane depolarization (Traynelis et al., 2010). In the dorsal vagal complex this could be result of converging inputs of the various metabolic, hormonal and synaptic inputs interpreted by the nuclei of the DVC.

Apart from the VGLUT2+ phenotype, a VGLUT3+ glutamatergic phenotype has also been shown to have high expression in NTS neurons. VGLUT2 and VGLUT3 do not colocalize in terminals of the NTS and are therefore thought to be distinct population. While either glutamatergic phenotype would be expected to lead to an enhanced excitatory neurotransmission in synaptically connected DMV neurons, an enhanced NMDA receptor mediated excitatory drive in GABAergic neurons would result in an inhibitory downstream effect. Moreover, it is possible that the glutamatergic neurons in question do not directly synapse onto DMV neurons but rather on local GABA or other network neurons. Both of these possibilities could result in an opposing functional outcome by enhancing the inhibitory drive to DMV neurons, but this form of plasticity would also be expected to modulate the release of GABA and an increase IPSC frequency. The failure to detect such an increase, therefore, argues against a presynaptic enhancement in GABAeregic neurons. As a result the most likely conclusion is that increased NMDA-mediated postsynaptic currents in VGLUT2+ positive neurons enhance excitatory neurotransmission.

Overall the array of phenotypes that could have vastly distinct changes in NMDA receptor expression and resultant electrophysiological responses, limits

the interpretation of protein expression or mRNA expression experiments conducted in slices of the DVC. Tissue extracts typically also contained other areas including the DMV and the AP. No recordings were made in the AP and potential NMDA receptor changes in T1-diabetic mice cannot be discussed as part of these studies.

Single-cell approached that can directly link electrophysiological responses with expression changes are as well as specific neuronal populations, would provide a better understanding the overall effect on excitatory neurotransmission. In studies of this dissertation, this approach was used for VGLUT2+ phenotypic identification. Apart from a VGLUT2+ phenotype, VGLUT3 expression has also been identified in the NTS and the two transporters are not thought to co-localize and therefore to make up independent populations of glutamatergic neurons (Lin et al., 2004; Lin and Talman, 2005). A primer VGLUT1 and VGLUT3 was not used to probe for this transporter, but an experiment to this effect could be conducted in the future. VGLUT1 has been shown to be expressed in the NTS but to a much more limited extent in subregions of the NTS (Hermes et al., 2013; Lin, 2009; Lin et al., 2004; Lin and Talman, 2005). Ideally expression of all three VGLUTs could be looked at with VGLUT1 and VGLUT3 being used as additional markers that should be able to target most glutamatergic NTS neurons. Apart from phenotypic identification it would be of particular interest in the context to link electrophysiological responses to quantitative changes of NMDA receptors and its subunits. Both TaqMan based PCR or single cell nCounter® NanoString has been shown to

have the necessary sensitivity to detect quantitative expression changes at the level of single-cells (Stahlberg, Bengtsson 2010).

Subunit specific modulation in the DVC

In addition to changes in the number of receptors, subunit changes may be involved in modulating NMDA receptor responses. As discussed in Chapter 1, NMDA receptor subunits confer distinct kinetic profiles on NMDA receptors.

To reiterate briefly, decay times span a ~50 fold range in the order NR2A< NR2B<NR2C<NR2D from fastest to slowest (Cull-Candy and Leszkiewicz, 2004). Mg^{2+} sensitivities correlate with Ca^{2+} permeability and are high for NR2A/B subunits, low for NR2C/D-subunits and do not play a role in NR3 subunit containing receptors (Ciabarra et al., 1995; Paoletti and Neyton, 2007). NR3 subunits, however, are not activated by NMDA or blocked by AP-5 and can therefore only be discussed as having an involvement in triheteromeric receptors (NMDA receptor dependent changes were observed in response to these pharmacological agents (Henson et al., 2010; Paoletti and Neyton, 2007).

The protein expression of these subunits was not tested but quantitative subunit expression changes were analyzed at the level of mRNA using NanoString®. No gene expression changes were observed between control and T1-diabetic mice. These results are subject, however, to the same limitation of brain slices containing heterogeneous cell populations of cells. More globally it argues that expression changes of pathological states of the DVC needs to be

investigated in phenotype specific cell populations. The subunit specific discussion is targeted to changes in specific phenotypic populations.

Based on electrophysiological current-voltage responses observed in this study, subunit switches in T1-diabetic animals were predicted. Both animal groups showed a nonlinear current voltage response suggestive of a Mg^{2+} dependent voltage sensitivity, but maintained a substantial inward current at negative potentials normally exhibiting Mg^{2+}-dependent block (Nowak et al., 1984). This limited voltage sensitivity in NTS neurons at baseline conditions (figure 4.6.B) is consistent with high NR3-subunit expression in the DVC as indicated by mRNA expression levels.

Current-voltage responses showed a trend towards increased voltage sensitivity in T1-diabetic mice and some neurons in a proportion of cells in T1-diabetic mice. This was enhanced in some neurons to a greater proportion in T1-diabetic mice, but phenotypic identifications were not made in sufficient number of neurons to link them to a particular phenotype. Increased voltage sensitivity would argue for an increase in magnesium sensitivity and a greater proportion of NR2A/B subunits over NR2C/D or NR3 subunits (Henson et al., 2010; Wyllie et al., 2013). During early development NR2B are thought to be the primary subunit type present in the brain and are gradually replaced by NR2A subunits making these subunits the primary subtype during adulthood (Monyer et al., 1994). Although adult mice were used in these studies, it is possible that under conditions of synaptic plasticity, a juvenile-phenotype becomes reinstated and allows the nucleus greater freedom to modulate its circuitry under pathological

states, possibly in an attempt to mount counter-regulatory responses such as decreasing liver gluconeogenesis.

The NR2B specific antagonist, Org 25-6981 (Tocris), could be used to address this question further. To address alterations in Ca^{2+} permeability, Ca^{2+} imaging studies could be conducted and may provide supporting evidence for subunit substitutions of subunits with low Ca^{2+} permeability. The NR3 subunit is essentially impermeable to Ca^{2+}, when expressed only in conjunction with NR1 subunits. While the expression of NR1/Nr3 subunits has been shown in heterologous expression systems to make functionally ion conducting channels, their expression in vivo is still being questioned. When expressed with NR2 subunits, however they are thought to exist as triheteromers in vivo and decrease the conduction when compared to NR/1NR2 containing of NMDA receptors. Ca^{2+} imaging studies in conjunction to the subunit specific pharmacological agents that are available aid in strengthening support for the significance in synaptic modulation as a function of the NR3 subunit (Henson et al., 2010; Pachernegg et al., 2012).

Receptor trafficking and LTP/LTD dependent synaptic plasticity

Finally, receptor trafficking from internal stores as well as from extrasynaptic sites into the PSD may contribute to altered excitatory inputs observed in studies throughout this dissertation. Trafficking can occur from internal as well as from extrasynaptic sites. Whole-cell currents were targeted to activate all NMDA receptor populations on NTS neurons, and trafficking of

extrasynaptic receptor as a result of T1-diabetes would be expected to activate similar population of NMDA receptors and lead to similar whole-cell current responses. Trafficking from internal, however, has been shown previously and would introduce a new receptor population to the membrane to increase current amplitudes. Consequently, receptor trafficking from internal stores presents itself as a plausible explanation of enhanced NMDA receptor function even in the absence of expression changes.

The frequency of sEPSC in downstream neurons may be more sensitive towards detecting changes in trafficking given that only receptors in the PSD or perisynaptic receptors would be expected to alter firing properties. Therefore receptor trafficking from extrasynaptic sites into to the PSD could explain increased sensitivity of AP-5 on sEPSCs (a greater relative percent decrease in frequency in response to AP-5).

The concept of receptor trafficking becomes more interesting in the context of LTP and LTD. Although studies to this effect were not conducted as part of this dissertation, precedent for changes in both of these mechanism in T1-diabetes exists and opens up a large array of future experimental approaches (Artola, A 2005). In the hippocampus for example, LTP and LTD are of comparable magnitude in T1-diabetic animals, but long term depression is facilitated and LTP is inhibited. These studies were conducted in rats maintained hyperglycemic for multiple months (Artola et al., 2005). It would be interesting to test whether responses over prolonged hyperglycemia would lead to similar changes in LTP and LTD mechanisms. Combining such studies with more short

term studies would be interesting in understanding whether these changes persist long term or are rather transient changes for a system in flux. Signaling mechanisms of LTP and LTD have been extensively studied and some of their players may eventually serve as targets for therapeutic approaches. In particular the NR3-subunit is thought to play a prominent role in LTD mechanisms, and would be an interesting player to focus on in studies of T1-diabetic mice in the DVC. Given that this subunit generally shows low expression in many other regions of the brain, but high expression in the DVC, future pharmacological advances in this subunit may prove themselves as relatively specific therapeutic agents for the DVC.

Final Conclusion

While NMDA mediated effects on normal physiological function in the DVC have been well established, this study is the first to identify preNMDA receptors on terminal contacts to DMV neurons and changes in NMDA receptor function under pathological conditions of T1-diabetes in the DVC. Evidence throughout this dissertation provides support that changes in NMDA receptors contribute to the mechanisms of augmenting excitatory neurotransmission in the DVC. The altered receptor responses in this dissertation, as a result of metabolic dyshomeostatis in pathological states of T1-diabetes, would argue for the need of more expansive studies. It remains unclear if this response serves a compensatory mechanism, possible by lowering gluconeogeneis or whether this is a physiological response spun out of control.

The predicted well known mechanism of synaptic plasticity, such as LTP, would be expected to strengthen and possibly alter synaptic circuitry and bestow urgency on the need to better understand its processes in the DVC. If the DVC preserves its ability to modulate synaptic circuitry, it may potentially serve as a target region to mount pharmacological counterregulatroy responses.

The high expression of an NMDA receptor subunit that lowers ionic conductance, notably of Ca^{2+}, is only minimally sensitive to Mg^{2+} and can be activated by glycine, should be explored further. This subunit may change the rules of synaptic conductance mediated by NMDA receptors in the DVC while possibly communicating closely with Glycine mediated inhibitory drives. It will be important to understand these mechanisms as NR3A subunit expression is thought to be low in adult animals in other regions of the brain. It may prove itself as a potential relatively specific pharmacological target.

Appendices

Appendix 1: List of Abbreviations

AMPA- α-amino-3-hydroxy-5-methyl-4-isoxazolepropionic acid

ACSF- Artificial cerebrospinal fluid

ABD- Agonist binding domain

AP- Area prostrema

AP-5- DL-2-Amino-5-phosphonopentanoic acid

Bic- Bicuculline methiodide

CaMKII- Calcium/calmodulin-dependent protein kinase II

CNQX- 6-Cyano-7-nitroquinoxaline-2,3-dione

CTD- C-terminus domain

DMV- Dorsal motor nucleus of the vagus nerve

DVC- Dorsal vagal complex

DTC- d-tubocurarine chloride

EPSC- Excitatory postsynaptic current

fwd- forward

IPSC- Inhibitory postsynaptic current

HFS- high frequency stimulation

Hz- hertz

GlyR- Glycine receptor

GlyT- Glycine transporter

LTD- long term depression

LTP- long term potentiation

mEPSC- miniature EPSC

mGLUR- metabotropic glutamate receptor

min- minutes

mIPSC- miniature IPSC

MK-801- -(+)-5-Methyl-10,11-dihydro-5H-dibenzo[a,d]cyclohepten-5,10-imine hydrogen maleate or dizocilpine

NMDA- *N*-methyl-D-aspartic acid

NTD- N-terminal domain

NTS- Nucleus of the solitary tract

P- Postnatal

preGlyR- presynaptic glycine receptor

preNMDA- presynaptic NMDA

PPr- Paired-pulse ratio

PSD- postsynaptic density

PTX- Picrotoxin

rev- reverse

RIN- RNA integrity number

RPM- revolution per minute

T1-diabetic- Type 1 diabetic

TMD- transmemrane domain

TTX- Tetrodotoxin

s- seconds

sEPSC- spontaneous EPSC

sIPSC- spontaneous IPSC

STZ- Streptozotocin

VGLUT- Vesicular glutamate transporter

Appendix 2: Equipment used for Electrophysiological data acquisition and brainstem slice preparation

List of Equipment

Vibrating Microtome (Vibratome 1000 Plus)

Pipette Puller (Sutter P-87)

Vibration Isolation Table (TMC)

Microscope (Olympus BX51WI)

Digitizer (Digidata 1320A and 1440A)

Patch-Clamp Amplifier (Axopatch 200B or Multiclamp 700B)

Signal timer for electrical stimulation (Master-8)

Neuro-corder (Model DR-484)

Set up and connection diagram of instruments used for electrophysiological recordings

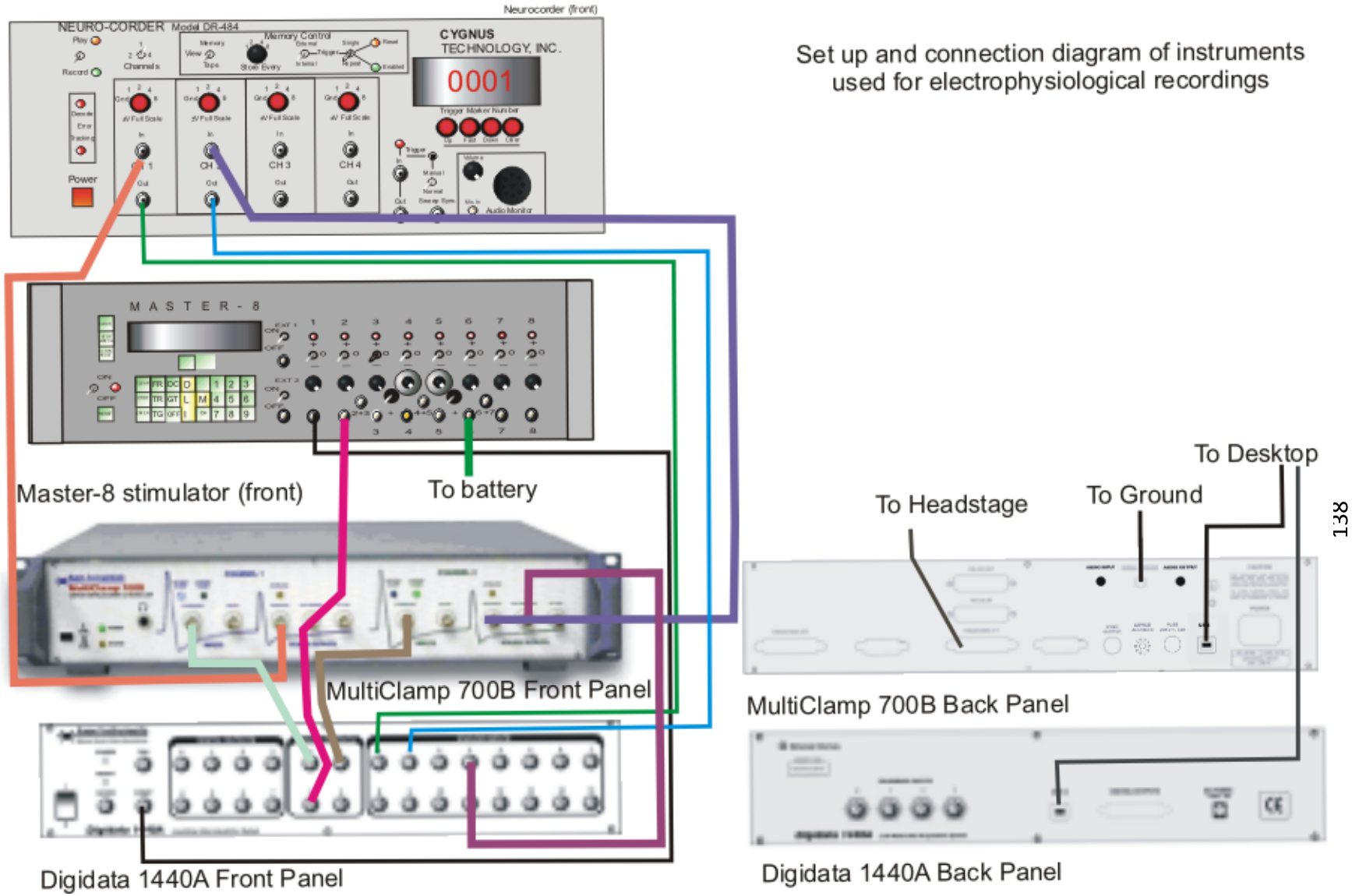

Appendix 3: Codeset for NanoString based experiments

Gene Name	NanoString Probe ID	Gene Name	NanoString Probe ID
Abcc8	NM_011510.3:1740	Grin3a	NM_001033351.1:1332
Actb	NM_007393.3:1138	Grin3b	NM_130455.2:2030
Dbh	NM_138942.3:254	Hprt	NM_013556.2:30
Gabra1	NM_010250.4:905	Insr	NM_010568.2:8314
Gabra4	NM_010251.2:3340	Itgam	NM_001082960.1:3025
Gabrd	NM_008072.2:475	Kcna1	NM_010595.3:5725
Gabrg2	NM_177408.5:1613	Kcnq2	NM_001003824.1:660
Gad1	NM_008077.4:3090	Mag	NM_010758.2:116
Gad2	NM_008078.2:769	Nr3c1	NM_008173.3:1800
Gapdh	NM_001001303.1:890	Pnmt	NM_008890.1:535
Gck	NM_010292.4:862	Ppif	NM_134084.1:534
Glra1	NM_020492.3:622	Rbfox3	NM_001024931.2:2700
Glrb	NM_010298.5:704	Scn8a	NM_001077499.1:8560
Glul	NM_008131.3:2145	Slc17a6	NM_080853.3:2825
Gria1	NM_001252403.1:2476	Slc17a8	NM_182959.3:2275
Gria2	NM_001039195.1:300	Slc2a4	NM_009204.2:275
Gria3	NM_016886.3:390	Slc32a1	NM_009508.2:2616
Gria4	NM_001113180.1:1274	Syn1	NM_013680.3:2930
Grin1	NM_008169.2:492	Th	NM_009377.1:235
Grin2a	NM_008170.2:4080	Ubc	NM_019639.4:21
Grin2b	NM_008171.3:6340	Vdac1	NM_011694.4:562
Grin2c	NM_010350.2:2720		
Grin2d	NM_008172.2:1201		

Appendix 4. Glucose concentrations of T1-diabetic animals used for experiments

T1-diabetic mice used for experiments in Chapter 4

sEPSCs T1-diabetic		
Date of experiment	**Cell**	**Glucose conc.**
5/19/2011	6	444
4/21/2011	3	596
4/9/2011	1	600
4/9/2011	3	600
4/9/2011	10	600
4/9/2011	10	600
4/4/2011	1	532
3/16/2011	2	600
3/15/2011	3	600
3/15/2011	4	600
3/14/2011	1	600
3/14/2011	1	600
1/10/2010	5	584
1/11/2011	3	579
1/10/2011	2	584
1/9/2011	3	600
12/9/2010	3	575
1/24/2011	2	600
1/11/2011	1	579
1/9/2011	1	600
group average (cells)		**583.65**
group average (animals)		**573.64**

mEPSCs T1-diabetic		
Date of experiment	**Cell**	**Glucose conc.**
3/14/2011	4	600
4/22/2011	4	541
4/21/2011	6	596
4/21/2011	5	596
3/15/2011	5	600
4/4/2011	4	582
4/9/2011 animal 1	5	600
4/9/2011 animal 2	14	600
5/19/2011	1	444
5/19/2011	2	444
5/27/2012	1	600
5/27/2012	2	600
5/4/2012	1	442
5/4/2012	3	442
5/4/2012	3	442
6/27/2012	9	335
7/6/2012	2	461
5/18/2011	1	600
5/18/2011	2	600
5/18/2011	4	600
group average (cells)		**536.25**
group average (animals)		**538.54**

sEPSC with AP-5 application T1-diabetic		
Date of experiment	**Cell**	**Glucose conc.**
1/10/2010	5	584
1/11/2011	3	579
1/10/2011	2	584
1/9/2011	3	600
12/9/2010	3	575
1/24/2011	2	600
	group average (cells)	**587.00**
	group average (animals)	**587.60**

mEPSC with AP-5 application T1-diabetic		
Date of experiment	**Cell**	**Glucose conc.**
3/14/2011	4	600
4/22/2011	4	541
4/21/2011	6	596
4/21/2011	5	596
3/15/2011	5	600
4/4/2011	4	582
4/9/2011 animal 1	5	600
4/9/2011 animal 2	14	600
5/19/2011	1	444
5/19/2011	2	444
group average (cells)		**560.30**
group average (animals)		**566.14**

WCC Currents and IV-responses T1-diabetic		
Date of experiment	**Cell**	**Glucose conc.**
4/22/2013	1	461
4/22/2013	2	461
4/22/2013	3	461
4/22/2013	4	461
4/22/2013	5	461
4/22/2013 animal 2	6	600
4/22/2013 animal 2	7	600
4/22/2013 animal 2	8	600
4/22/2013 animal 2	9	600
4/22/2013 animal 2	10	600
4/27/2013	1	461
4/27/2013	2	461
4/27/2013	4	461
5/15/2013	1	505
5/15/2013	2	505
5/15/2013	3	505
5/15/2013	4	505
5/16/2013	1	407
5/16/2013	2	407
5/16/2013	3	407
6/9/2013	2	477
	group average (cells)	**495.52**
	group average (animals)	**485.17**

Table 8.

Protein Expression NR1 T1-diabetic	
Animal	**Glucose conc.**
T1-diabetic 1	491
T1-diabetic 2	600
T1-diabetic 3	429
T1-diabetic 4	600
T1-diabetic 5	600
T1-diabetic 6	434
group average (animals)	**525.67**

Protein Expression NR1 T1-diabetic	
Animal	**Glucose conc.**
T1-diabetic 1	600
T1-diabetic 2	599
T1-diabetic 3	600
T1-diabetic 4	600
T1-diabetic 5	600
group average (animals)	**599.80**

Mice used for experiments in Chapter 5

Strychnine application T1-diabetic		
Date of experiment	**Cell**	**Glucose conc.**
11/16/2012	4	335
11/21/2012	2	600
2/25/2013	1	490
7/23/2013	4	470
	group average (cells)	**473.75**
	group average (animals)	**473.75**

Glycine Transport Inhibitors T1-diabetic		
Date of experiment	**Cell**	**Glucose conc.**
9/27/2012	3	528
9/27/2012	2	528
9/25/2012	3	600
	group average (cells)	**552.00**
	group average (animals)	**564.00**

References

Ahren, B., G. Sundkvist, H. Mulder, and F. Sundler. 1996. Blockade of muscarinic transmission increases the frequency of diabetes after low-dose alloxan challenge in the mouse. *Diabetologia*. 39:383-390.

Aoki, C., C.G. Go, K. Wu, and P. Siekevitz. 1992. Light and electron microscopic localization of alpha subunits of GTP-binding proteins, G(o) and Gi, in the cerebral cortex and hippocampus of rat brain. *Brain Res*. 596:189-201.

Aoki, C., C. Venkatesan, C.G. Go, J.A. Mong, and T.M. Dawson. 1994. Cellular and subcellular localization of NMDA-R1 subunit immunoreactivity in the visual cortex of adult and neonatal rats. *The Journal of neuroscience : the official journal of the Society for Neuroscience*. 14:5202-5222.

Aragon, M.C., C. Gimenez, and F. Mayor. 1987. Stoichiometry of sodium- and chloride-coupled glycine transport in synaptic plasma membrane vesicles derived from rat brain. *FEBS letters*. 212:87-90.

Aroeira, R.I., A.M. Sebastiao, and C.A. Valente. 2013. GlyT1 and GlyT2 in brain astrocytes: expression, distribution and function. *Brain structure & function*.

Artola, A. 2008. Diabetes-, stress- and ageing-related changes in synaptic plasticity in hippocampus and neocortex--the same metaplastic process? *European journal of pharmacology*. 585:153-162.

Artola, A., A. Kamal, G.M. Ramakers, G.J. Biessels, and W.H. Gispen. 2005. Diabetes mellitus concomitantly facilitates the induction of long-term depression and inhibits that of long-term potentiation in hippocampus. *The European journal of neuroscience*. 22:169-178.

Babic, T., K.N. Browning, Y. Kawaguchi, X. Tang, and R.A. Travagli. 2012. Pancreatic insulin and exocrine secretion are under the modulatory control of distinct subpopulations of vagal motoneurones in the rat. *The Journal of physiology*. 590:3611-3622.

Bach, E.C., and B.N. Smith. 2012. Presynaptic NMDA receptor-mediated modulation of excitatory neurotransmission in the mouse dorsal motor nucleus of the vagus. *Journal of neurophysiology*. 108:1484-1491.

Balfour, R.H., A.M. Hansen, and S. Trapp. 2006. Neuronal responses to transient hypoglycaemia in the dorsal vagal complex of the rat brainstem. *The Journal of physiology*. 570:469-484.

Balfour, R.H., and S. Trapp. 2007. Ionic currents underlying the response of rat dorsal vagal neurones to hypoglycaemia and chemical anoxia. *The Journal of physiology*. 579:691-702.

Barber, W.D., and T.F. Burks. 1983. Brain stem response to phasic gastric distension. *The American journal of physiology*. 245:G242-248.

Barber, W.D., and T.F. Burks. 1987. The response of brainstem neurons to chemical activation of gastric sensory receptors. *Gastroenterology clinics of North America*. 16:521-524.

Barria, A., D. Muller, V. Derkach, L.C. Griffith, and T.R. Soderling. 1997. Regulatory phosphorylation of AMPA-type glutamate receptors by CaM-KII during long-term potentiation. *Science*. 276:2042-2045.

Batten, T.F., D.V. Pow, and S. Saha. 2010. Co-localisation of markers for glycinergic and GABAergic neurones in rat nucleus of the solitary tract: implications for co-transmission. *Journal of chemical neuroanatomy*. 40:160-176.

Beato, M., P.J. Groot-Kormelink, D. Colquhoun, and L.G. Sivilotti. 2004. The activation mechanism of alpha1 homomeric glycine receptors. *The Journal of neuroscience : the official journal of the Society for Neuroscience*. 24:895-906.

Bellone, C., and R.A. Nicoll. 2007. Rapid bidirectional switching of synaptic NMDA receptors. *Neuron*. 55:779-785.

Benke, T.A., A. Luthi, J.T. Isaac, and G.L. Collingridge. 1998. Modulation of AMPA receptor unitary conductance by synaptic activity. *Nature*. 393:793-797.

Berger, A.J., S. Dieudonne, and P. Ascher. 1998. Glycine uptake governs glycine site occupancy at NMDA receptors of excitatory synapses. *Journal of neurophysiology*. 80:3336-3340.

Bergeron, R., T.M. Meyer, J.T. Coyle, and R.W. Greene. 1998. Modulation of N-methyl-D-aspartate receptor function by glycine transport. *Proceedings of the National Academy of Sciences of the United States of America*. 95:15730-15734.

Berretta, N., and R.S. Jones. 1996. Tonic facilitation of glutamate release by presynaptic N-methyl-D-aspartate autoreceptors in the entorhinal cortex. *Neuroscience*. 75:339-344.

Betz, H., J. Gomeza, W. Armsen, P. Scholze, and V. Eulenburg. 2006. Glycine transporters: essential regulators of synaptic transmission. *Biochemical Society transactions*. 34:55-58.

Bidoret, C., A. Ayon, B. Barbour, and M. Casado. 2009. Presynaptic NR2A-containing NMDA receptors implement a high-pass filter synaptic plasticity rule. *Proceedings of the National Academy of Sciences of the United States of America*. 106:14126-14131.

Blake, C.B., and B.N. Smith. 2012. Insulin reduces excitation in gastric-related neurons of the dorsal motor nucleus of the vagus. *American journal of physiology. Regulatory, integrative and comparative physiology*. 303:R807-814.

Bliss, T.V., and T. Lomo. 1973. Long-lasting potentiation of synaptic transmission in the dentate area of the anaesthetized rabbit following stimulation of the perforant path. *The Journal of physiology*. 232:331-356.

Bolshakov, V.Y., H. Golan, E.R. Kandel, and S.A. Siegelbaum. 1997. Recruitment of new sites of synaptic transmission during the cAMP-dependent late phase of LTP at CA3-CA1 synapses in the hippocampus. *Neuron*. 19:635-651.

Bonham, A.C., and E.M. Hasser. 1993. Area postrema and aortic or vagal afferents converge to excite cells in nucleus tractus solitarius. *The American journal of physiology*. 264:H1674-1685.

Brasier, D.J., and D.E. Feldman. 2008. Synapse-specific expression of functional presynaptic NMDA receptors in rat somatosensory cortex. *J Neurosci*. 28:2199-2211.

Browning, K.N., and R.A. Travagli. 1999. Characterization of the in vitro effects of 5-hydroxytryptamine (5-HT) on identified neurones of the rat dorsal motor nucleus of the vagus (DMV). *British journal of pharmacology*. 128:1307-1315.

Browning, K.N., and R.A. Travagli. 2003. Neuropeptide Y and peptide YY inhibit excitatory synaptic transmission in the rat dorsal motor nucleus of the vagus. *The Journal of physiology*. 549:775-785.

Browning, K.N., and R.A. Travagli. 2007. Functional organization of presynaptic metabotropic glutamate receptors in vagal brainstem circuits. *The Journal of neuroscience : the official journal of the Society for Neuroscience*. 27:8979-8988.

Browning, K.N., and R.A. Travagli. 2009. Modulation of inhibitory neurotransmission in brainstem vagal circuits by NPY and PYY is controlled by cAMP levels. *Neurogastroenterology and motility : the official journal of the European Gastrointestinal Motility Society*. 21:1309-e1126.

Browning, K.N., and R.A. Travagli. 2010. Plasticity of vagal brainstem circuits in the control of gastric function. *Neurogastroenterology and motility : the official journal of the European Gastrointestinal Motility Society*. 22:1154-1163.

Browning, K.N., and R.A. Travagli. 2011. Plasticity of vagal brainstem circuits in the control of gastrointestinal function. *Autonomic neuroscience : basic & clinical*. 161:6-13.

Burzomato, V., M. Beato, P.J. Groot-Kormelink, D. Colquhoun, and L.G. Sivilotti. 2004. Single-channel behavior of heteromeric alpha1beta glycine receptors: an attempt to detect a conformational change before the channel opens. *The Journal of neuroscience : the official journal of the Society for Neuroscience*. 24:10924-10940.

Carnethon, M.R., D.R. Jacobs, Jr., S. Sidney, K. Liu, and C. study. 2003. Influence of autonomic nervous system dysfunction on the development of type 2 diabetes: the CARDIA study. *Diabetes care*. 26:3035-3041.

Casado, M., P. Isope, and P. Ascher. 2002. Involvement of presynaptic N-methyl-D-aspartate receptors in cerebellar long-term depression. *Neuron*. 33:123-130.

Chabot, C., G. Massicotte, M. Milot, F. Trudeau, and J. Gagne. 1997. Impaired modulation of AMPA receptors by calcium-dependent processes in streptozotocin-induced diabetic rats. *Brain research*. 768:249-256.

Charton, J.P., M. Herkert, C.M. Becker, and H. Schroder. 1999. Cellular and subcellular localization of the 2B-subunit of the NMDA receptor in the adult rat telencephalon. *Brain Res*. 816:609-617.

Chattipakorn, S.C., and L.L. McMahon. 2003. Strychnine-sensitive glycine receptors depress hyperexcitability in rat dentate gyrus. *Journal of neurophysiology*. 89:1339-1342.
Christie, J.M., and C.E. Jahr. 2008. Dendritic NMDA receptors activate axonal calcium channels. *Neuron*. 60:298-307.
Ciabarra, A.M., J.M. Sullivan, L.G. Gahn, G. Pecht, S. Heinemann, and K.A. Sevarino. 1995. Cloning and characterization of chi-1: a developmentally regulated member of a novel class of the ionotropic glutamate receptor family. *The Journal of neuroscience : the official journal of the Society for Neuroscience*. 15:6498-6508.
Citri, A., and R.C. Malenka. 2008. Synaptic plasticity: multiple forms, functions, and mechanisms. *Neuropsychopharmacology : official publication of the American College of Neuropsychopharmacology*. 33:18-41.
Collingridge, G.L., J.T. Isaac, and Y.T. Wang. 2004. Receptor trafficking and synaptic plasticity. *Nature reviews. Neuroscience*. 5:952-962.
Collingridge, G.L., S.J. Kehl, and H. McLennan. 1983. Excitatory amino acids in synaptic transmission in the Schaffer collateral-commissural pathway of the rat hippocampus. *The Journal of physiology*. 334:33-46.
Corlew, R., D.J. Brasier, D.E. Feldman, and B.D. Philpot. 2008. Presynaptic NMDA receptors: newly appreciated roles in cortical synaptic function and plasticity. *Neuroscientist*. 14:609-625.
Craighead, J.E. 1980. Experimental models of juvenile onset (insulin-dependent) diabetes mellitus. *Monographs in pathology*. 21:166-176.
Cubelos, B., C. Gimenez, and F. Zafra. 2005. Localization of the GLYT1 glycine transporter at glutamatergic synapses in the rat brain. *Cerebral cortex*. 15:448-459.
Cubelos, B., C. Leite, C. Gimenez, and F. Zafra. 2013. Localization of the glycine transporter GLYT1 in glutamatergic synaptic vesicles. *Neurochemistry international*.
Cull-Candy, S.G., and D.N. Leszkiewicz. 2004. Role of distinct NMDA receptor subtypes at central synapses. *Science's STKE : signal transduction knowledge environment*. 2004:re16.
Cummings, J.A., R.M. Mulkey, R.A. Nicoll, and R.C. Malenka. 1996. Ca2+ signaling requirements for long-term depression in the hippocampus. *Neuron*. 16:825-833.
Davis, S.F., A.V. Derbenev, K.W. Williams, N.R. Glatzer, and B.N. Smith. 2004. Excitatory and inhibitory local circuit input to the rat dorsal motor nucleus of the vagus originating from the nucleus tractus solitarius. *Brain research*. 1017:208-217.
Davis, S.F., K.W. Williams, W. Xu, N.R. Glatzer, and B.N. Smith. 2003. Selective enhancement of synaptic inhibition by hypocretin (orexin) in rat vagal motor neurons: implications for autonomic regulation. *The Journal of neuroscience : the official journal of the Society for Neuroscience*. 23:3844-3854.

Debanne, D., N.C. Guerineau, B.H. Gahwiler, and S.M. Thompson. 1996. Paired-pulse facilitation and depression at unitary synapses in rat hippocampus: quantal fluctuation affects subsequent release. *The Journal of physiology*. 491 (Pt 1):163-176.

Derbenev, A.V., M.J. Monroe, N.R. Glatzer, and B.N. Smith. 2006. Vanilloid-mediated heterosynaptic facilitation of inhibitory synaptic input to neurons of the rat dorsal motor nucleus of the vagus. *The Journal of neuroscience : the official journal of the Society for Neuroscience*. 26:9666-9672.

Derbenev, A.V., T.C. Stuart, and B.N. Smith. 2004. Cannabinoids suppress synaptic input to neurones of the rat dorsal motor nucleus of the vagus nerve. *The Journal of physiology*. 559:923-938.

Di Luca, M., L. Ruts, F. Gardoni, F. Cattabeni, G.J. Biessels, and W.H. Gispen. 1999. NMDA receptor subunits are modified transcriptionally and post-translationally in the brain of streptozotocin-diabetic rats. *Diabetologia*. 42:693-701.

Dobrunz, L.E., E.P. Huang, and C.F. Stevens. 1997. Very short-term plasticity in hippocampal synapses. *Proceedings of the National Academy of Sciences of the United States of America*. 94:14843-14847.

Dobrunz, L.E., and C.F. Stevens. 1997. Heterogeneity of release probability, facilitation, and depletion at central synapses. *Neuron*. 18:995-1008.

Dudek, S.M., and M.F. Bear. 1992. Homosynaptic long-term depression in area CA1 of hippocampus and effects of N-methyl-D-aspartate receptor blockade. *Proceedings of the National Academy of Sciences of the United States of America*. 89:4363-4367.

Duguid, I.C., and T.G. Smart. 2004. Retrograde activation of presynaptic NMDA receptors enhances GABA release at cerebellar interneuron-Purkinje cell synapses. *Nat Neurosci*. 7:525-533.

Durand, G.M., Y. Kovalchuk, and A. Konnerth. 1996. Long-term potentiation and functional synapse induction in developing hippocampus. *Nature*. 381:71-75.

Dutertre, S., C.M. Becker, and H. Betz. 2012. Inhibitory glycine receptors: an update. *The Journal of biological chemistry*. 287:40216-40223.

El Mestikawy, S., A. Wallen-Mackenzie, G.M. Fortin, L. Descarries, and L.E. Trudeau. 2011. From glutamate co-release to vesicular synergy: vesicular glutamate transporters. *Nature reviews. Neuroscience*. 12:204-216.

Engelman, H.S., and A.B. MacDermott. 2004. Presynaptic ionotropic receptors and control of transmitter release. *Nat Rev Neurosci*. 5:135-145.

Eulenburg, V., W. Armsen, H. Betz, and J. Gomeza. 2005. Glycine transporters: essential regulators of neurotransmission. *Trends in biochemical sciences*. 30:325-333.

Ferreira, M., Jr., K.N. Browning, N. Sahibzada, J.G. Verbalis, R.A. Gillis, and R.A. Travagli. 2001. Glucose effects on gastric motility and tone evoked from the rat dorsal vagal complex. *J Physiol*. 536:141-152.

Fremeau, R.T., Jr., K. Kam, T. Qureshi, J. Johnson, D.R. Copenhagen, J. Storm-Mathisen, F.A. Chaudhry, R.A. Nicoll, and R.H. Edwards. 2004. Vesicular

glutamate transporters 1 and 2 target to functionally distinct synaptic release sites. *Science*. 304:1815-1819.
Fukunaga, K., D. Muller, and E. Miyamoto. 1995. Increased phosphorylation of Ca2+/calmodulin-dependent protein kinase II and its endogenous substrates in the induction of long-term potentiation. *The Journal of biological chemistry*. 270:6119-6124.
Gao, H., and B.N. Smith. 2010. Tonic GABAA receptor-mediated inhibition in the rat dorsal motor nucleus of the vagus. *Journal of neurophysiology*. 103:904-914.
Geiss, G.K., R.E. Bumgarner, B. Birditt, T. Dahl, N. Dowidar, D.L. Dunaway, H.P. Fell, S. Ferree, R.D. George, T. Grogan, J.J. James, M. Maysuria, J.D. Mitton, P. Oliveri, J.L. Osborn, T. Peng, A.L. Ratcliffe, P.J. Webster, E.H. Davidson, L. Hood, and K. Dimitrov. 2008. Direct multiplexed measurement of gene expression with color-coded probe pairs. *Nature biotechnology*. 26:317-325.
Gerdeman, G.L., J. Ronesi, and D.M. Lovinger. 2002. Postsynaptic endocannabinoid release is critical to long-term depression in the striatum. *Nature neuroscience*. 5:446-451.
Glatzer, N.R., A.V. Derbenev, B.W. Banfield, and B.N. Smith. 2007. Endomorphin-1 modulates intrinsic inhibition in the dorsal vagal complex. *Journal of neurophysiology*. 98:1591-1599.
Glatzer, N.R., and B.N. Smith. 2005. Modulation of synaptic transmission in the rat nucleus of the solitary tract by endomorphin-1. *Journal of neurophysiology*. 93:2530-2540.
Glitsch, M., and A. Marty. 1999. Presynaptic effects of NMDA in cerebellar Purkinje cells and interneurons. *The Journal of neuroscience : the official journal of the Society for Neuroscience*. 19:511-519.
Gross, P.M., K.M. Wall, J.J. Pang, S.W. Shaver, and D.S. Wainman. 1990. Microvascular specializations promoting rapid interstitial solute dispersion in nucleus tractus solitarius. *The American journal of physiology*. 259:R1131-1138.
Harvey, R.J., E. Carta, B.R. Pearce, S.K. Chung, S. Supplisson, M.I. Rees, and K. Harvey. 2008. A critical role for glycine transporters in hyperexcitability disorders. *Frontiers in molecular neuroscience*. 1:1.
Henson, M.A., A.C. Roberts, I. Perez-Otano, and B.D. Philpot. 2010. Influence of the NR3A subunit on NMDA receptor functions. *Progress in neurobiology*. 91:23-37.
Hermes, S.M., J.F. Colbert, and S.A. Aicher. 2013. Differential content of vesicular glutamate transporters in subsets of vagal afferents projecting to the nucleus tractus solitarii in the rat. *The Journal of comparative neurology*.
Herzog, E., G.C. Bellenchi, C. Gras, V. Bernard, P. Ravassard, C. Bedet, B. Gasnier, B. Giros, and S. El Mestikawy. 2001. The existence of a second vesicular glutamate transporter specifies subpopulations of glutamatergic

neurons. *The Journal of neuroscience : the official journal of the Society for Neuroscience*. 21:RC181.
Herzog, E., J. Gilchrist, C. Gras, A. Muzerelle, P. Ravassard, B. Giros, P. Gaspar, and S. El Mestikawy. 2004. Localization of VGLUT3, the vesicular glutamate transporter type 3, in the rat brain. *Neuroscience*. 123:983-1002.
Hrabetova, S., and T.C. Sacktor. 1996. Bidirectional regulation of protein kinase M zeta in the maintenance of long-term potentiation and long-term depression. *The Journal of neuroscience : the official journal of the Society for Neuroscience*. 16:5324-5333.
Jeong, H.J., I.S. Jang, A.J. Moorhouse, and N. Akaike. 2003. Activation of presynaptic glycine receptors facilitates glycine release from presynaptic terminals synapsing onto rat spinal sacral dorsal commissural nucleus neurons. *The Journal of physiology*. 550:373-383.
Kalappa, B.I., L. Feng, W.R. Kem, A.G. Gusev, and V.V. Uteshev. 2011. Mechanisms of facilitation of synaptic glutamate release by nicotinic agonists in the nucleus of the solitary tract. *American journal of physiology. Cell physiology*. 301:C347-361.
Kalia, M., and M.M. Mesulam. 1980a. Brain stem projections of sensory and motor components of the vagus complex in the cat: I. The cervical vagus and nodose ganglion. *J Comp Neurol*. 193:435-465.
Kalia, M., and M.M. Mesulam. 1980b. Brain stem projections of sensory and motor components of the vagus complex in the cat: II. Laryngeal, tracheobronchial, pulmonary, cardiac, and gastrointestinal branches. *J Comp Neurol*. 193:467-508.
Kamal, A., G.J. Biessels, I.J. Urban, and W.H. Gispen. 1999. Hippocampal synaptic plasticity in streptozotocin-diabetic rats: impairment of long-term potentiation and facilitation of long-term depression. *Neuroscience*. 90:737-745.
Kameyama, K., H.K. Lee, M.F. Bear, and R.L. Huganir. 1998. Involvement of a postsynaptic protein kinase A substrate in the expression of homosynaptic long-term depression. *Neuron*. 21:1163-1175.
Kandel, E.R., J.H. Schwartz, and T.M. Jessell. 2000. Principles of neural science. McGraw-Hill, Health Professions Division, New York. xli, 1414 p. pp.
Kirchner, A., J. Breustedt, B. Rosche, U.F. Heinemann, and V. Schmieden. 2003. Effects of taurine and glycine on epileptiform activity induced by removal of Mg2+ in combined rat entorhinal cortex-hippocampal slices. *Epilepsia*. 44:1145-1152.
Kulkarni, M.M. 2011. Digital multiplexed gene expression analysis using the NanoString nCounter system. *Current protocols in molecular biology / edited by Frederick M. Ausubel ... [et al.]*. Chapter 25:Unit25B 10.
Kunz, P.A., A.C. Burette, R.J. Weinberg, and B.D. Philpot. 2012. Glycine receptors support excitatory neurotransmitter release in developing mouse visual cortex. *The Journal of physiology*. 590:5749-5764.

Lam, C.K., M. Chari, G.A. Rutter, and T.K. Lam. 2011. Hypothalamic nutrient sensing activates a forebrain-hindbrain neuronal circuit to regulate glucose production in vivo. *Diabetes*. 60:107-113.

Lam, C.K., M. Chari, B.B. Su, G.W. Cheung, A. Kokorovic, C.S. Yang, P.Y. Wang, T.Y. Lai, and T.K. Lam. 2010. Activation of N-methyl-D-aspartate (NMDA) receptors in the dorsal vagal complex lowers glucose production. *The Journal of biological chemistry*. 285:21913-21921.

Lanore, F., C. Blanchet, A. Fejtova, P. Pinheiro, K. Richter, D. Balschun, E. Gundelfinger, and C. Mulle. 2010. Impaired development of hippocampal mossy fibre synapses in mouse mutants for the presynaptic scaffold protein Bassoon. *The Journal of physiology*. 588:2133-2145.

Larsen, R.S., R.J. Corlew, M.A. Henson, A.C. Roberts, M. Mishina, M. Watanabe, S.A. Lipton, N. Nakanishi, I. Perez-Otano, R.J. Weinberg, and B.D. Philpot. 2011. NR3A-containing NMDARs promote neurotransmitter release and spike timing-dependent plasticity. *Nature neuroscience*. 14:338-344.

Lau, C.G., and R.S. Zukin. 2007. NMDA receptor trafficking in synaptic plasticity and neuropsychiatric disorders. *Nature reviews. Neuroscience*. 8:413-426.

Levin, B.E., A.A. Dunn-Meynell, and V.H. Routh. 1999. Brain glucose sensing and body energy homeostasis: role in obesity and diabetes. *The American journal of physiology*. 276:R1223-1231.

Lin, L.H. 2009. Glutamatergic neurons say NO in the nucleus tractus solitarii. *Journal of chemical neuroanatomy*. 38:154-165.

Lin, L.H., R.H. Edwards, R.T. Fremeau, F. Fujiyama, T. Kaneko, and W.T. Talman. 2004. Localization of vesicular glutamate transporters and neuronal nitric oxide synthase in rat nucleus tractus solitarii. *Neuroscience*. 123:247-255.

Lin, L.H., and W.T. Talman. 2005. Nitroxidergic neurons in rat nucleus tractus solitarii express vesicular glutamate transporter 3. *Journal of chemical neuroanatomy*. 29:179-191.

Lin, L.H., and W.T. Talman. 2006. Vesicular glutamate transporters and neuronal nitric oxide synthase colocalize in aortic depressor afferent neurons. *Journal of chemical neuroanatomy*. 32:54-64.

Lisman, J. 1989. A mechanism for the Hebb and the anti-Hebb processes underlying learning and memory. *Proceedings of the National Academy of Sciences of the United States of America*. 86:9574-9578.

Liu, Q., and M.T. Wong-Riley. 2010. Postnatal development of N-methyl-D-aspartate receptor subunits 2A, 2B, 2C, 2D, and 3B immunoreactivity in brain stem respiratory nuclei of the rat. *Neuroscience*. 171:637-654.

Low, C.M., and K.S. Wee. 2010. New insights into the not-so-new NR3 subunits of N-methyl-D-aspartate receptor: localization, structure, and function. *Molecular pharmacology*. 78:1-11.

Lujan, R., R. Shigemoto, and G. Lopez-Bendito. 2005. Glutamate and GABA receptor signalling in the developing brain. *Neuroscience*. 130:567-580.

Lynch, J.W. 2009. Native glycine receptor subtypes and their physiological roles. *Neuropharmacology*. 56:303-309.
Ma, Q.P., and R.J. Hargreaves. 2000. Localization of N-methyl-D-aspartate NR2B subunits on primary sensory neurons that give rise to small-caliber sciatic nerve fibers in rats. *Neuroscience*. 101:699-707.
MacDermott, A.B., L.W. Role, and S.A. Siegelbaum. 1999. Presynaptic ionotropic receptors and the control of transmitter release. *Annu Rev Neurosci*. 22:443-485.
Malenka, R.C., J.A. Kauer, D.J. Perkel, M.D. Mauk, P.T. Kelly, R.A. Nicoll, and M.N. Waxham. 1989. An essential role for postsynaptic calmodulin and protein kinase activity in long-term potentiation. *Nature*. 340:554-557.
Malenka, R.C., and R.A. Nicoll. 1993. NMDA-receptor-dependent synaptic plasticity: multiple forms and mechanisms. *Trends in neurosciences*. 16:521-527.
Malenka, R.C., and R.A. Nicoll. 1997. Silent synapses speak up. *Neuron*. 19:473-476.
Malkov, V.A., K.A. Serikawa, N. Balantac, J. Watters, G. Geiss, A. Mashadi-Hossein, and T. Fare. 2009. Multiplexed measurements of gene signatures in different analytes using the Nanostring nCounter Assay System. *BMC research notes*. 2:80.
Mathew, S.S., and J.J. Hablitz. 2011. Presynaptic NMDA receptors mediate IPSC potentiation at GABAergic synapses in developing rat neocortex. *PLoS One*. 6:e17311.
Matsubayashi, H., M. Alkondon, E.F. Pereira, K.L. Swanson, and E.X. Albuquerque. 1998. Strychnine: a potent competitive antagonist of alpha-bungarotoxin-sensitive nicotinic acetylcholine receptors in rat hippocampal neurons. *The Journal of pharmacology and experimental therapeutics*. 284:904-913.
Mayer, M.L., G.L. Westbrook, and P.B. Guthrie. 1984. Voltage-dependent block by Mg2+ of NMDA responses in spinal cord neurones. *Nature*. 309:261-263.
Mayor, F., Jr., J.G. Marvizon, M.C. Aragon, C. Gimenez, and F. Valdivieso. 1981. Glycine transport into plasma-membrane vesicles derived from rat brain synaptosomes. *The Biochemical journal*. 198:535-541.
McDougall, S.J., and M.C. Andresen. 2012. Low-fidelity GABA transmission within a dense excitatory network of the solitary tract nucleus. *The Journal of physiology*. 590:5677-5689.
McDougall, S.J., and M.C. Andresen. 2013. Independent transmission of convergent visceral primary afferents in the solitary tract nucleus. *Journal of neurophysiology*. 109:507-517.
Meddows, E., B. Le Bourdelles, S. Grimwood, K. Wafford, S. Sandhu, P. Whiting, and R.A. McIlhinney. 2001. Identification of molecular determinants that are important in the assembly of N-methyl-D-aspartate receptors. *The Journal of biological chemistry*. 276:18795-18803.

Menger, N., D.V. Pow, and H. Wassle. 1998. Glycinergic amacrine cells of the rat retina. *The Journal of comparative neurology*. 401:34-46.
Merchenthaler, I. 1991. Neurons with access to the general circulation in the central nervous system of the rat: a retrograde tracing study with fluoro-gold. *Neuroscience*. 44:655-662.
Monyer, H., N. Burnashev, D.J. Laurie, B. Sakmann, and P.H. Seeburg. 1994. Developmental and regional expression in the rat brain and functional properties of four NMDA receptors. *Neuron*. 12:529-540.
Mothet, J.P., A.T. Parent, H. Wolosker, R.O. Brady, Jr., D.J. Linden, C.D. Ferris, M.A. Rogawski, and S.H. Snyder. 2000. D-serine is an endogenous ligand for the glycine site of the N-methyl-D-aspartate receptor. *Proceedings of the National Academy of Sciences of the United States of America*. 97:4926-4931.
Nowak, L., P. Bregestovski, P. Ascher, A. Herbet, and A. Prochiantz. 1984. Magnesium gates glutamate-activated channels in mouse central neurones. *Nature*. 307:462-465.
Obici, S., B.B. Zhang, G. Karkanias, and L. Rossetti. 2002. Hypothalamic insulin signaling is required for inhibition of glucose production. *Nature medicine*. 8:1376-1382.
Oliet, S.H., R.C. Malenka, and R.A. Nicoll. 1997. Two distinct forms of long-term depression coexist in CA1 hippocampal pyramidal cells. *Neuron*. 18:969-982.
Pachernegg, S., N. Strutz-Seebohm, and M. Hollmann. 2012. GluN3 subunit-containing NMDA receptors: not just one-trick ponies. *Trends in neurosciences*. 35:240-249.
Paoletti, P. 2011. Molecular basis of NMDA receptor functional diversity. *The European journal of neuroscience*. 33:1351-1365.
Paoletti, P., P. Ascher, and J. Neyton. 1997. High-affinity zinc inhibition of NMDA NR1-NR2A receptors. *The Journal of neuroscience : the official journal of the Society for Neuroscience*. 17:5711-5725.
Paoletti, P., C. Bellone, and Q. Zhou. 2013. NMDA receptor subunit diversity: impact on receptor properties, synaptic plasticity and disease. *Nature reviews. Neuroscience*. 14:383-400.
Paoletti, P., and J. Neyton. 2007. NMDA receptor subunits: function and pharmacology. *Current opinion in pharmacology*. 7:39-47.
Payne, J.A., C. Rivera, J. Voipio, and K. Kaila. 2003. Cation-chloride co-transporters in neuronal communication, development and trauma. *Trends in neurosciences*. 26:199-206.
Payne, J.A., T.J. Stevenson, and L.F. Donaldson. 1996. Molecular characterization of a putative K-Cl cotransporter in rat brain. A neuronal-specific isoform. *The Journal of biological chemistry*. 271:16245-16252.
Pocai, A., T.K. Lam, R. Gutierrez-Juarez, S. Obici, G.J. Schwartz, J. Bryan, L. Aguilar-Bryan, and L. Rossetti. 2005a. Hypothalamic K(ATP) channels control hepatic glucose production. *Nature*. 434:1026-1031.

Pocai, A., S. Obici, G.J. Schwartz, and L. Rossetti. 2005b. A brain-liver circuit regulates glucose homeostasis. *Cell metabolism*. 1:53-61.
Poyatos, I., J. Ponce, C. Aragon, C. Gimenez, and F. Zafra. 1997. The glycine transporter GLYT2 is a reliable marker for glycine-immunoreactive neurons. *Brain research. Molecular brain research*. 49:63-70.
Pribilla, I., T. Takagi, D. Langosch, J. Bormann, and H. Betz. 1992. The atypical M2 segment of the beta subunit confers picrotoxinin resistance to inhibitory glycine receptor channels. *The EMBO journal*. 11:4305-4311.
Quinlan, E.M., D.H. Olstein, and M.F. Bear. 1999. Bidirectional, experience-dependent regulation of N-methyl-D-aspartate receptor subunit composition in the rat visual cortex during postnatal development. *Proc Natl Acad Sci U S A*. 96:12876-12880.
Raiteri, L., S. Stigliani, C. Usai, A. Diaspro, S. Paluzzi, M. Milanese, M. Raiteri, and G. Bonanno. 2008. Functional expression of release-regulating glycine transporters GLYT1 on GABAergic neurons and GLYT2 on astrocytes in mouse spinal cord. *Neurochemistry international*. 52:103-112.
Reymann, K.G., and J.U. Frey. 2007. The late maintenance of hippocampal LTP: requirements, phases, 'synaptic tagging', 'late-associativity' and implications. *Neuropharmacology*. 52:24-40.
Ritter, R.C. 2011. A tale of two endings: modulation of satiation by NMDA receptors on or near central and peripheral vagal afferent terminals. *Physiology & behavior*. 105:94-99.
Ritter, R.C., P.G. Slusser, and S. Stone. 1981. Glucoreceptors controlling feeding and blood glucose: location in the hindbrain. *Science*. 213:451-452.
Ritter, S., T.T. Dinh, and Y. Zhang. 2000. Localization of hindbrain glucoreceptive sites controlling food intake and blood glucose. *Brain research*. 856:37-47.
Saltzman, M.B., and R.W. McCallum. 1983. Diabetes and the stomach. *The Yale journal of biology and medicine*. 56:179-187.
Santos, M.S., H. Li, and S.M. Voglmaier. 2009. Synaptic vesicle protein trafficking at the glutamate synapse. *Neuroscience*. 158:189-203.
Sanz-Clemente, A., R.A. Nicoll, and K.W. Roche. 2013. Diversity in NMDA receptor composition: many regulators, many consequences. *The Neuroscientist : a review journal bringing neurobiology, neurology and psychiatry*. 19:62-75.
Seagard, J.L., C. Dean, and F.A. Hopp. 1999. Role of glutamate receptors in transmission of vagal cardiac input to neurones in the nucleus tractus solitarii in dogs. *The Journal of physiology*. 520 Pt 1:243-253.
Sheng, M., J. Cummings, L.A. Roldan, Y.N. Jan, and L.Y. Jan. 1994. Changing subunit composition of heteromeric NMDA receptors during development of rat cortex. *Nature*. 368:144-147.
Sjostrom, P.J., G.G. Turrigiano, and S.B. Nelson. 2003. Neocortical LTD via coincident activation of presynaptic NMDA and cannabinoid receptors. *Neuron*. 39:641-654.

Smith, B.N., S.F. Davis, A.N. Van Den Pol, and W. Xu. 2002. Selective enhancement of excitatory synaptic activity in the rat nucleus tractus solitarius by hypocretin 2. *Neuroscience*. 115:707-714.
Smith, B.N., P. Dou, W.D. Barber, and F.E. Dudek. 1998. Vagally evoked synaptic currents in the immature rat nucleus tractus solitarii in an intact in vitro preparation. *The Journal of physiology*. 512 (Pt 1):149-162.
Song, W., S.C. Chattipakorn, and L.L. McMahon. 2006. Glycine-gated chloride channels depress synaptic transmission in rat hippocampus. *Journal of neurophysiology*. 95:2366-2379.
Stil, A., S. Liabeuf, C. Jean-Xavier, C. Brocard, J.C. Viemari, and L. Vinay. 2009. Developmental up-regulation of the potassium-chloride cotransporter type 2 in the rat lumbar spinal cord. *Neuroscience*. 164:809-821.
Supplisson, S., and C. Bergman. 1997. Control of NMDA receptor activation by a glycine transporter co-expressed in Xenopus oocytes. *The Journal of neuroscience : the official journal of the Society for Neuroscience*. 17:4580-4590.
Thomas, G.M., and R.L. Huganir. 2004. MAPK cascade signalling and synaptic plasticity. *Nature reviews. Neuroscience*. 5:173-183.
Travagli, R.A. 2007. The nucleus tractus solitarius: an integrative centre with 'task-matching' capabilities. *The Journal of physiology*. 582:471.
Travagli, R.A. 2012. Of apples and oranges: GABA and glutamate transmission in neurones of the nucleus tractus solitarii could not be more different. *The Journal of physiology*. 590:5559.
Travagli, R.A., and R.A. Gillis. 1995. Effects of 5-HT alone and its interaction with TRH on neurons in rat dorsal motor nucleus of the vagus. *The American journal of physiology*. 268:G292-299.
Travagli, R.A., R.A. Gillis, C.D. Rossiter, and S. Vicini. 1991a. Glutamate and GABA-mediated synaptic currents in neurons of the rat dorsal motor nucleus of the vagus. *The American journal of physiology*. 260:G531-536.
Travagli RA, G.R., Rossiter CD, Vicini S. 1991. Glutamate and GABA-mediated synaptic currents in neurons of the rat dorsal motor nucleus of the vagus. *Am J Physiol Gas Liv Phy*. 260:6.
Travagli, R.A., G.E. Hermann, K.N. Browning, and R.C. Rogers. 2006. Brainstem circuits regulating gastric function. *Annual review of physiology*. 68:279-305.
Travagli, R.A., M. Ulivi, and W.J. Wojcik. 1991b. gamma-Aminobutyric acid-B receptors inhibit glutamate release from cerebellar granule cells: consequences of inhibiting cyclic AMP formation and calcium influx. *The Journal of pharmacology and experimental therapeutics*. 258:903-909.
Traynelis, S.F., L.P. Wollmuth, C.J. McBain, F.S. Menniti, K.M. Vance, K.K. Ogden, K.B. Hansen, H. Yuan, S.J. Myers, and R. Dingledine. 2010. Glutamate receptor ion channels: structure, regulation, and function. *Pharmacological reviews*. 62:405-496.
Turecek, R., and L.O. Trussell. 2001. Presynaptic glycine receptors enhance transmitter release at a mammalian central synapse. *Nature*. 411:587-590.

Undeland, K.A., T. Hausken, O.H. Gilja, S. Aanderud, and A. Berstad. 1998. Gastric meal accommodation studied by ultrasound in diabetes. Relation to vagal tone. *Scandinavian journal of gastroenterology*. 33:236-241.

Wan, S., and K.N. Browning. 2008. D-glucose modulates synaptic transmission from the central terminals of vagal afferent fibers. *American journal of physiology. Gastrointestinal and liver physiology*. 294:G757-763.

Wan, S., F.H. Coleman, and R.A. Travagli. 2007. Glucagon-like peptide-1 excites pancreas-projecting preganglionic vagal motoneurons. *American journal of physiology. Gastrointestinal and liver physiology*. 292:G1474-1482.

Wee, K.S., Y. Zhang, S. Khanna, and C.M. Low. 2008. Immunolocalization of NMDA receptor subunit NR3B in selected structures in the rat forebrain, cerebellum, and lumbar spinal cord. *The Journal of comparative neurology*. 509:118-135.

Werner, A., L. Dehmelt, and P. Nalbant. 1998. Na+-dependent phosphate cotransporters: the NaPi protein families. *The Journal of experimental biology*. 201:3135-3142.

Williams, K.W., and B.N. Smith. 2006. Rapid inhibition of neural excitability in the nucleus tractus solitarii by leptin: implications for ingestive behaviour. *The Journal of physiology*. 573:395-412.

Williams, K.W., A. Zsombok, and B.N. Smith. 2007. Rapid inhibition of neurons in the dorsal motor nucleus of the vagus by leptin. *Endocrinology*. 148:1868-1881.

Wong, H.K., X.B. Liu, M.F. Matos, S.F. Chan, I. Perez-Otano, M. Boysen, J. Cui, N. Nakanishi, J.S. Trimmer, E.G. Jones, S.A. Lipton, and N.J. Sucher. 2002. Temporal and regional expression of NMDA receptor subunit NR3A in the mammalian brain. *The Journal of comparative neurology*. 450:303-317.

Woodhall, G., D.I. Evans, M.O. Cunningham, and R.S. Jones. 2001. NR2B-containing NMDA autoreceptors at synapses on entorhinal cortical neurons. *J Neurophysiol*. 86:1644-1651.

Wright, J., C. Campos, T. Herzog, M. Covasa, K. Czaja, and R.C. Ritter. 2011. Reduction of food intake by cholecystokinin requires activation of hindbrain NMDA-type glutamate receptors. *American journal of physiology. Regulatory, integrative and comparative physiology*. 301:R448-455.

Wyllie, D.J., M.R. Livesey, and G.E. Hardingham. 2013. Influence of GluN2 subunit identity on NMDA receptor function. *Neuropharmacology*.

Yang, J., G.L. Woodhall, and R.S. Jones. 2006. Tonic facilitation of glutamate release by presynaptic NR2B-containing NMDA receptors is increased in the entorhinal cortex of chronically epileptic rats. *The Journal of neuroscience : the official journal of the Society for Neuroscience*. 26:406-410.

Ye, J.H., F. Wang, K. Krnjevic, W. Wang, Z.G. Xiong, and J. Zhang. 2004. Presynaptic glycine receptors on GABAergic terminals facilitate discharge of dopaminergic neurons in ventral tegmental area. *The Journal of*

neuroscience : the official journal of the Society for Neuroscience. 24:8961-8974.

Zafra, F., C. Aragon, and C. Gimenez. 1997a. Molecular biology of glycinergic neurotransmission. *Molecular neurobiology*. 14:117-142.

Zafra, F., C. Aragon, L. Olivares, N.C. Danbolt, C. Gimenez, and J. Storm-Mathisen. 1995. Glycine transporters are differentially expressed among CNS cells. *The Journal of neuroscience : the official journal of the Society for Neuroscience*. 15:3952-3969.

Zafra, F., I. Poyatos, and C. Gimenez. 1997b. Neuronal dependency of the glycine transporter GLYT1 expression in glial cells. *Glia*. 20:155-162.

Zhang, L., K. Meng, Y.H. Li, and T.Z. Han. 2009. NR2A-containing NMDA receptors are required for L-LTP induction and depotentiation in CA1 region of hippocampal slices. *Eur J Neurosci*. 29:2137-2144.

Zimmet, P., K.G. Alberti, and J. Shaw. 2001. Global and societal implications of the diabetes epidemic. *Nature*. 414:782-787.

Zsombok, A., M.D. Bhaskaran, H. Gao, A.V. Derbenev, and B.N. Smith. 2011. Functional plasticity of central TRPV1 receptors in brainstem dorsal vagal complex circuits of streptozotocin-treated hyperglycemic mice. *The Journal of neuroscience : the official journal of the Society for Neuroscience*. 31:14024-14031.

Zsombok, A., and B.N. Smith. 2009. Plasticity of central autonomic neural circuits in diabetes. *Biochimica et biophysica acta*. 1792:423-431.

Vita

Eva Claudia Bach

Education

University of Kentucky 2008-2013
Anticipated PhD in Physiology December 2013

University of Kentucky 2006-2008
Bachelor of Science in Biology May 2008

University of Idaho 2004-2006

Academic and Professional Honors

Travel Award (2011 and 2012)
Delta Epsilon Iota Honor Society (member since 2008)
Awarded Magna Cum Laude from the University of Kentucky (2008)
Trustees Scholarship (2007-2008)
National Honor Society (member since 2001)

Professional Society Affiliations

Society for Neuroscience (SfN), Student Member

Publications
Research Papers

Bach EC, Halmos KC, Smith BN. NMDA receptors in normal and T1-diabetic mice. In preparation.

Bach EC, Smith BN. Presynaptic NMDA receptor-mediated modulation of excitatory neurotransmission in the mouse dorsal motor nucleus of the vagus. Journal of Neurophysiology. 2012 Sep;108(5):1484-91

Hunt RF, Haselhorst LA, Schoch KM, **Bach EC**, Rios-Pilier J, Scheff SW,

Saatman KE, Smith BN. Posttraumatic mossy fiber sprouting is related to the

degree of cortical damage in three mouse strains. Epilepsy Research. 2012

Mar;99(1-2):167-70.

Fannon M, Forsten-Williams K, Zhao B, **Bach E**, Parekh PP, Chu CL, Goerges-Wildt AL, Buczek-Thomas JA, Nugent MA. Facilitated diffusion of VEGF165 through descemet's membrane with sucrose octasulfate. Journal of Cell Physiology. 2012 Nov;227(11):3693-700.

Abstracts

EC Bach; BN Smith. Enhanced NMDA receptor-mediated currents in NTS neurons of T1-Diabetic mice.

1. Abstract submitted to be presented at the Society of Neuroscience, San Diego (2013)

EC Bach; BN Smith. NMDA receptors in the vagal complex in normal and diabetic mice.
1. Society of Neuroscience Meeting, New Orleans, LA (2012)
2. Department of Physiology Research Retreat, Cumberland Falls, KY (2012)
3. Blue Grass Society for Neuroscience Spring Neuroscience Day, Lexington KY (2012)
4. Barnstable Brown Obesity & Diabetes Research Day, Lexington, KY (2012)

EC Bach; BN Smith. Presynaptic NMDA receptors modulate glutamate release in the dorsal motor nucleus of the vagus in normal and diabetic mice.
Presented at: the Society of Neuroscience, Washington, DC. 2011
1. Society of Neuroscience, Washington, DC (2011)
2. Barnstable Brown Obesity & Diabetes Research Day, Lexington, KY (2012)

EC Bach; BN Smith. Presynaptic NMDA receptor facilitation in the dorsal vagal complex.
Poster Prestented at:
1. Blue Grass Society for Neuroscience Spring Neuroscience Day, Lexington KY (2011)
2. Society for Neuroscience, San Diego, CA (2010)
3. Department of Physiology 50th Anniversary, Lexington, KY (2010)
4. Department of Physiology Research Retreat, Cumberland Falls, KY (2010)

RF Hunt; LA Haselhorst; **EC Bach**; J Rios-Pilier; KM Schoch; SW Scheff; K Saatman; BN Smith. Relationship between injury severity and posttraumatic

epileptogenesis after controlled cortical impact in mice. Presented at the Society for Neuroscience, Chicago, OH (2009)

Research Experience

October 2008- present

Bret N. Smith, PhD, Department of Physiology, University of Kentucky

May 2007- August 2008

Michael Fannon, PhD, Department of Ophthalmology, University of Kentucky

August 2007- May 2008

James MacLeod, VMD, PhD, Department of Veterinary Sciences, University of Kentucky

January 2006- May 2006

Eva Top, PhD, Department of Biological Sciences, University of Idaho